

**Changes in the HIV-1 *env* gene:
Implications at the RNA and protein structure levels**

Francesc Cunyat Viaplana

Doctoral Thesis UAB 2012

Universitat Autònoma de Barcelona

Facultat de Medicina, Departament de Biologia Cel·lular, Fisiologia i Immunologia

Thesis Director: **Dr. Cecília Cabrera Navarro**

Tutor: **Dr. Dolores Jaraquemada**



La doctora **Cecilia Cabrera Navarro**, investigadora principal en el Laboratori de Retrovirologia de l'Institut de Recerca en Sida (IrsiCaixa) de l'Hospital Germans Trias i Pujol i l'Institut d'Investigació en Ciències de la Salut Germans Trias i Pujol (IGTP),

Certifica:

Que el treball experimental realitzat i la redacció de la memòria de la Tesi Doctoral titulada "*Changes in the HIV-1 env gene: Implications at the RNA and protein structure levels*" han estat realitzats per en Francesc Cunyat Viaplana sota la seva direcció i considera que és apte per a ser presentat per a optar al grau de Doctor en Immunologia per la Universitat Autònoma de Barcelona.

I per tal que en quedi constància, signa aquest document a Badalona, 25 de Maig del 2012.

Dr. Cecilia Cabrera Navarro



La doctora **Dolores Jaraquemada**, professora del Departament de Biologia Cel·lular, Fisiologia i Immunologia de la Unitat d'Immunologia de la Universitat Autònoma de Barcelona,

Certifica:

Que el treball experimental realitzat i la redacció de la memòria de la Tesi Doctoral titulada "*Changes in the HIV-1 env gene: Implications at the RNA and protein structure levels*" han estat realitzats per en Francesc Cunyat Viaplana sota la seva direcció i considera que és apte per a ser presentat per a optar al grau de Doctor en Immunologia per la Universitat Autònoma de Barcelona.

I per tal que en quedi constància, signa aquest document a Barcelona, 25 de Maig del 2012.

Dr. Dolores Jaraquemada

This work has been supported by the “*Fondo de Investigación Santitaria (FIS)*”, project 07/0418, and by the “*Institut de Recerca de la Sida IrsiCaixa*”. This work was also supported by fund from the “*Fundación para la Investigación y la Prevención del Sida en España (FIPSE)*”, project 36725/08.

The printing of this thesis was made possible by the financial aid of the UAB.

Cris Mascort, an excellent professional and a good friend, made the cover design of this thesis.

**A la meva família,
i de manera especial, a la Bea**

SUMMARY

The Env glycoprotein is one of the key proteins used by HIV-1 to mediate its pathogenicity. The sequence of the *env* gene is important to encode the Env glycoprotein but also for the secondary structure of the RRE that harbor its transcripts. The relevance of both elements has been extensively proved, although functional assays were needed in both cases to study the impact of specific changes. Treatment with the fusion inhibitor T-20 in patients infected with HIV-1 select resistant viruses to this drug after acquiring changes in their *env* gene. Therefore, we decided to use T-20-associated changes in order to functionally study relevant *in vivo env* variants. Predictions of the RRE secondary structures showed alterations when they were encoding for the changes G36V/D, V38A, Q40H and L45M, but not when harboring N43D and Q40H-L45M. Functional data showed that only the mutants harboring the L45M mutation had impairments in their binding capacity to Rev when this protein was at low concentrations, suggesting that the nucleotide changes affecting the encoding of the amino acid 45 in gp41 plays a role in Rev binding. However, none of the RRE variants were affected in their ability to being transported to the cytoplasm. Thus, it was found that alterations in RRE secondary structures predicted from nucleotide sequences might not necessary imply functional impairments and that the L45M change was not incorporated as a secondary mutation due to a restoration of the RRE functions. As it is important to functionally characterize patient-derived Envs to understand their *in vivo* pathogenesis, we established a complete methodology to study them by focusing on the main role of the subunit gp41. Based on our results, the correct selection of the effector cell line is essential to optimize the sensitivity of the assays. The 293T cell line might be used for fusogenic experiments and the HeLa for analyzing death parameters. Clinical trials had suggested that V38A viral mutants arising in an Env context containing the N140I polymorphism, were low pathogenic due to they were associated with virological failure and immunologic benefits. In order to understand these *in vivo* discordant data, we used our complete methodology to analyze patient-derived Envs that harbored these changes. We found that the V38A mutant Envs that were arisen in a N140I context were less able to induce single-cell death to target cells despite not having an altered fusogenic capacity. Thus, these data supports the importance of the Env context and the main role of gp41 in HIV-1 pathogenesis.

RESUM

La glicoproteïna de l'envolta (Env) és una de les proteïnes claus del VIH-1 en patogènesi. La seqüència del gen *env* és important per a codificar l'Env però també per les estructures secundàries dels RREs que contenen els seus trànscrips. La rellevància dels dos elements s'ha comprovat extensament, tot i que assajos funcionals són requerits en ambdós casos per estudiar l'impacte de canvis específics. El tractament amb l'inhibidor de fusió T-20 selecciona virus resistents després d'adquirir canvis al gen *env*. Per estudiar variants funcionalment rellevants d'*env* que es trobessin *in vivo* vam decidir utilitzar mutacions associades a T-20. Les prediccions de les estructures secundàries dels RRE van resultar alterades en els canvis que codificaven per G36V/D, V38A, Q40H i L45M, però no per N43D o Q40H-L45M. Funcionalment vam demostrar que només els mutants que presenten el canvi L45M a la seva seqüència pateixen un impacte en la capacitat d'unir-se a la proteïna viral Rev quan aquesta es troba en baixes concentracions, suggerint que els canvis nucleotídics que afecten a la formació de l'aminoàcid 45 de gp41 juguen un paper en la unió a Rev. De totes maneres, ninguna variant d'RRE va ser afectada en la seva capacitat per a ser transportada al citoplasma. Per tant, alteracions en les prediccions d'estructures secundàries a partir de seqüències nucleotídiques no necessàriament impliquen impactes funcionals i la mutació L45M no s'incorpora com a mutació secundària degut a un restaurament de les funcions del RRE. Com que és important caracteritzar funcionalment Envs derivades de pacients per a estudiar la seva patogenicitat, vam establir una metodologia completa per a estudiar-les basant-nos en el paper principal que hi juga la subunitat gp41. Els resultats demostren que la selecció de la línia cel·lular efectora és essencial per optimitzar la sensibilitat dels assajos. La línia cel·lular 293T hauria de ser utilitzada per experiments fusogènics i la HeLa per analitzar paràmetres relacionats amb la mort. Estudis clínics havien suggerit que virus que contenen la mutació V38A i que havien aparegut sota un context que tinguessin el polimorfisme viral N140I eren menys patogènics degut a que estaven associats amb fallada virològica i beneficis immunològics. Per tal d'entendre aquestes dades discordants vam basar-nos en la nostra metodologia per a analitzar Envs derivades de pacients que tinguessin aquests canvis. Aquestes Envs V38A-N140I van resultar tenir menys capacitat per induir la mort per cèl·lula individual tot i no veure's alterada la seva capacitat fusogènica, remarcant la importància del context de l'Env i el paper central de gp41 a la patogènesi del VIH-1.

RESUMEN

La glicoproteína de la envuelta (Env) es una de las proteínas claves del VIH-1 en patogénesis. La secuencia del gen *env* es importante para codificar la Env pero también para las estructuras secundarias de los RREs presentes en sus transcritos. La relevancia de estos dos elementos ha sido comprobada extensamente, pese a que ensayos funcionales aún son requeridos en ambos casos para estudiar el impacto de cambios específicos. El tratamiento con el inhibidor de fusión T-20 selecciona virus resistentes después de adquirir cambios en el gen *env*. Para estudiar variantes funcionalmente relevantes de *env* que se encontraran *in vivo* decidimos utilizar mutaciones asociadas a T-20. Las predicciones de las estructuras secundarias de los RRE resultaron alteradas en los cambios que codificaban para G36V/D, V38A, Q40H y L45M, pero no para N43D o Q40H-L45M. Funcionalmente demostramos que sólo los mutantes que presentan el cambio L45M en su secuencia sufren un impacto de unión a la proteína viral Rev cuando ésta se encuentra en bajas concentraciones, sugiriendo que los cambios nucleotídicos que afectan a la formación del aminoácido 45 de gp41 juegan un papel en la unión a Rev. No obstante, la capacidad de transporte al citoplasma de estos RRE no está afectada. Por lo tanto, alteraciones en las estructuras secundarias predictivas a partir de secuencias nucleotídicas no necesariamente implican impactos funcionales y la mutación L45M tampoco se incorpora como mutación secundaria debido a la restauración de las funciones del RRE. Como es importante caracterizar funcionalmente Envs derivadas de pacientes para estudiar su patogenicidad, establecimos una metodología completa basándonos en el papel principal de la subunidad gp41. Los resultados demostraron que la línea celular efectora es esencial para optimizar la sensibilidad de los ensayos. La línea celular 293T debería utilizarse para experimentos de fusión y la HeLa per analizar parámetros de citopaticidad. Estudios clínicos habían sugerido que virus que contenían la mutación V38A y el polimorfismo viral N140I estaban asociados a una fallo virológico y beneficios inmunológicos del paciente debido a que eran menos patogénicos. Para entender estos datos discordantes analizamos Envs derivadas de pacientes y vimos que cuando éstas tenían los cambios V38A-N140I tenían menos capacidad para matar células diana de forma individual pese a no tener alterada su capacidad fusogénica. Estos datos remarcan la importancia del contexto de la Env y el papel central de gp41 en la patogénesis del VIH-1.

ABBREVIATIONS

AIDS	Acquired Immunodeficiency Syndrome
APC	Antigen presenting cell
bp	Base pairs
C1-C5	Constant domains 1-5 of gp120
CA	HIV capsid protein (p24)
CCR5	Chemokine receptor 5
CXCR4	CXC Chemokine receptor 4
CT	Cytoplasmic tail of gp41
DDAO	Dichloro-DimethylAcridin-One
DiI	1,1'-dioctadecyl-3,3',3'-tetramethylindocarbocyanine perchlorate
DMSO	Dimethyl sulfoxide
DNA	Deoxyribonucleic acid
EDTA	Ethylenediaminetetraacetic acid
EMSA	Electrophoretic mobility shift assay
Env	HIV Envelope glycoprotein (Envs in plural)
F primer	Forward primer
FACS	Flow cytometry , acronym from Beckton Dickinson
FP	Fusion peptide of gp41
FSC	Forward Scatter
GALT	Gut-associated lymphoid tissue
GDP	Guanosine diphosphate
GI	Gastrointestinal
HAART	Highly Active Antiretroviral Therapy
HIV	Human Immunodeficiency Virus
HIV-1	Human Immunodeficiency Virus type 1
HR1/2	Heptad repeats 1/2 of gp41
IN	HIV Integrase enzyme
kb	Kilo-bases

LTR	Long terminal repeat
MA	HIV Matrix protein (p17)
min	Minutes
MPER	Membrane proximal external region
mRNA	Messenger RNA
NC	HIV Nucleocapsid (p7)
NES	Nuclear export signal
NIH	National institute of health
NIH ARRRP	NIH AIDS Research and Reference Reagent Program
NLS	Nuclear localization signal
nm	nanometers
nt	Nucleotide
PBS	Phosphate buffered saline
PCR	Polymerase chain reaction
PR	HIV Protease
PROT	Protein
R primer	Reverse primer
R5	With tropism R5
R5-tropic	With tropism R5
R5X4	With tropism X4 and R5
RBD	RNA binding domain
Rev	Regulator of virion protein expression
RFI	Relative fluorescence intensity
RLU	Relative Luminiscence Units
RNA	Ribonucleic acid
RRE	Rev responsive element (RREs in plural)
RT	HIV reverse transcriptase enzyme
Sec	Seconds
SHAPE	Selective 2'-hydroxyl acylation analyzed by primer extension
SSC	Side scatter

Tat	Trans-activator of transcription
TCR	T-cell receptor
TMD	Transmembrane domain of gp41
V1-V5	Variable domains 1-5
VS	Virological synapse
X4	With tropism X4
X4-tropic	With tropism X4

TABLE OF CONTENTS

SUMMARY.....	I
RESUM	III
RESUMEN.....	V
INTRODUCTION.....	15
1.- HISTORY	17
2.- DIVERSITY AND ORIGINS	17
3.- HIV-1	18
3.1.- <i>Morphology</i>	18
3.2.- <i>Genome</i>	19
3.3.- <i>Replication cycle of HIV-1 and antiretroviral drugs</i>	20
3.3.1.- Virus Entry	20
3.3.2.- Uncoating of the capsid core, reverse transcription, nuclear import and integration.....	20
3.3.3.- Transcription and translation.....	20
3.3.4.- Assembly, budding and proteolytic maturation	22
4.- mRNA TRANSCRIPTION AND REGULATION.....	23
5.- THE ESSENTIAL ROLE OF REV-RRE IN HIV-1 mRNA NUCLEAR EXPORT ...	27
5.1.- <i>Rev</i>	27
5.2.- <i>The Rev responsive element (RRE) and its interaction with Rev</i>	27
6.- IMMUNOPATHOGENESIS OF HIV-1 INFECTION	30
6.1.- <i>Viral receptors and tropisms</i>	30
6.2.- <i>Phases of HIV-1 infection</i>	31
6.2.1.- Acute phase	31
6.2.2.- Chronic phase.....	31
6.3.- <i>Envelope glycoprotein (Env)</i>	33
6.3.1.- Synthesis	33
6.3.2.- Structure	33
6.3.2.1.- Functionally relevant sequences of the gp160 polyproteins.....	33

6.3.2.2.- Quaternary structure of the Env trimers	34
6.3.3.- Entry process	35
6.3.4.- Env-mediated pathogenesis	38
6.3.4.1.- Soluble gp120 subunits	38
6.3.4.2.-Envs expressed on the surface of HIV-1 and infected cells..	38
6.3.5.- Fusion inhibitor T-20 (Enfuvirtide)	41
6.3.5.1.- Treatment with T-20	41
6.3.5.2.- T-20 resistance.....	42
HYPOTHESES & OBJECTIVES.....	47
MATERIALS & METHODS	51
1.- Reagents	53
1.1.- <i>Antiretroviral Drugs</i>	53
1.2.- <i>Antibodies</i>	53
1.3.- <i>Plasmids</i>	53
1.4.- <i>Membrane and cell trackers</i>	53
1.5.- <i>Other reagents</i>	53
2.- Cells.....	54
2.1.- <i>Cell lines</i>	54
2.1.1.- Adherent cells.....	54
2.1.2.- Suspension cells	54
2.2.- <i>Primary cells</i>	55
3.- Patients	55
4.- Plasmid constructions	56
4.1.- <i>Full-length Env-expressing plasmids</i>	56
4.2.- <i>Plasmids expressing Hybrid-Envs</i>	58
4.3.- <i>RRE-expressing plasmids for in vitro RNA production</i>	59
4.4.- <i>RRE-expressing plasmids to measure RNA transport</i>	60
4.5.- <i>Site-directed mutants</i>	61
5.- Secondary structure model analysis for RRE RNAs.....	63
6.- Rev binding assays	63
7.- Rev exporting assays.....	63
8.- HeLa and 293T transfections: Env-expressing cells.....	64

9.- Quantification of the Env expression	65
9.1.- <i>Flow cytometry</i>	65
9.2.- <i>Western Blot</i>	65
10.- Cell-to-Cell fusion assays.....	66
11.- Envelope-induced cytopathicity in CD4 ⁺ T cells: absolute cell loss and bystander apoptosis	66
12.- Hemifusion assay	66
13.- Statistical analysis	67
RESULTS	69
CHAPTER 1.-Predicted structures and functional evaluations of patient-derived Rev responsive elements (RRE)	71
1.- <i>Prediction of the patient-derived RRE secondary structures</i>	75
2.- <i>Analyses of the RRE functions</i>	82
2.1.- RRE-Rev binding assay	82
2.2.- Rev-dependent RNA transport assay	84
3.- <i>Sequences of the Rev proteins</i>	85
CHAPTER 2.-Methodological approach to study the cytopathicity of patient-derived HIV-1 envelope glycoproteins	89
1.- <i>Plasmids expressing hybrid Envs</i>	93
2.- <i>Cell lines used to transfect hybrid-Env expressing plasmids</i>	93
3.- <i>Cell surface expression of HIV-1 hybrid-Env glycoproteins</i>	93
4.- <i>Analysis of envelope fusogenicity</i>	96
5.- <i>Quantification of the Env-induced cytopathicity in CD4⁺ T cells</i>	101
5.1.- Analysis of Env-induced bystander apoptosis.....	101
5.2.- Analysis of the Env-induced absolute loss of CD4 ⁺ cells.....	104
6.- <i>Analysis of the Env-induced hemifusion activity</i>	104
CHAPTER 3.-Pathogenicity of patient-derived gp41 glycoproteins with specific changes in HR1 and HR2.....	107
1.- <i>Patients and plasmids expressing hybrid Envelopes</i>	111
2.- <i>Cell surface expression of HIV-1 hybrid-Env glycoproteins</i>	116
3.- <i>Analysis of the Env protein fusogenicity</i>	118
4.- <i>Quantification of Env-induced absolute loss of CD4⁺ T cells</i>	120

5.- <i>Analysis of Env-induced bystander apoptosis</i>	120
DISCUSSION & PERSPECTIVES	123
CONCLUSIONS	141
PUBLISHED ARTICLES	145
REFERENCES	149
ACKNOWLEDGMENTS	165

INTRODUCTION

1.- History

Lots of efforts have been done to characterize the causative agent of the Acquired Immunodeficiency Syndrome (AIDS) since the first detected cases in 1981 [2]. Its first isolation in 1983 [3], further confirmed by other research groups [4,5], identified the infective agent as a novel human retrovirus, which later was officially designated as the Human Immunodeficiency Virus (HIV) by the International Committee on the Taxonomy of Viruses [6]. The five identified cases in Los Angeles in 1981 raised to 33.3 million cases estimated worldwide in 2010, according to the last report of the Joint United Nations Program on HIV/AIDS [7], converting HIV as one of the major threatening diseases known by mankind.

2.- Diversity and origins

HIV is a Lentivirus that belongs to the Retrovirus family and can be divided into two different types: the worldwide predominant HIV-1 and the HIV-2 [8], which is mainly concentrated in West Africa. HIV-1 is further subdivided into 3 distinct groups and 11 different clades. Phylogenetic analyses have identified the M group as the major responsible for the epidemic, and within this group the sub-type B is the clade that infects the majority of people with AIDS in America, Europe, Asia and Australia [9].

HIV is thought to have originated through a cross-species transmission (zoonosis) of the Simian Immunodeficiency Virus (SIV). The three different groups of HIV-1 are thought to have arisen as a consequence of independent transmissions from a subspecies of Chimpanzee (*Pan troglodytes troglodytes*) [10], being estimated that the founder virus of the M group might have originated somewhere between 1915 and 1941, as predicted by genetic divergence models [11]. However, HIV-2 is thought to have been transmitted from Sooty mangabeys (*Cercocebus atys*) [12], which is a species of African primate that is endemic of West Africa.

Introduction

3.- HIV-1

HIV-1 infects a variety of cells of the immune system, including CD4⁺ T lymphocytes, macrophages and dendritic cells [13]. This infection is characterized by a profound depression of protective immunity and the appearance of opportunistic infections, malignant tumors and central nervous system degeneration, which ultimately may lead to AIDS. HIV-1 is transmitted by sexual contact, mother-to-child (in utero, during delivery or through breast milk) and through blood inoculations.

3.1.- Morphology

The mature HIV-1 virions have spherical shapes with average diameters of 110 nm and consist of an exterior lipid bilayer and a conical capsid core in which the viral genome is located (**Figure 1**).

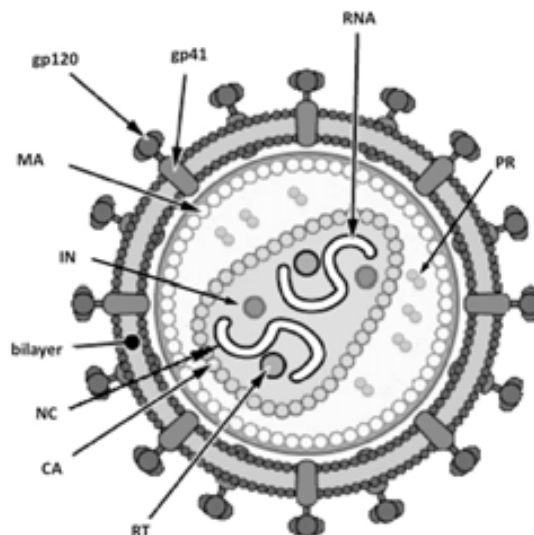


Figure 1: Morphology of an HIV-1 virion. Schematic representation of a mature virion displaying its genomic RNA and the following viral proteins: Envelope (gp120 and gp41); MA: Matrix; CA: Structural Capsid; NC: Nucleocapsid; RT: Reverse Transcriptase; PR: Protease; IN: Integrase. [9]

The surface of the virions contains an average of 14 envelope glycoproteins (Env) [14], each of them formed by two different subunits: the surface glycoprotein (gp120, SU) and the transmembrane glycoprotein (gp41, TM), which is anchored into the viral membrane. Besides, internally, the viral membrane is coated with a shell formed with approximately 2000 copies of the matrix protein (MA, p17).

The conical capsid core is formed by 2000 copies of the capsid protein (CA, p24) and is situated in the center of the virus particle. HIV genomic RNA is found encapsidated inside this core as two copies of single-stranded RNA (diploid genome) and stabilized with 2000 copies of the nucleocapsid protein (NC, p7). The viral enzymes: protease (PR, p11), reverse transcriptase (RT, p51 and p66) and integrase (IN, p32); the accessory proteins: Nef, Vif and Vpr; and p6, which help the incorporation of Vpr into the viral particles; are also thought to be packed into the capsid core (**Figure 1**). The regulatory proteins Rev and Tat and the accessory protein Vpu are not packed into the virions although they have functions in the infected cell [15].

3.2.- Genome

The HIV-1 genome encodes nine open reading frames in a ~9-kb molecule of RNA delimited by the 5' and 3' LTRs (Long terminal Repeats), which serve some structural and regulatory functions (**Figure 2**). The three major polyproteins encoded are Gag, Gag-Pol and Env. The structural components: MA, CA, NC and p6 are derived from Gag polyproteins and the three HIV-1 enzymes, PR, RT and IN from the Gag-Pol polyprotein. The gp120 and gp41 glycoproteins are encoded by the Env polyproteins. The rest of the genes encode for the regulatory proteins, Tat and Rev, and the accessory proteins Vif, Vpr, Vpu and Nef.

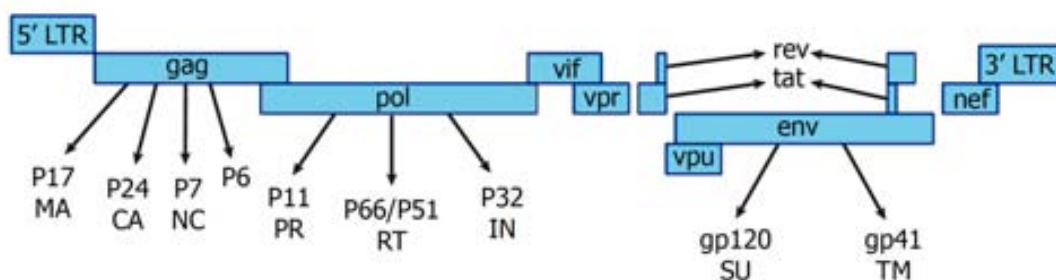


Figure 2: Schematic structure of the HIV-1 genome showing the 9 open reading frames (in boxes) encoding the main viral proteins and delimited by the LTRs. Figure adapted from [16].

3.3.- *Replication cycle of HIV-1 and antiretroviral drugs*

The sequential steps that represent the life cycle of HIV-1, which span from the initial infection of a host cell to the viral replication and release of the new virion, and the targets for antiviral intervention are described below (**Figure 3**):

3.3.1.- *Virus Entry*

HIV-1 particles bind to target cells through the Envs. These glycoproteins are embedded into the viral membrane and are able to bind to specific receptors and coreceptors located on the surface of the target cells. These interactions lead to conformational changes of the Env and enable the fusion between the viral and the target cell membranes. The merge of both membranes triggers the release of the capsid core into the host cell cytoplasm. This first step in the replication cycle of HIV-1 can be inhibited by coreceptor antagonists, such as the CCR5 antagonist Maraviroc, and by fusion inhibitors, such as Enfuvirtide (T-20).

3.3.2.- *Uncoating of the capsid core, reverse transcription, nuclear import and integration.*

The virion core is then uncoated and the viral proteins and the genomic RNA are released to the cytoplasm. The single-stranded RNA is retro-transcribed by the RT into a double-stranded DNA. Then, is helped to enter into the nucleus by binding to Vpr, MA [17] and host proteins. The RT process can be inhibited using non-nucleoside reverse transcriptase inhibitors (NNRTIs) and nucleoside reverse transcriptase inhibitors (NRTIs). Finally, the random integration into the host genome is catalyzed by IN and LTRs, generating the integrated form of HIV, called provirus. Integrase inhibitors can inhibit this latter step.

3.3.3.- *Transcription and translation*

Initiation of the HIV gene transcription is associated with the activation state of the cell. Therefore, the provirus may remain transcriptionally inactive if the cell is not activated, producing few or no new viral proteins, and hence, virions. Conditions that restrict transcription initiation may induce that these proviruses stay latent and that remain invisible for the immune system. If the cells are stimulated with antigens, cytokines or

Introduction

other cellular factors [19] the expression of the viral transcripts begins. The generated transcripts will be exported to the cytoplasm where they will be translated into viral proteins (*see section 4*).

3.3.4.- Assembly, budding and proteolytic maturation

The viruses assemble into immature virions after recruiting the newly produced viral proteins and two copies of the viral genomic RNA (**Figure 4A and 4C**). A layer of Gag proteins is associated with the inner viral membrane and upon budding from the plasma membrane immature particles dramatically rearrange to form mature, infectious virions (**Figure 4B and 4D**). This is done through the activation of the PR, which cleaves Gag to generate MA, CA, NC and p6 [20]. Mature virions then are ready to initiate a new viral cycle by infecting new target cells. An infected cell produces many virions, each one capable of infecting a new cell, thereby amplifying the infectious cycle. Protease inhibitors can block the catalytic activity of the PR, allowing only the production of immature noninfectious viral particles [21].

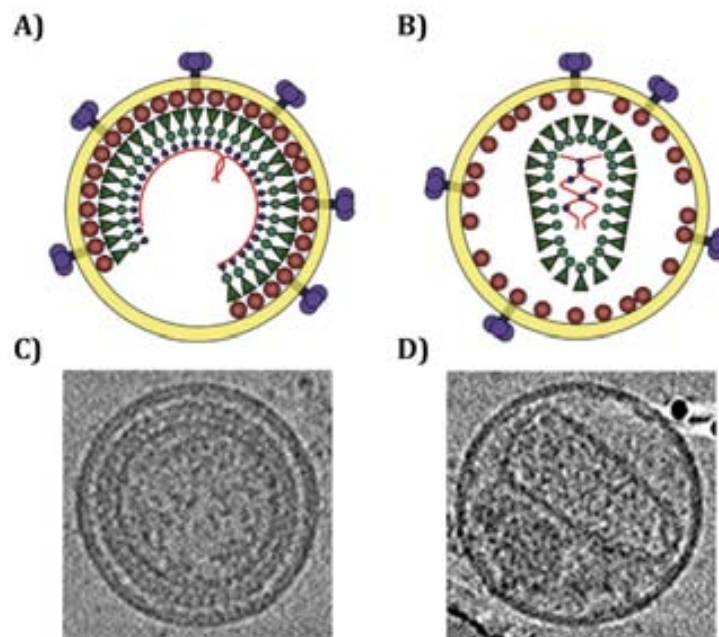


Figure 4: HIV-1 virions. Schematic representations and images obtained by electron cryotomography of immature (**A-C**) and mature (**B-D**) HIV-1 virions. [18]

4.- mRNA transcription and regulation

The HIV-1 primary transcript contains multiple splice donors (5' splice sites) and splice acceptors (3' splice sites) that can be processed to yield more than 40 different spliced mRNAs species in infected cells [22,23](**Figure 5**). Many of the mRNAs are polycistronic; i.e., they contain different open reading frames that encode for more than one protein. HIV-1 mRNAs fall into three size classes: an *unspliced mRNA*, which is the 9-kb primary transcript that generates the Gag and Gag-Pol precursor proteins or that is used to be directly packaged into virions to serve as the genomic RNA; *Incompletely spliced mRNAs (singly spliced)*, which are produced after using the splice donor site located nearest the 5' end of the HIV RNA genome in combination with any of the splice acceptors located in the central region of the virus. These heterogeneous mRNAs are 4- to 5-kb long and can potentially express Env, Vif, Vpu, Vpr, and the single-exon form of Tat; and *fully spliced mRNAs*, which have also spliced out the fragment between the splice donor site located nearest the 3' end of the transcript and the last splice acceptor of HIV and have the potential to express Rev, Nef, and the two-exon form of Tat. These heterogeneous mRNAs do not require the action of the Rev protein like the other two types to being exported to the cytoplasm, and are about 1.8-kb long.

Introduction

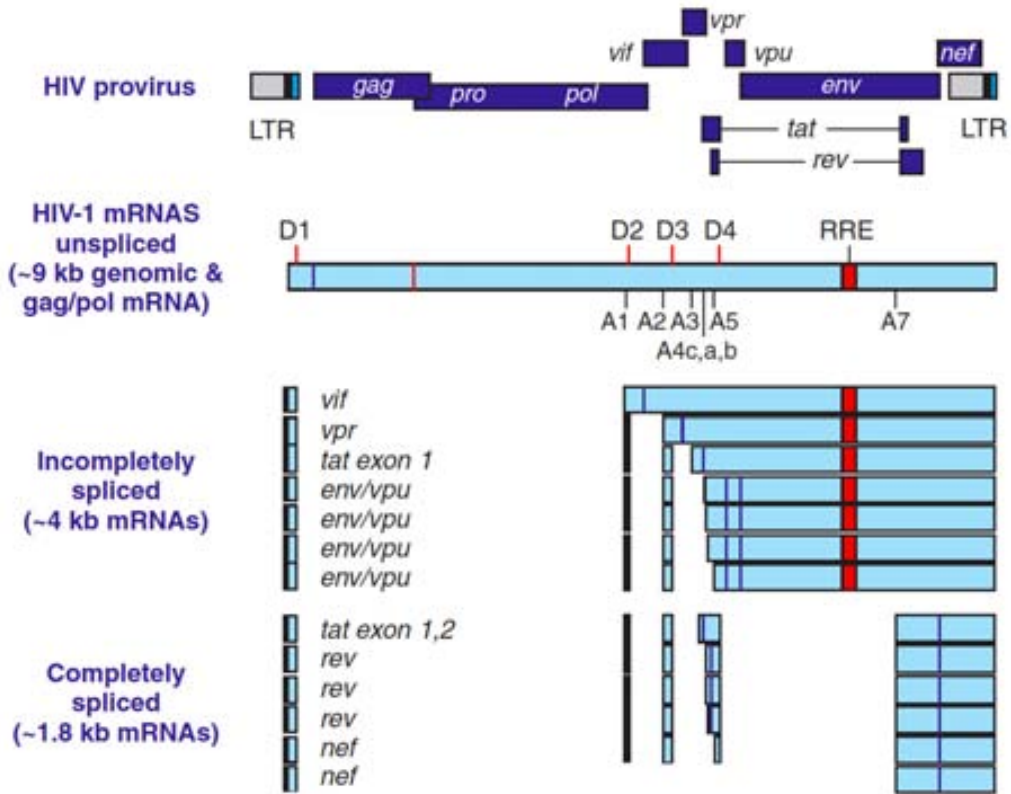


Figure 5: Locations of splice sites and representation of the main viral transcripts. Schematic diagram of the HIV-1 genome and the main viral transcripts, being marked in a red rectangle the RRE. The HIV-1 genes that are encoded in each transcript are shown on their left side. [22]

The HIV-1 gene transcription is highly regulated and the HIV-1 mRNA expression can be divided into two phases (**Figure 6**): [22]:

- *Early phase of mRNA expression*

The 5' long terminal repeat acts as the HIV-1 viral promoter. Normally, intron-containing mRNAs are completely spliced before they can exit the nucleus. This regulation is essential because it prevents the translation of intronic sequences contained in partially spliced mRNAs. For this reason, only the short completely spliced mRNAs that are encoding the viral regulatory proteins: Tat, Rev and Nef, are exported outside the nucleus by an endogenous cellular pathway (**Figure 3 and 6A**). Subsequently, the encoded regulatory proteins are imported again into the nucleus through interactions with cellular proteins to control the complex pattern of gene expression.

- *Late phase of mRNA expression*

At this phase, Tat promotes the transcription of the long HIV-1 mRNAs by interacting with the transactivation-response region (TAR), a secondary structure that lays downstream to the transcription initiation, to stimulate their elongation. These mRNA species correspond to the unspliced and singly spliced transcripts, which encode for the rest of the viral proteins. Both mRNAs have a highly structured RNA element situated in the *env* gene and referred to as the Rev-responsive element (RRE) that allows their nuclear export by Rev [24] (**Figure 6B**). The Rev protein binds to the RRE and directs the export of these unconventional viral mRNAs to bypass the normal "check point" of RNA splicing. Certain threshold levels of Rev are necessary to export intron-containing HIV mRNAs, explaining why these transcripts encode the viral late gene products. Once in the cytoplasm, viral transcripts will be translated into the viral proteins and new viral particles will be produced.

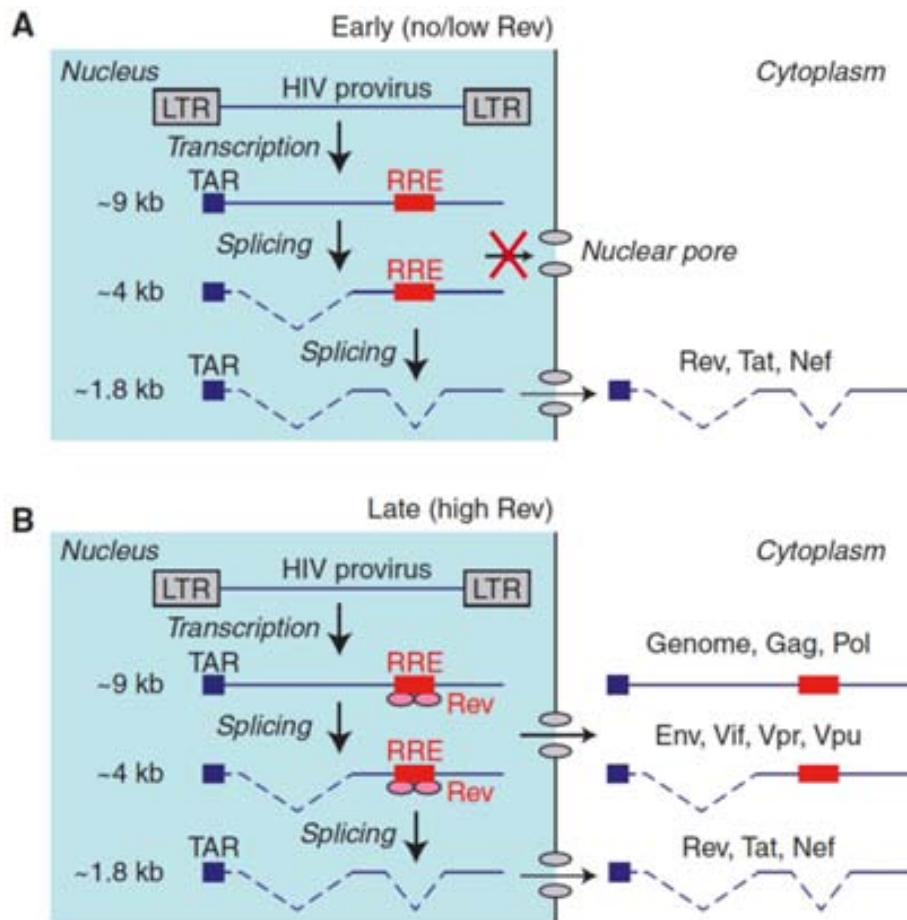


Figure 6: Early (A) and late (B) phases of HIV-1 mRNA expression. In the early phase only the fully spliced mRNAs are able to reach the cytoplasm and produce the Rev, Tat and Nef viral proteins. Later, when the nuclear concentration of Rev protein expressed in the previous phase reaches a certain threshold, the long mRNA transcripts are able to being exported by these Rev proteins upon binding to the RREs. TAR: transactivation-response region; RRE: Rev responsive element. [22]

5.- The essential role of Rev-RRE in HIV-1 mRNA nuclear export

As noted above, HIV-1 encodes six regulatory and/or accessory genes in addition to *gag*, *pol*, and *env*. One of the first to be identified was *tat*, which encodes the viral protein Tat, whose function is to potently trans-activate the expression of all viral genes [25,26]. Disruptions of neighboring sequences of the *tat* gene were shown to give rise to viruses that still expressed Tat but were unable to express Gag, Pol, or Env and were therefore unable to replicate [27,28]. A gene that overlaps with *tat* was immediately recognized and in accordance with its initially described function, this essential gene was termed *rev* (an acronym for regulator of expression of virion proteins).

5.1.- Rev

HIV-1 Rev protein is encoded by two exons and is produced from fully spliced mRNAs. This sequence-specific RNA binding protein consists in 116 amino acids and accumulates within the nuclei of infected cells [29] to induce the transition from the early to the late phase of HIV gene expression [30]. Rev has three main functional domains [1] (**Figure 7A**): an arginine-rich sequence that serves as nuclear localization signal (NLS) and as RNA-binding domain (RBD) [31]; a multimerization domain [32,33]; and a leucine-rich effector domain, which works as a nuclear export signal (NES) [34,35].

Once Rev is translated in the cytoplasm, it binds to the nuclear import factor, importin- β , through its NLS and it is translocated into the nucleus, where an interaction with the molecule Ran-GTP will disassemble the Rev/Importin- β complex (**Figure 7D**). Because the NLS domain also functions as the RBD, the dissociation of the complex results in Rev becoming available for binding to the RRE [24]. Rev is absolutely required for HIV-1 replication: proviruses that lack Rev function are transcriptionally active but do not express viral late genes and thus do not produce virions.

5.2.- The Rev responsive element (RRE) and its interaction with Rev

The RRE is a large RNA stem-loop structure of ~350 nt [1,36] (nts 7710-8061) that resides within the *env* gene (expands from the end of gp120 to the loop of gp41) and thus, is present in all ~9-kb and ~4-kb HIV-1 mRNAs (**Figure 5**). This RRE is well conserved across all subtypes of the major group M, highlighting its importance in HIV-

Introduction

1 pathogenesis. This element is characterized by a highly branched secondary structure with multiple stem-loops and bulges that are important for the recognition and binding of the viral regulatory Rev protein, which allows the exportation of the non-completely spliced viral transcripts outside the nucleus [37-39]) (**Figure 7B**).

Specific sequences within the RRE that determine Rev responsiveness are surprisingly limited. In fact, recognition by Rev appears to be controlled by the presence of a single high-affinity binding site. This fragment contains a "bubble" structure constituted by a non-Watson-Crick G-G base pair [40]), known as the Rev high affinity binding site, which is located at the base of the stem loop IIB [41] (**Figure 7B**). Following this RRE-Rev first interaction in the stem IIB, a conformational change occurs allowing the binding of additional Rev monomers that oligomerize on the RRE along stems IIA and I [31,42-50], a fact that is directly correlated with its export competence [33,51-53]. Rev assemble cooperatively on the RRE in a symmetrical tail-to-tail and head-to-head protein-protein interactions [48], which was confirmed by the crystal structure obtained of a Rev dimer [54]. This high stoichiometry of Rev monomers bound on the RRE turns these complexes into export-competent [51]. The ratio Rev:RNA for these complexes is variable between the different reports, although the most accurate appears to be 4 [50,55]. However other assays have also showed ratios Rev:RNA of 8 [44] or 13 [52].

Subsequently, these Rev/RRE complexes can interact with Crm1 (exportin 1) through the NES domains of the Rev proteins (**Figure 7C**) and can be transported to the cytoplasm through the nuclear pore complexes (**Figure 7D**). There, the complex is destabilized and all factors release from the RRE. Then, transported mRNAs can be translated or directly assembled into nascent virions; on the other hand, Rev proteins are able to reenter into the nucleus by binding other importin- β and reenter into the nucleus [24,56].

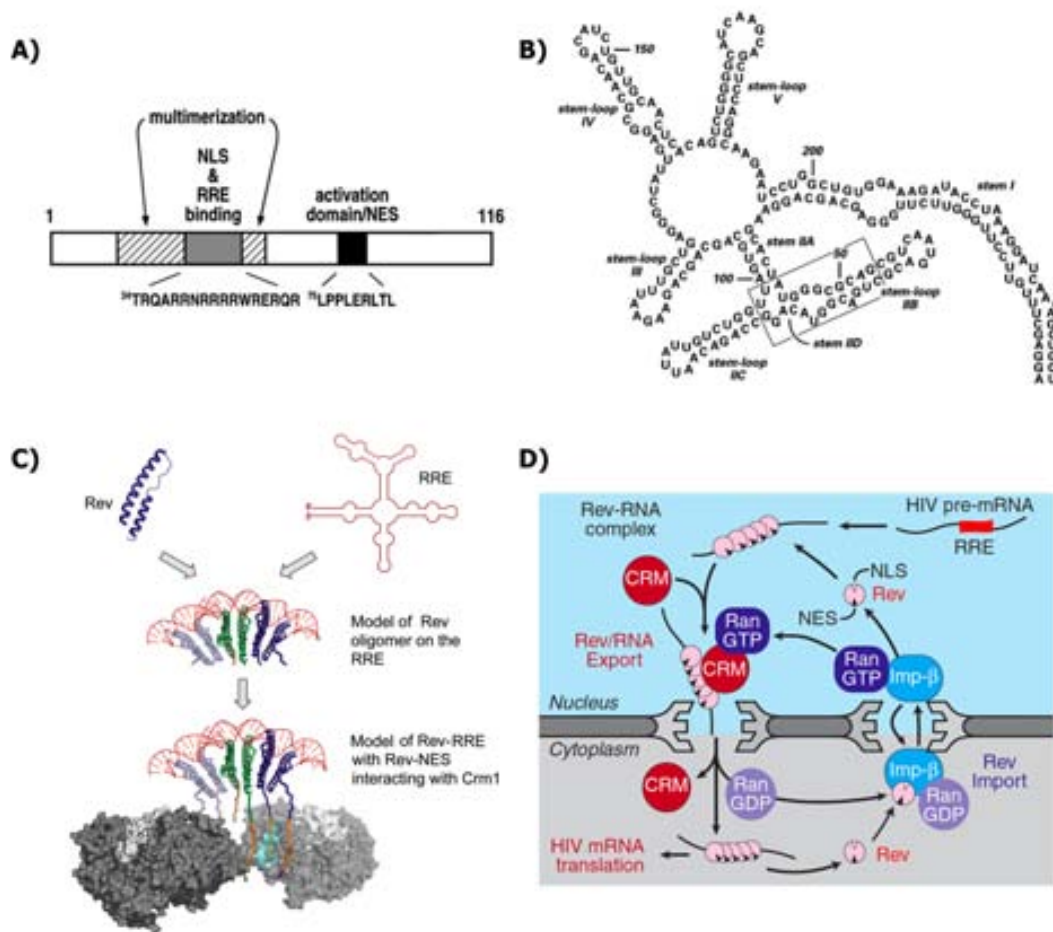


Figure 7: Rev protein, RRE and their interactions. A) Schematic representation of the main domains present in the regulatory Rev protein. Amino acid sequences of the regions rich in Arginines (R) and Leucines (L) from HIV-1_{HXB} are shown; NLS: Nuclear Localization Signal NES; Nuclear Export Signal. **B)** Predicted secondary structure of the partial RRE of HIV-1_{HXB}. The structure shows the different stems and loops. The high-affinity Rev binding site is boxed. [24] **C)** Oligomerization of Rev proteins along the RRE and their binding to Crm1. Subsequent binding of this complex to Ran-GTP allows the exportation of the RNA to the cytoplasm. [53] **D)** Rev-exporting cycle of viral mRNAs containing the RRE structure (unspliced and singly spliced mRNAs). [22]; RRE: Rev Responsive Element;

6.- Immunopathogenesis of HIV-1 infection

6.1.- Viral receptors and tropisms

The **CD4** cell surface receptor is mainly expressed in CD4⁺ T cells, but also at low levels in monocytes, macrophages, dendritic cells and microglia in the central nervous system. This CD4 receptor molecule is the main receptor of HIV and is required for productive HIV infection. The first interaction between the gp120 subunit from the Env glycoprotein and the CD4 receptor promotes conformational changes that allow the interaction of gp120 with the viral coreceptor, which in turn will induce an additional refolding of the Env structure to promote the gp41-mediated fusion [57,58].

The **chemokine receptors** CCR5 and the CXCR4 are the main coreceptors involved in HIV-1 entry. Depending on the amino acid composition of the Env, the different HIV-1 strains will use CCR5, CXCR4 or both to enter into target cells. According to the capacity to use each of the coreceptors, HIV strains can be referred as X4 (X4-tropic) if they only infect cells that express CXCR4; R5 (R5-tropic) if they only use CCR5; or R5X4 (dual tropic) if they can use both CCR5 and CXCR4, although one co-receptor may be favored. Different mixtures of R5, X4 and R5X4 virus strains may be present in HIV-infected individuals and in these cases the virus populations are described as being mixed tropic. The viral tropism is also a marker of disease status. The HIV-1 population in infected individuals is mainly composed of R5-tropic strains at primary stages of HIV-1 infection, while X4-using strains appear at the late stages and when there is a sharp decline in CD4⁺ T cell counts. However, it is not clear if this is a consequence of disease progression and immunological deterioration, or its cause.

6.2.- Phases of HIV-1 infection

The amount of T lymphocytes in the human body remains constant by homeostatic mechanisms. However, these mechanisms fail after HIV-1 infection, which induces a progressive immune deficiency caused by the loss of CD4⁺ T cells and systemic immune activation.

The HIV infection can be divided in two main phases:

6.2.1.- Acute phase

The infection of HIV-1 in a new host displays a characteristic initial peak of viraemia followed by a decline of the virus replication in peripheral blood because of the emergence of HIV-specific humoral and cell-mediated immune responses. Neutralizing antibodies generally develop within the first 6 months after the initial HIV infection [59]. In this acute phase there is a dramatic loss of the CD4⁺ T cells that reside in mucosal tissues during this primary HIV-1 infection, especially in the gastrointestinal (GI) tract, and this depletion is correlated with the high levels of viraemia that is observed before the onset of antiviral immune response. Contrasting to the gradual depletion of the CD4⁺ T cells observed in peripheral blood, 90% of the CD4⁺ T lymphocytes in the gut-associated lymphoid tissue (GALT) are destroyed independently of the transmission route [60] during the first 2 weeks after infection [61,62].

6.2.2.- Chronic phase

The emergence of potent, but ultimately ineffective, cell-mediated and humoral responses to HIV leads to the chronic phase of infection, which is characterized by partial control of viral replication, chronic immune activation, progressive decline of the naïve and memory T-cell pool, and systemic CD4⁺ T-cell depletion in the periphery. This impairment in the homeostasis is partially driven by a reduction in the input of naïve CD4⁺ T cells produced in the thymus and spilled into the peripheral naïve T cell pool [63]. The thymus is the primary organ of thymopoiesis and is severely damaged upon HIV infection. Then, when the individuals infected with HIV-1 develop AIDS, this decline is accelerated. Currently, the loss of CD4⁺ T cells can be partially reversed by successful antiretroviral treatments, although unfortunately these drugs are not able to reach the level of a cure.

Introduction

The mechanism used by HIV-1 to massively destroy CD4⁺ T cells, remains unknown. The cell depletion can be produced by virus-mediated cytolysis, elimination of infected cells through cellular responses triggered by the immune system, syncytium formation or an indirect killing of bystander cells through apoptosis. In the GALT, several mechanisms have been described as responsible for the massive loss of cells. Mattapallil et al. showed that the cellular depletion was mediated by a direct cytopathic effect executed by the virus, because a 60% of the CD4⁺ T cells of the tissue were infected, while Li's study showed that only a 7% of the CD4⁺ T lymphocytes were infected and that majority of the lymphocytes were dying through apoptosis.

Apoptosis was proposed as a potential mechanism of destruction of T cells in individuals infected with HIV-1 in 1991. Since that link was described, the study of the mechanisms that HIV-1 uses to induce apoptosis has been in a key field of basic research. Multiple mechanisms have been postulated that would contribute to the bystander cell death: a mechanism associated with cellular factors such as the tumor necrosis factor (TNF), Fas and TRAIL ligands, or associated with soluble viral factors like the proteins: Tat, Vpr and Nef, which would be released by the infected cells [64]. In addition, another mechanism of indirect cell death has recently been described, the abortive infection. This mechanism is based on the fact that naïve CD4⁺ T cells in tissue are refractory to productive HIV infection [65]. The viruses can enter into these cells but are not able to complete the reverse transcription and hence, prematurely finishes the transcription and abort their infection [66]. Accumulation of these incomplete reverse transcripts in the cytoplasm of the uninfected cell finally leads to their death through proapoptotic and proinflammatory responses [67]. However, over the past few years it has been established that one of the main determinants of HIV-1-induced apoptosis is the viral Envelope (Env) glycoprotein [68,69].

6.3.- Envelope glycoprotein (Env)

Envelope glycoproteins are expressed on the surface of HIV-1 virions and on the plasma membrane of infected cells. Although the function of the HIV-1 envelope glycoprotein complex (gp120/gp41, Env) is to facilitate the entry of the viral nucleocapsid into the target cell by mediating fusion of the viral and cellular membranes, it has also been shown that this glycoprotein plays a crucial role in the depletion of CD4⁺ cells.

6.3.1.- *Synthesis*

Envs are synthesized as polyprotein precursors (gp160) on the rough endoplasmic reticulum (RER) [70], where they are glycosylated and trafficked to the Golgi complex. In the secretory pathway the glycosylated gp160 acquire further complex modifications and are proteolytically cleaved by cellular furin or furin-like proteases, yielding the mature surface glycoprotein (gp120) and the transmembrane glycoprotein (gp41). Both subunits remain associated by non-covalent interactions and are anchored to the membrane through gp41. The Env, consistent of both gp41 and gp120 subunits, are bound by non-covalent interactions and oligomerize in homotrimers to form the Env spikes. Part of the Env spikes when reach the plasma membrane are rapidly recycled via endocytosis, which contribute to the relatively low incorporation of Env into the virus particles and helps HIV-1 evade the host immune response [70].

6.3.2.- *Structure*

6.3.2.1.- *Functionally relevant sequences of the gp160 polyproteins*

Gp120 is characterized by a high degree of genetic variability between HIV-1 isolates. However, the amino acid changes are not distributed homogenously along the whole subunit. Amino acid alignments of the viral isolates led to the identification of 5 variable protein domains (V1-V5) that are separated with 5 constant segments (C1-C5) [71,72] (**Figure 8**).

Gp41 is organized into three major domains: an extracellular domain (ectodomain), a transmembrane domain (TMD) and an intracellular domain (endodomain or cytoplasmic tail, CT) (**Figure 8**). The ectodomain consists in different subdomains: an hydrophobic region known as the fusion peptide (FP), which is located at the N-terminus; two hydrophobic regions that form α -helical coiled-coil structures referred to

Introduction

as the heptad-repeat regions HR1 and HR2 (N- and C-heptad repeat, respectively; also designated as NHR and CHR) that are separated by a loop region, which harbors two importantly conserved cysteines [73]; and the membrane-proximal external region (MPER).

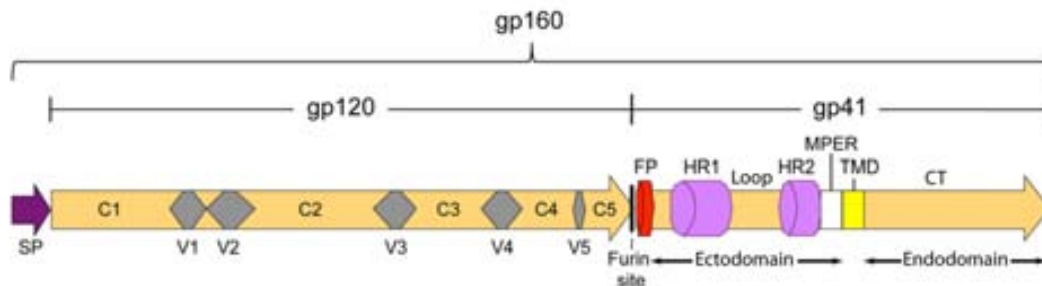


Figure 8: Functionally relevant domains of the gp160 polyprotein (gp120 and gp41). SP: Signal peptide; C1-C5: Constant domains; V1-V5: Variable domains; FP: Fusion peptide; HR1/2: Heptad repeats 1 and 2; MPER: Membrane-proximal external region; TMD: Transmembrane domain; CT: Cytoplasmic tail. Adapted from [70].

6.3.2.2.- Quaternary structure of the Env trimers

Gp120 is the subunit that enables host tropism and gp41 is the responsible for the fusion development. The formation of the tertiary structure of the Env is maintained through 9 important disulfide bonds in gp120 that are formed by 18 covalently bound cysteine residues [74]. The five variable domains that are encoded by gp120 are located near the surface of the molecule and are heavily glycosylated. These Env glycosylations, which account for half of the molecular mass of gp120 [75], mask Env from immune recognition [76,77] by creating a “glycan shield” that prevents recognition by most antibodies [78], help Env to correctly fold [79] and help virions to bind host cell membranes [79,80]. The Env evolved to admit a number of sequence variations and to keep key functional domains hidden from host immune responses to efficiently escape. The gp41 ectodomain seems to be necessary for the trimeric oligomerization of the Envelope spikes [81] and it is also glycosylated (**Figure 9**); however, the four glycosylations located in this domain appear to be dispensable for viral replication [82]. The CT also influences multiple properties of Env, such as the incorporation into virus particles, virus infectivity, cell-surface Env expression, gp120 shedding and Env-induced fusion [70].

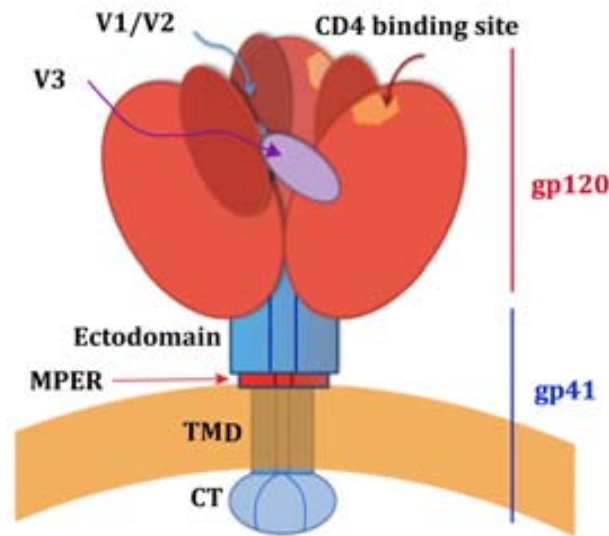


Figure 9: Schematic diagram of trimeric HIV-1 Env. Trimeric Envs are anchored into the plasma membrane through TMD of the gp41 glycoproteins. Some of the domains of gp120 are depicted in the figure as: light red (core), dark red (V1/V2 loops), purple (V3 loop) and orange (CD4 binding site). The main domains of gp41 are depicted as: light blue (Ectodomain and CT), red (MPER) and dark blue TMD. V1, V2 and V3: Variable domains; MPER: Membrane proximal region; TMD: Transmembrane domain; CT: Cytoplasmic tail. Figure adapted from [83].

6.3.3.- *Entry process*

During the entry process mediated by Env, this glycoprotein adopt three main states [84]:

- *Native (Non-fusogenic state)*

This is the native conformation. Gp41 subunits stay in the inner part of the spike and are being shield by gp120 (**Figure 9 and 10A**).

- *Extended pre-hairpin (intermediate state)*

This intermediate state is reached after the binding of gp120 to cellular receptors (**Figure 10A**). The residues of gp120 that allow the binding to the CD4 receptor are folded into proximity in the inner side of the Env tertiary structure and are located mainly in C1, C3 and C4 domains [85]. Subsequently to the interaction with this receptor, gp120 refolds and this conformational change exposes a new surface that is able to bind to the HIV-1 coreceptors [86], [87]. After coreceptor binding, gp41

Introduction

is released in an extended conformation, exposing HR1 and HR2, and inserting the FP into the membrane of the target cell (**Figure 10A** and **10B**).

○ *Hairpin (fusogenic state)*

The fusogenic ability of the Env glycoprotein is acquired when, after reaching an extended conformation, the three gp41 subunits that form the spike fold into a six-helix bundle structure, also called the core structure. This stable structure, which is essential for the fusion process, is reached when the gp41 heptad repeat domains interact with each other (HR1-HR2). The six-helix bundles help to bring the cellular and viral membranes in a sufficient close proximity to enable membrane fusion (**Figure 10A** and **10B**). Subsequent higher-order clustering of additional Envs also at the fusogenic state is needed to facilitate membrane fusion [88] (**Figure 10C**). The first fusion event that is reached is hemifusion, which is a fusion intermediate characterized by the mixing of the outer leaflets of both viral and target cell lipid bilayers without progression to fusion pore formation [89], and hence, without cytoplasmic content exchange (**Figure 10A** and **10C**). At this point, distal membrane leaflets remain separated and progression to the fusion pore formation can be stopped and reversed. The rate-limiting step of the fusion process is overcoming this hemifusion stage, because it is highly energy-demanding [90]. The productive fusion requires overpassing this hemifusion intermediate and performing a transition to a posthemifusion intermediate. If these posthemifusion intermediates are formed, then fusion can be facilitated. Triggering of these fusion pores might be done by multiple adjacent coreceptor interactions and gp41 rearrangements, which will finally irreversibly lead to the content exchange [91]. Factors that might regulate the formation of a wide fusion pore might be the number of receptors and gp120 molecules and the degree of fluidity of the target membrane [92]. Furthermore, cellular components [93], such as caveolin or tetraspanins, have been shown to modulate the ability of Env to mediate hemifusion and induce fusion by interacting with gp41 [94] and also to reduce the budding efficiency [95]. This highlights the importance of cellular factors in the process of HIV infection.

Introduction

6.3.4.- Env-mediated pathogenesis

The HIV-1 Env can induce the depletion of CD4⁺ T cells through different mechanisms depending on its presentation. Env can kill target cells when the gp120 subunits are presented dissociated in the medium or when the Env trimers are expressed on the viral surface or on the plasma membrane of infected cells.

6.3.4.1.- Soluble gp120 subunits

Soluble gp120 subunits resulting from shedding of the surface of the viral particles or infected cells are toxic to cells when they interact with the cellular coreceptors (**Figure 11A**). These dissociated gp120 induce apoptosis in a caspase-9-dependent form [97] and they also are able to downregulate CD4 receptors [98].

6.3.4.2.- Envs expressed on the surface of HIV-1 and infected cells

o Direct killing

Cell-free viruses infect target CD4⁺ T cells and induce their death in a so-called “direct killing”. HIV-1 infected cells can also mediate a “direct killing” of target cells by fusing with them via their cell-surface expressed Envs (**Figure 11C**). The joining of both membranes produces multinucleated cells, syncytia, which will die in a p53-dependent manner. A small number of reports showed multinucleated cells in *in vivo* samples [99-102], suggesting that although some small syncytia could be viable and functional [103], the vast number of multinucleated cells might be condemned to die due to genomic instability [104,105].

o Indirect killing

HIV-1 infected cells can also interact with bystander target cells without developing complete fusion. The interactions, which are gp41-dependent and stuck at the Hairpin (**Figure 10A** and dashed box of **10C**), involve the development of hemifusion processes and the death of the target cells in a single-cell manner [68,106] (**Figure 11B**). The mixing of lipids between infected and uninfected cells, which is developed by these hemifusion processes, induces the death of the target cells through a rapid apoptotic pathway that is dependent on the activation of caspase-3. The *in vivo* relevance of each of these death mechanisms remains unknown, although it has been suggested that the

bystander cell death could be playing an important role. The main reasons that support the relevance of the indirect cell killing are:

- The low amount of productively infected cells that are observed *in vivo*, which cannot account for the huge depletion obtained in CD4⁺ T cell counts [107].
- Less than 1% of the circulating viruses seem to be infectious [108,109].
- Syncytia are rarely seen *in vivo* [99-102].
- The extent of apoptosis has been correlated with AIDS progression [110].
- The extent of apoptosis and the number of apoptotic cells greatly exceeds the number of HIV-1 infected cells, confirming that not only infected cells develop apoptosis [111].
- *In situ* labeling of lymph nodes showed that apoptosis occurs mainly in bystander cells but not in productively infected cells [112], which are more resistant to apoptosis [113] due to a modulation of the mitochondrial pathway that develops apoptosis [114].

Introduction

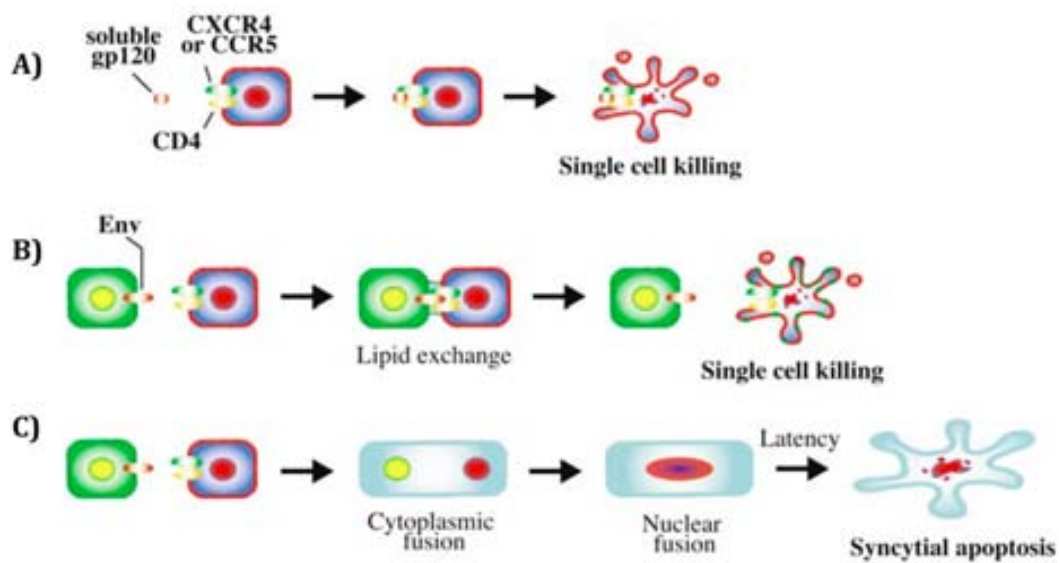


Figure 11: Mechanisms of Env-mediated pathogenesis. Soluble gp120 (A) and Env expressed on the plasma membrane of infected cells (B-C) can kill target cells upon interacting with CD4 receptors and CCR5/CXCR4 coreceptors. If the Env expressed on the effector cell is able to do a lipid exchange through hemifusion processes but the fusion pore is not completed, cells will separate and the target cell will die rapidly in a single-cell manner (B). However, if the interactions between both cells are able to induce a complete fusion pore, cytoplasmic and nuclear fusions will promote a slow killing of this multinucleated cell (C). [104]

Therefore, research focused on the characterization of the Env-mediated pathogenesis is needed to understand its importance *in vivo*. The vast majority of the studies that evaluate the role of the Env in the HIV-1 pathogenicity are using full-length Env that are derived from laboratory-adapted HIV-1 strains and the main endpoint is the quantification of the fusion capacity. Because of the central role of gp41 in mediating CD4⁺ cell death, it is important to address the pathogenesis associated to the gp41 subunit and especially, gp41 glycoproteins that are derived from patients. This would be useful in order to evaluate how changes present in gp41 glycoproteins of HIV-1 infected patients modify the pathogenesis of the Env glycoprotein. As the Env laboratory-adapted strains are more capable to developing complete fusion and syncytia, the measurements of indirect cell death for these reports would be underestimated, because of the masking effects of complete fusion processes. Furthermore, because gp41 is involved in the depletion of CD4⁺ cells by different mechanisms, it seems important to evaluate not only the fusion capacity, but also killing potential (ability to induce CD4⁺

T-cell loss or bystander death) in order to fully characterize the HIV-1 cytopathicity of patient-derived Env/gp41-glycoproteins.

6.3.5.- Fusion inhibitor T-20 (Enfuvirtide)

6.3.5.1.- Treatment with T-20

Enfuvirtide (ENF, T-20) is an HIV fusion inhibitor, the first of a novel class of antiretroviral drugs used in combination therapy for the treatment of HIV-1 infection. This drug is a 36-amino acid peptide that was designed based on the amino acid sequence of the HR2 domain of the gp41 subunit (**Figure 12A and 12B**). This peptide prevents the HR1-HR2 interaction by binding to the HR1 domain and avoids the six-helix bundle formation that are needed in the development of fusion and hemifusion processes [115-117] (**Figure 12C**). T-20 is indicated for the treatment of patients infected with HIV-1 who are multiresistant to antiretrovirals. Its administration is always in combination therapy with other drugs. The therapeutic benefits of T-20 therapy have been demonstrated by increases in CD4⁺ T cell counts and a significant reduction in HIV RNA levels [118-120], although its high cost and inconvenient dosing regimen are factors that have limited its use in clinical practice to "salvage" therapy in patients with multi-drug resistant HIV.

Introduction

6.3.5.2.- T-20 resistance

Several factors lead to the emergence of drug-resistant variants in patients infected with HIV-1 that are under the highly active antiretroviral treatment (HAART): rapid HIV-1 turnover, huge viral productions for long periods of time, high error rate or the RT, recombination events between distinct isolates, incomplete suppression of viral replication in patients under HAART, low genetic barrier of antiretroviral drugs and poor adherences to treatments [121]. Drug-resistant variants may replicate in the presence of the antiretroviral drugs and may escape from their inhibitory effect. Alteration of the environment generated upon the introduction of a new drug induces a change in the quasispecies distribution to favor viral variants with the best fitness [122]. While the predominant variants in the absence of antiretrovirals are wild type viruses (wt), in the presence of optimal drug concentrations, the main viral populations are mutants with advantages in fitness. If HAART is removed due to the presence of resistant mutants, the environment, in terms of fitness, might become better for wt viruses again. However, resistant mutants will not disappear in these conditions and will be still present, although at very low levels (minority variants). Thus, a rapid rebound of these mutant variants will be reached if the same drugs, and hence, the same environment, were introduced again.

T-20-resistant HIV-1 variants rapidly emerge under drug pressure when virus replication is not completely suppressed [123-125]. Sequence analysis of T-20-resistant viral populations revealed the acquisition of mutations within the HR1 domain at positions 36-45, which were associated with a reduction in viral infectivity, probably as a consequence of an impaired interaction between HR1 and HR2 [126,127] (**Figure 12B**). However, certain compensatory mutations within HR2 may arise and restore viral infectivity [128-131].

➤ *T-20-associated mutations correlated with immunological recovery.*

Despite virological failure, specific changes (the cluster V38A+N140I) have been associated with an increase in CD4⁺ T cell counts in patients infected with HIV-1 and treated with T-20 [132-134]. The V38A correspond to a primary mutation located in the HR1 domain of gp41, while the N140I is a viral polymorphism placed in HR2. As explained, the Env glycoprotein plays a crucial role in the depletion of CD4⁺ T cells by inducing the death of single bystander cells, which is mediated by gp41 [31,68,106,135]. Therefore, those changes in gp41 that emerge under T-20 pressure could induce a change in the viral pathogenicity. Previously, site-directed point mutations at position 38 in gp41 have been shown to exhibit deficiency in cell-to-cell fusion activity and apoptosis induction *in vitro* and in a humanized mouse model [136,137]. However, it is important to note that genetic context is extremely important in the characterization of the biological properties of Env. In the case of T20 resistance, previous studies have shown that the Env genetic background contributes to both the T20 resistance and to the function of Env. The selection for resistance is a coevolutionary process in which HR1 mutations are selected in combination with Env variants that permit optimal phenotypic expression of HR1 mutations [138]. It is well established that when HR1 mutations are introduced out of context (i.e., in a gp41 where they were not originally found), they can reduce the rate of membrane fusion, but the introduction of changes in HR2, or even in gp120, can compensate for this defect [123,126,128-131,139] Point mutations introduced into gp41 may perturb the folding of the protein into a six-helix bundle along the HR1 and HR2 coiled-coil domains. In contrast, a native gp41 background may stabilize the fusogenic six-helix bundle with compensatory changes in the HR1 mutants, thereby minimizing the effect of the original mutation. Thus, highlighting the importance of assessing the pathogenicity of primary ENV/gp41 in which is maintained the genetic context and where changes have been generated.

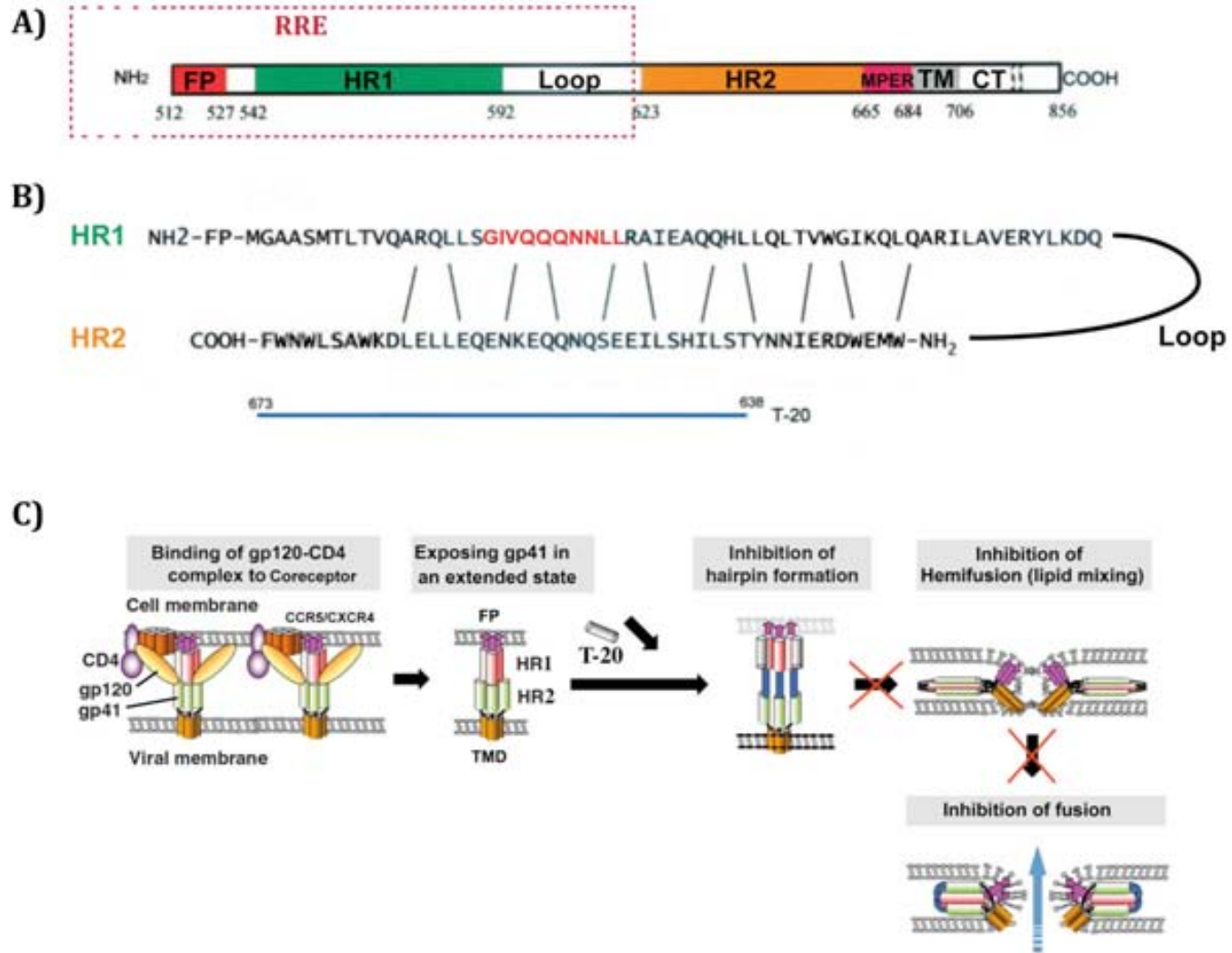


Figure 12: Fusion inhibition by T-20 (*Figure shown in the following page*). **A)** A schematic representation with the main domains of the gp41 glycoprotein is shown. The dashed box shows the fragment of gp41 that includes the RRE in the viral transcripts (at the nucleotide level). The residue numbers shown in the figure correspond to the positions in gp160 of HIV-1_{HXB2}. **B)** Representation of the interaction between HR1 and HR2, showing the important interactions with vertical lines. T-20 overlaps and mimics HR2, and hence it is able to bind to HR1. The red sequence inside HR1 is the main determinant of T-20 primary resistance (positions 36-45 of gp41). Note that inside the dashed box identifying the RRE region is also placed the segment in which the primary resistance mutations to T-20 appear (HR1). The region encoding for the Rev responsive element (RRE) also incorporates part of gp120 (not shown in the figure). **C)** During the fusion process the T-20 inhibitor avoids the interaction between HR1 and HR2 of gp41, and hence, the formation of the hairpin state. Thus, T-20 blocks the hemifusion and complete fusion processes. Figure adapted from [96,140-143]

➤ *T20-associated mutations correlated with changes in the RRE structure.*

The primary resistance mutations that appear in the HR1 domain of gp41 are not only affecting the Env glycoprotein but also the viral RNA secondary structure by altering the region where the RRE is localized (**Figure 12A**). The nucleotide changes emerge under drug pressure in the region that forms the RRE and can modify its conserved secondary structure, and consequently, affect the functions that develops in the viral transcription. The secondary structures of the RREs are usually determined through computational predictions based on their primary sequences and bioinformatics algorithms. More recently a new methodology has been developed and allowed to describe the secondary structure of the entire HIV-1 RNA genome [123,144-146]. These experiments of SHAPE (selective 2'-hydroxyl acylation analyzed by primer extension) are based on chemical reactions that determine the reactivity of each nucleotide in the analyzed RNA fragment and these values are subsequently converted into free energies, which are finally used to predict the secondary structures. Thus, these predictions give an idea of the overall RRE secondary structure conservation when compared to other predicted structures, but their alterations cannot be extrapolated to functional data.

Introduction

The main studies performed analyzing nucleotide changes in the RRE have been focused on the characterization of the RRE-Rev binding, the multimerization of Rev and the identification of the regions that were important for these functions. All these reports have been centered studying the high affinity binding site (localized at the base of the stem IIB) and the relevance of the other stems (III, IV and V). Mutations in the high-affinity binding site of Rev showed disruptions in the predicted secondary structures of this region and involved a direct impact on Rev binding [31,147]. For the rest of the stems, big deletions or multiple mutations were shown to create non-functional RREs [148,149]; however, few efforts have been done analyzing single nucleotide substitutions present *in vivo* in this region situated in the *env* gene.

Two reports associated the decrease in replication capacities of viruses harboring primary resistance mutations to T-20 with alterations in the predicted secondary structure of their RREs [139,146,150,151]. However, these assays did not specifically test the functions of these mutated RREs, which might be the ability to interact with Rev and the ability to allow the transportation of long viral transcripts to the cytoplasm. Besides, the T-20 primary resistance mutations Q40H and L45M were suggested to be selected together in order to restore the RRE secondary structure, which was abrogated when the nucleotide substitutions that encoded for these changes were present alone [139]. These hypotheses were based on predicted secondary structures but functional impact of these changes, which were situated in the gp41 protein (*env* gene) have not been tested so far.

HYPOTHESES & OBJECTIVES

The secondary structure of the RRE is determined at the nucleotide level and has been shown to be important for the correct export of the HIV viral transcripts, and hence, viral replication. Nucleotide changes in the *env* gene have been associated with the emergence of drug resistance and alterations in the predicted secondary structure of the RREs, which could lead to changes in their replication capacity. However, the impact of these changes on the RRE functionalities has not been reported to date.

- **Objective 1.-** To select nucleotide substitutions in the *env* gene (gp41/RRE) from patients receiving a T-20-containing salvage therapy and to analyze their impact on the RRE predicted secondary structures and functionalities. This objective is addressed in *Chapter 1*.

The role of the Env/gp41 glycoprotein in HIV pathogenesis has been extensively studied in the last three decades. However, experiments were mainly based on the introduction of mutations by site-directed mutagenesis or the analysis of laboratory-adapted HIV strains, which may not reflect exactly the *in vivo* phenotype due to the importance of the Env context for its function. The establishment of a methodology able to fully evaluate the Env pathogenicity would be a useful tool for the characterization of Env/gp41 isolated from patients.

- **Objective 2.-** To establish an *in vitro* methodology to evaluate the pathogenicity of patient-derived Env glycoproteins. This objective is addressed in *Chapter 2*.

Changes in gp41 associated with resistance to the fusion inhibitor T-20 have been correlated with immunological recovery, even after virological failure, suggesting that the acquisition of T-20 resistance alters gp41 pathogenicity.

- **Objective 3.-** To analyze the pathogenicity of several patient-derived gp41 glycoproteins isolated from patients receiving a T-20 containing therapy with changes at positions 38 and 140. This objective is addressed in *Chapter 3*.

MATERIALS & METHODS

1.- Reagents

1.1.- Antiretroviral Drugs

The fusion inhibitor C34 [152], the CXCR4-antagonist JM-2987 (hydrobromide salt of AMD-3100) [153] and the CCR5-antagonist TAK-779 [154,155] were obtained through the NIH AIDS Research and Reference Reagent Program (NIH ARRRP), Division of AIDS, NIAID, NIH.

1.2.- Antibodies

The antibodies targeting CD4 (FITC-labeled) and CD3 (APC-Cy7-labeled) were obtained from BD Bioscience (San José, CA, USA). The anti-gp120 antibodies 2G12 and IgG1 b12 were obtained from Polymun (Vienna, Austria) and through the NIH ARRRP, respectively. PE- and HRP-labeled secondary antibodies goat anti-Human IgG were obtained from Jackson ImmunoResearch Laboratories (Pennsylvania, USA).

1.3.- Plasmids

The Tat-expressing plasmid pcTat [142,156] was obtained from Dr. Abhay Patki and Dr. Michael Lederman through the NIH ARRRP. The pNL4-3 was obtained through the NIH ARRRP from Dr. Malcolm Martin [143,157]. The pLAI.2 was obtained through the NIH ARRRP from Dr. Keith Peden, courtesy of the MRC AIDS Directed Program [140]. The fusion defective mutant 41.2 was obtained from Dr. Eric O. Freed through the HIV Drug Resistance Program National Cancer Institute NCI-Frederick (Frederick, MD, USA). The luciferase-RRE expressing plasmid pDM628 was kindly provided by Dr. J. Kjems (Aarhus University, Denmark).

1.4.- Membrane and cell trackers

Dichloro-DimethylAcridin-One (DDAO) and the lipophilic probe Di1C₁₈(3) (DiI) were purchased from Molecular Probes (Invitrogen, Madrid, Spain).

1.5.- Other reagents

The cationic fluorescent dye propidium iodide (PI) and the potentiometric mitochondrial probe DiOC₆(3) were purchased from Sigma-Aldrich and Invitrogen, respectively. Sterile phosphate buffered saline (PBS), low and high DNA mass ladders, DMSO, LB-Agar, LB-liquid, Lipofectamine 2000, OPTIMEM, Versene, Trypsin, Dulbecco's modified Eagle's

Materials & Methods

medium (DMEM), RPMI 1640, fetal bovine serum (FBS), cell extraction buffer, NuPAGE® Bis-Tris mini gels 4-12% polyacrylamide and iBlot® Dry Blotting System, were obtained from Invitrogen. Calphos was purchased from Clontech Laboratories (Mountain View, CA, USA). 96-well plates were purchased from BD Bioscience. Lymphoprep was purchased from Axis-shield (Oslo, Norway). Perfect-Count Microspheres were obtained from Cytognos (Salamanca, Spain). The BCA protein assay kit and the SuperSignal West Pico Chemiluminescent Substrate were purchased from Thermo Scientific Pierce (Madrid, Spain).

2.- Cells

2.1.- Cell lines

2.1.1.- Adherent cells

The primary human embryonic kidney 293T cell line was obtained from the American Type Culture Collection (ATCC, LGC Standards, Middlesex, UK). The human cervical epithelial carcinoma cell lines HeLa and TZM-bl were supplied by the NIH ARRRP. TZM-bl cells harbor an integrated copy of the *luciferase* gene under control of the HIV-1. The transactivation of the *luciferase* gene leads to the production of the Luciferase enzyme that in the presence of its specific substrate, D-luciferin, catalyzes the oxidation of specific substrates to produce light.

Adherent cells were grown in DMEM supplemented with 10% of heat-inactivated FBS (referred from now on as D10) and maintained at 37°C in a 5% CO₂ incubator. Cells were subcultured twice a week using Versene and Trypsin.

2.1.2.- Suspension cells

MOLT_{NL4-3} is an X4-tropic HIV-1 chronically infected cell line previously generated in our laboratory through infecting the MOLT_{Uninfected} cell line with the NL4-3 viral strain by Dr. Julià Blanco.

Cells were grown in suspension and were maintained in RPMI supplemented with 10% FBS (referred from now on as R10). Cells were subcultured twice a week.

2.2.- Primary cells

Fresh buffy coats, enriched fractions in leukocytes and erythrocytes of human peripheral blood, from healthy donors were obtained from a local blood bank (Banc de Sang i Teixits, BST, Barcelona, Spain). Purification of the PBMCs was performed by a density gradient centrifugation using Lymphoprep and subsequently used to purify primary CD4⁺ T lymphocytes. To purify CD4⁺ T cells we used the CD4⁺ T cell Isolation kit II (Miltenyi Biotec, Madrid, Spain), a negative selection kit to avoid undesired effects in activation or behavior in the target cells. Final preparations were >95% of CD4⁺ T cells, as determined by flow cytometry. The isolated CD4⁺ lymphocytes were incubated overnight at 37°C in R10.

3.- Patients

Previously, we characterized gp41 proteins derived from 13 heavily pre-treated HIV-1-infected patients receiving an T-20-containing salvage therapy. Several drug-resistance mutations were detected along the entire gp41 ectodomain, mainly mapping in the HR1 domain at positions 36, 38 and 43 [123](**Table 1**). Plasma samples from those characterized patients collected at different time points during the treatment were used to generate Envelope-expressing plasmids.

Table 1. Genotypic changes within HR1 in gp41 during follow-up (Population-based sequencing).

Patient ID	Weeks on T-20 Treatment				
	4	12	24	48	96
1 ¹	36G/V, 38V/A	36G/V, 38V/A	36V	36V	36V
2	43 N/D	43D	43D	43D	43D
3		-		42N/D	43D
4 ²	43N/D	43D	43D	43D	43D
5 ²	36G/V, 40Q/H	36G/V, 40Q/H, 45L/M	40H, 45M	40H, 45M	40H, 45M
6	44L/M	38M, 44L/M	38M, 44L/M	44M ³	
7	43N/D/S	34M,43N/D/S	34M,43N/D/S	34M,43N/D/S	34M,43D
8	-	43D	43D	43D ¹	
9 ⁴	-	38E	38E/A	38A, 42T ¹	
10 ^{2,5}	38V/A	43N/D	34M, 43N/D ¹		
11	38V/A	33M, 42N/T	33M1, 42T	33M, 42T ¹	
12	-	43D	36G/S, 43D, 45L/M ¹		
13	-	36G/D,43N/D	43D, 49D ¹		

¹End of follow-up.

²Patients with changes at position 36 before week 4

³Patient harboring viruses with the 140I.

⁴Patient harboring viruses with the 140N.

⁵Patient harboring viruses with the 140T.

- not available samples.

4.- Plasmid constructions

4.1.- Full-length Env-expressing plasmids

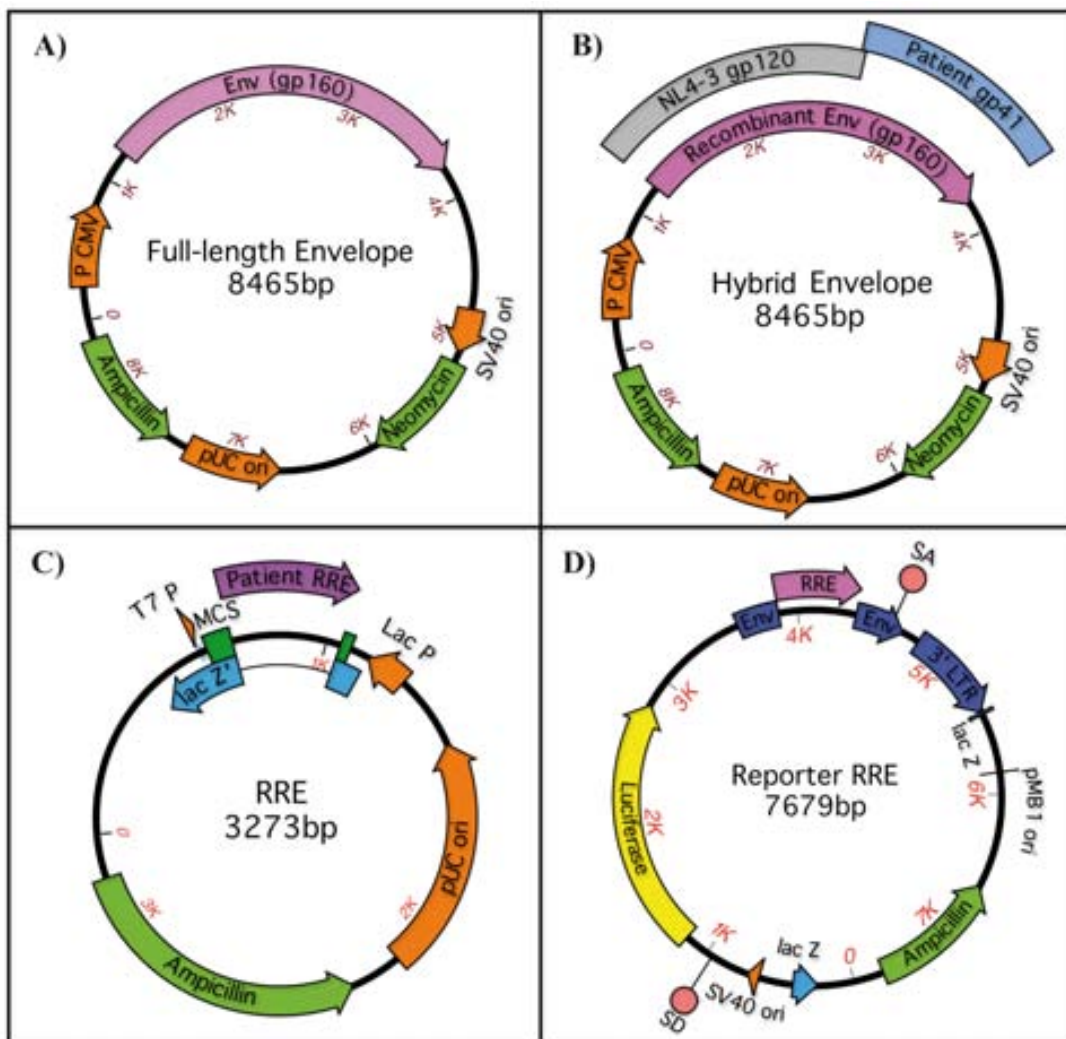
Full-length Env-expressing plasmids from patients 1, 5, 9 and 10 at baseline and at different time points during treatment were constructed. Viral RNA was isolated (QIAamp Viral RNA kit, QIAGEN, Spain) following manufacturer's instructions and a fragment corresponding to the *rev*, *vpu* and *env* genes was amplified through RetroTranscription-PCR using specific primers (NLEcoRIF and NLXhoIR, see **Table 2**) and the SuperScriptIII One-Step RT-PCR system with Platinum Taq High Fidelity (Invitrogen). The program used in the PCR was the following: First, 1 cycle of 30 min at 55°C; 2 min at 94°C. Second, 30 cycles of 1min at 94°C, 1min at 58°C and 5min at 68°C; and finally 1 cycle of 10 min at 68°C. A nested PCR was carried out using Platinum Taq DNA Polymerase High Fidelity (Invitrogen) using the RNA-NestedF and the RNA-NestedR primers (**Table 2**) to obtain the fragment that encodes the full-length Env protein (2951bp) in addition to the Rev and Vpu. The PCR program was: 1 cycle of 5 min at 94°C; 35 cycles of: 1 min at 94°C, 1 min at 55°C and 4 min at 68°C; and 1 cycle of 10 min at 68°C. The purification of the PCR products was performed with the SNAP UV-free gel purification kit (Invitrogen) as described by the manufacturer and were subsequently directionally cloned into the expression vector pcDNA.3.1D/V5/His-TOPO (Invitrogen) in a 1:1 molar ratio of PCR product:TOPO vector (**Figure 13A**).

The TOPO cloning reaction constructs were transformed into One Shot TOP10 chemically competent E.coli (Invitrogen) by heat shocking at 42 °C for 30 seconds, spread on LB plates containing 100 µg/ml ampicillin (Sigma-Aldrich) and incubated overnight at 37°C. The next day several individual colonies (between 30-60) were selected and analyzed by PCR, using a forward primer that hybridized within the insert (BGHR) and that were coupled with Egp41F to confirm the presence and the correct orientation of the insert into the vector (**Table 2**). The PCR products were analyzed by agarose gel electrophoresis and positive clones were selected and grown overnight at 37°C in liquid LB medium containing 100 µg/ml ampicillin. Plasmids of each selected clone were isolated and purified using the QIAprep Spin Miniprep Kit (Qiagen) and glycerolates were stored at -80°C to preserve the transformed cells.

All Env-expressing plasmids were sequenced using 14 specific primers (RNA-NestedF, EnvF, 6855R, U6923, 7030R, U7316, L7344, L7692, Egp41F, Egp41R, RNA-NestedR, U6835, L7764 and EnvR) (**Table 2**). The regions corresponding to the first and the second

exons of Rev were also sequenced in some of the plasmids adding the T7promoter primer. The sequencing was performed using the Big Dye Terminator v3.1 cycle sequencing kit (Applied Biosystems) with a standard sequencing reaction procedure: 1 cycle of 95°C for 5 min and 35 cycles of: 95°C for 30 secs, 56,5°C for 15 secs and 60°C for 3 min. DNA clean-up of the sequencing reactions was performed by centrifugation using absolute ethanol and EDTA. Purified DNA was subsequently sequenced using a 4-capillar automatic DNA sequencer (3100 Genetic Analyzer) and the sequences were aligned and edited using the Sequencher v4.7 (Gene Codes Corporation, Ann Arbor, MI) and the GeneDoc v2.6 (Nicholas Karl B et al 1997) programs. Full-length envelope clones were classified and used depending on their mutations.

Figure 13



Materials & Methods

Figure 13: Main features of the constructed plasmids. A) Full-length Envelope-expressing constructs were inserted into the pcDNA3.1D TOPO vector and remained under the CMV promoter. **B) Hybrid Envelopes** were cloned also into the pcDNA3.1D TOPO vector. The PCR-amplified fragment corresponding to the gp120 and gp41 subunits that overlapped in 22 bp is shown in the figure in parallel to the sequence. **C) RRE-expressing plasmids for *in vitro* RNA production** were constructed into the pPCR Script Amp SK(+) vector by inserting the RRE fragments into the multi cloning site (MCS) and situating the inserts downstream to the T7 promoter (T7 P). **D) Reporter RRE-expressing plasmids** were constructed in the pDM628 vector by digestion with the restriction enzymes XmaI and SpeI. This process could be made only after introducing the cleavage sites by PCR-amplification to both the RRE inserts and the vectors. Genes corresponding to HIV that are colored in dark blue were derived from the SF2 strain and were part of the pDM628 vector itself. The fragment of the *envelope* gene previously inserted in the construction of the pDM628 corresponded to the nts 6006 to 8376 of the X4-tropic SF2 clone. The *luciferase* reporter gene (yellow) is shown downstream the SV40 promoter (orange) but upstream to the envelope fragment. Splicing donor (SD) and splicing acceptors (SA) were displayed as circles. Only the plasmids constructed in pcDNA3.1D TOPO (in **A**) and **B**) were resistant to Neomycin but all of them were resistant to Ampicillin (from **A**) to **D**). The *lac Z'* gene (light blue) showed in **C**) and **D**) is not functional due to become broken after inserting the fragments. Promoters were shown in orange.

4.2.- Plasmids expressing Hybrid-Envs

Hybrid gp160 proteins were constructed with gp120 derived from an NL4-3 virus and gp41 derived from the patients (**Figure 13B**). Full-length Env-expressing plasmids created previously (described above) from patients 1, 9 and 10, who had mutations associated with T-20 resistance at position 38 in the gp41 viral protein but differed in the amino acid found at position 140, were selected to PCR-amplify the gp41 subunits using MluIF2 and RNA-NestedR primers (**Table 2**). In parallel, gp120 was PCR-amplified from pNL4-3 using the RNA-NestedF and MluIR2 primers (**Table 2**). Both PCR thermal cycle conditions were: 1 cycle of 5 min at 94°C; 35 cycles of 1min at 94°, 1 min at 58°C and 3 min at 68°C; and 1 cycle of 10 min at 68°C.

The joining of the NL4-3-derived gp120 and the different patient-derived gp41 subunits was done using a strategy called overlapping PCR. This method benefits from an overlapping sequence between both subunits, since the primers MluIF2 and MluIR2 are complementary to each other. Both PCR products (gp120 and gp41), previously gel-purified, were mixed and

re-amplified to generate a final PCR product (an hybrid Env with gp120 from an NL4-3 virus and gp41 derived from patients). The PCR consisted in an initial cycle of denaturation at 94°C for 5 min and 15 cycles of: 94°C 30 secs, 60°C 30 secs and 68°C 5min. These cycles were performed with all the reagents used in a standard PCR mix but without specific primers. Following these cycles the RNA-NestedF and the RNA-NestedR primers were added to the preparations and were used to exponentially amplify the recombinant hybrid envelopes (**Table 2**). A denaturation step of 15 min at 94°C was followed by 20 cycles of: 94°C for 1 min, 60°C for 1 min and 68°C for 6 min; and 10 min at 68°C. The PCR products were purified (**Figure 14**), cloned in the pcDNA.3.1D/V5/His-TOPO and sequenced as previously described. Forty-eight hybrid envelope clones with changes at positions 38 and 140 were selected and characterized (*Chapter 3*).

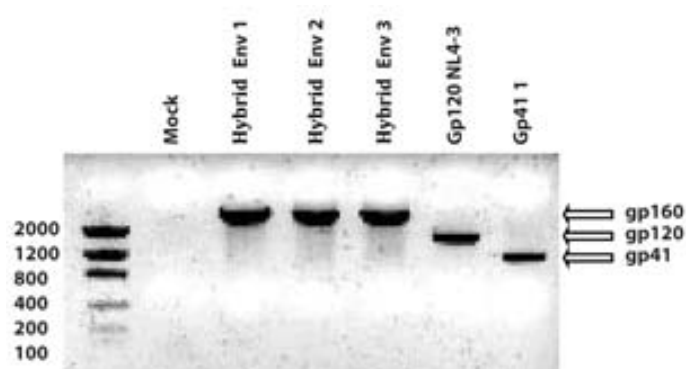


Figure 14: Agarose gel electrophoresis showing the DNA fragments that allowed the construction of the hybrid Envelopes. Purified DNA fragments obtained by PCR-amplification are displayed as gel bands in the figure. Gp160 fragments (2951 bp) were obtained by an overlapping PCR using the gp120 (1794 bp) and the gp41 (1179 bp) subunits as templates. Both subunits and three hybrid envelopes constructed with a common gp120 subunit, derived from a NL4-3 virus, and three different gp41 subunits, derived from viruses circulating in distinct patients, were used to run the gel Electrophoresis.

4.3.- RRE-expressing plasmids for *in vitro* RNA production

RRE-expressing plasmids for *in vitro* RNA synthesis were constructed from full-length Env-expressing plasmids that were derived from patient 10, who had mutations at positions 36, 38 and 43. The fragment that corresponded to the RRE was PCR-amplified from the full-Env plasmids using RREF and RRER primers and the following thermal cycle conditions: 1 cycle of 5 minutes at 94°C; 35 cycles of: 1 min at 94°C, 1 min at 50°C and 3min at 68°C; and 10

Materials & Methods

min at 68°C (**Table 2**). PCR fragments of 329 bp were purified by gel-excision as described before and subsequently cloned into the pPCR-Script Amp SK(+) cloning vector (Cultek, Granollers, Spain) as described by the manufacturer (**Figure 13C**). Several clones were selected and a PCR was performed using the primers T3Strata, which hybridized to the vector, and Ngp41F, to confirm the presence and the correct orientation of the insert (**Table 2**). Plasmid isolation from positive clones was performed and 26 individual clones were selected after checking for the harbored mutations by sequencing analyses using primers that were flanking the insert, T7Strata and T3Strata (**Table 2**). Two plasmids containing each of the desired mutations were subsequently used for *in vitro* RNA production (*Chapter 1*).

4.4.- RRE-expressing plasmids to measure RNA transport

In order to perform an RNA transport assay to test the different RRE mutants, we selected the same full-length Env that were used to generate the RRE-expressing plasmids for the *in vitro* RNA production and we cloned their RRE fragments into the reporter vector pDM628ΔRRE.

We constructed this reporter vector after modifying the preexistent pDM628, which was a Rev-dependent luciferase-based vector. PDM628ΔRRE was constructed by introducing into pDM628 two cleavage sites for the restriction enzymes XmaI and SpeI at the 5' and 3' ends of the RRE, respectively. The introduction of these enzymatic cleavage sites was performed by PCR using primers that added these cleavage sequences (SpeIRREFpDM628 and XmaIRRER) before and after of the RRE sequence that was present on the pDM628 (**Table 2**). Subsequently to the digestion with these two enzymes, the polylinker 5'PO4 CCGGGACCGGTGGCGCGCCACCGGTA was introduced into the modified pDM628 vector in order to close it in a circular form lacking the RRE.

The RRE fragments were PCR-amplified from the full-length Env-expressing plasmids also using primers that harbored these enzymatic restriction sites (SpeIRREF and XmaIRRER) (**Table 2**). Then, both pDM628ΔRRE vector and RRE fragments were digested with SpeI and XmaI restriction enzymes and were purified. Finally, the inserts (533 bp) were cloned into the vector (**Figure 13D**), transformed into bacteria and the transformants were analyzed and sequenced as described before. These plasmids were subsequently used to measure the capacity of the mutant RREs to being transported to the cytoplasm (*Chapter 1*).

4.5.- Site-directed mutants

D589L Env-expressing plasmids were constructed by introducing a point mutation in two different envelopes, pNL4-3 and pLAI.2, by using the GeneTailor Site-Directed Mutagenesis Kit (Invitrogen) and specific primers. The originated full envelopes that harbored the D589L mutation in both viral strain backgrounds were subsequently cloned into a pcDNA3.1 vector as previously described.

RRE-expressing plasmids having Q40H, L45M and 40Q-45L were generated by site directed mutagenesis, using the GeneTailor Site-Directed Mutagenesis Kit (Invitrogen), for *in vitro* RNA production and to perform a transport assay. Site-directed mutants were created using as a template a full Env-expressing plasmid that was derived from patient 5 and which harbored the double mutation Q40H-L45M. The RRE fragments generated after the site-directed mutagenesis were subsequently cloned into the pPCR-Script Amp SK(+) cloning vector and into the pDM628 Δ RRE, as previously described.

Table 2. Primers used to PCR-amplify, sequence and construct the different envelope fragments and plasmids described in this thesis.

Primer name	Sequence in 5'→3' direction	Orientation	HXB2 loc.	CDS	Method	Observations
NLEcoRIF	GGTCAGGGAGTCTCCATAGAATGGAGG	F	5284→5310	vif	RT PCR	Full
NLXhoIR	GATCTACAGCTGCCTTGTAAATCATTGGT	R	9055→9027	nef	RT PCR	Full
RNA-NestedF	CACCTAGGCATCTCCTATGGCAGGAAGAAG	F	5954→5983	tat ₁ , rev ₁	Nest. PCR, S.A.	Full, hybrid
RNA-NestedR	GTCTCGAGATACTGCTCCCACCC	R	8904→8882	nef	Nest. PCR, S.A.	Full, hybrid
BGHR	TAGAAGGCACAGTCGAGG	R	Vector (a.i.)	pcDNA3.1	Col. PCR	Full, hybrid
EnvF	AGCAGAAGACAGTGGCAATGAGAGTGAAG	F	6208→6236	env(gp120), vpu	S.A.	Full, hybrid
6855R	GGAATTGGCTCAAAGGATAACC	R	6865→6845	env (gp120)	S.A.	Full, hybrid
U6923	GGACCATGTACAAATGTCAGCA	F	6933→6954	env (gp120)	S.A.	Full, hybrid
7030R	TCTTCTTCTGCTAGACTGCCATTTA	R	7030→7006	env (gp120)	S.A.	Full, hybrid
U7316	CTCAGGAGGGGACCCAGAAA	F	7316→7335	env (gp120)	S.A.	Full, hybrid
L7344	CCTCCACAATTAATACTGTG	R	7363→7344	env (gp120)	S.A.	Full, hybrid
L7692	TTGGTGGGTGCTACTCCTAATG	R	7723→7702	env (gp120)	S.A.	Full, hybrid
Egp41F	AAGAGAAGAGTGGTGCAGAGAG	F	7728→7749	env (gp120)	Col. PCR, S.A.	Full, hybrid
Egp41R	ATTCCTTCGGGCTGTCCG	R	8422→8404	env (gp41), tat ₂ , rev ₂	S.A.	Full, hybrid
U6835	GGTATCCTTTGAGCCAATTCC	F	6845→6865	env (gp120)	S.A.	Full, hybrid
L7764	CCAAGAACCAAGGAACAIAAG	R	7794→7774	env (gp41)	S.A.	Full, hybrid
EnvR	TTTTGACCACTTGCCACCCATCTTATAG	R	8817→8790	env (gp41), nef	S.A.	Full, hybrid
T7promoter	TAATACGACTCACTATAGGG	F	Vector (b.i.)	pcDNA3.1	S.A.	Full, hybrid
MluIF2	CAAAGAGACGCGTGGTGCAGAG	F	7726→7747	env (gp120)	Nest. PCR	Hybrid
MluIR2	CTCTGCACCACGCGTCTCTTTG	R	7747→7726	env (gp120)	Nest. PCR	Hybrid
RREF	GAGAAGAGTGGTGCAGAGAG	F	7730→7749	env (gp120)	Nest. PCR	RRE R.P.
RRER	CATTCCAAGGCACAGCAG	R	8058→8041	env (gp41)	Nest. PCR	RRE R.P.
Ngp41F	GCAGCAGGAAGCACTATGGG	F	7797→7816	env (gp41)	Col. PCR	RRE R.P.
T3strata	AATTAACCCTCACTAAAGGG	R	Vector (a.i.)	pPCR-Script	Col. PCR, S.A.	RRE R.P.
T7strata	GTAATACGACTCACTATAGGGC	F	Vector (b.i.)	pPCR-Script	S.A.	RRE R.P.
SpeIRREFpDM628	TTGACAATTACACTAGTACAATATACACC	F	8128→8156	env (gp41)	I.E.R.S.	RRE T.A.
XmaIRRER	TATCTCCTCCCCGGGTCTGAAGA	R	7647→7624	env (gp120)	I.E.R.S.	RRE T.A.
SpeIRREF	TTAACAATTACACTAGTTTAATACACTCC	F	8128→8156	env (gp41)	I.E.R.S.	RRE T.A.

HXB2 loc.: Number of position relative to HXB2 genome start; *CDS*: Coding sequence; *F*: Forward; *R*: Reverse; *b.i.*: before insert; *a.i.*: after insert; *tat*_{1/2}: Exons 1/2 of *tat*; *rev*_{1/2}: Exons 1/2 of *rev*; *RT PCR*: Retrotranscription PCR; *S.A.*: Sequencing analysis; *Col. PCR*: Colony PCR; *Nest. PCR*: Nested PCR; *I.E.R.S.*: Introduction of enzymatic restriction sites; *Full*: Full-length envelopes; *Hybrid*: Hybrid envelopes; *RRE R.P.*: RRE for RNA production; *RRE T.A.*: RRE for RNA transport.

5.- Secondary structure model analysis for RRE RNAs

The secondary structures of the RREs harboring different nucleotide substitutions were predicted by bioinformatics tools using the sequences obtained from full-length Env-expressing plasmids and from the ones produced for *in vitro* RNA production. To predict differences in the RNA folding of these RREs depending on the harbored mutations, it was used the RNA Fold server (Vienna RNA Webservers [158], <http://rna.tbi.univie.ac.at/>), which predicts the minimum free energy structures and base pair probabilities from single RNA sequences using dynamic programming algorithms [144]; and the MFold web server ([147,158]; <http://mfold.rna.albany.edu/?q=mfold/RNA-Folding-Form>), which uses different algorithms than the RNA Fold program. In order to predict these secondary structures, sequences corresponding to the nts 7730-8058 (329 bp), which correspond to the positions relative to HXB2 genome start, were introduced to generate them.

6.- Rev binding assays

Rev binding assays were performed in collaboration with Dr Nancy Beerens at the Aarhus University (Aarhus, Denmark). RRE RNA was generated through *in vitro* transcription by T7 RNA polymerase and radiolabeled UTPs from the constructed RRE-expressing plasmids (**Figure 13C**). The RNA products were separated on a denaturing gel and the full-length products were isolated. After elution, the RNA was precipitated and the % of ³²P-UTP incorporation was determined. Equal amounts of RNA were used for Rev binding assays. Recombinant Rev protein was produced in E.coli, purified, and then mixed with RNA_{RRE}. Then, the products were analyzed on a native gel (EMSA) and the gel shifts were quantified by phosphorimage.

7.- Rev exporting assays

Rev exporting assays were performed in collaboration with Dr Nancy Beerens at the Aarhus University. 293T cells were cotransfected with pcRev and RRE-expressing plasmids, which were generated using the Rev-dependent luciferase-based pDM628ΔRRE, and luminescence was measured in order to determine the rate of exportation to the cytoplasm of the full-length transcripts using a kit of luciferase.

8.- HeLa and 293T transfections: Env-expressing cells

HeLa and 293T cells were plated at a density of 8×10^5 cells/well in six-well plates and allowed to grow overnight. Both cell lines were transfected with 1.3 μg of Env-expressing plasmids, for bystander apoptosis, absolute loss of CD4^+ T cells and hemifusion analyses or cotransfected with the Env-expressing plasmids and 2.7 μg of pcTat for the fusion assays, to obtain Env^+ cells. Transient transfections of subconfluent 293T cells were accomplished using the Calphos Mammalian transfection kit and confluent HeLa cells were transfected with the Lipofectamine 2000 kit, according to the manufacturer's instructions. Twenty-four hours post-transfection, the cells were collected for further analyses. As negative controls, cells were mock-transfected (with the pcDNA 3.1 vector) or transfected with pcTat alone.

9.- Quantification of the Env expression

9.1.- Flow cytometry

Detection of Envelope expression on the membrane of effector cells was performed through an indirect-staining by flow cytometry twenty-four hours post-transfection. To assess this, 3×10^5 Env-transfected cells were incubated with the anti-gp120 monoclonal antibodies 2G12 or IgG1 b12 (4 μ g/ml) for 20 min at 37°C and after washing the cells with sterile PBS, incubated at RT for 15min with the PE-labeled goat anti-human IgG. Two more washing steps were performed and thereafter, the cells were fixed in formaldehyde 1%, acquired in a FACS LSRII flow cytometer and analyzed by the FACSdiva software (BD Biosciences). Mock-transfected cells were used as a negative staining control. The percentage of Env-positive cells and the geometric mean fluorescence intensity (geoMFI) of these cells were considered as individual parameters or used to calculate the relative fluorescence intensity (RFI= % of Env-positive cells x geoMFI of Env-positive cells), as described previously [39,148]. MOLT_{NL4-3} and MOLT_{Uninfected} were used as positive and negative controls in each assay.

9.2.- Western Blot

293T and HeLa Env-transfected cells were lysed with cell extraction buffer (Invitrogen) following manufacturer's instructions. Total protein amounts were quantified using the BCA protein assay kit (Thermo Scientific Pierce) and 20 μ g of total protein for each sample were analyzed in SDS-PAGE using NuPAGE® Bis-Tris mini gels with 4 to 12% gradient of polyacrylamide concentration (Invitrogen). Proteins were transferred to a nitrocellulose membrane using the iBlot® Dry Blotting System (Invitrogen). Western blotting was conducted using anti-Env 2G12 antibody (Polymun) at 2 μ g/ml for 2 hours at room temperature, followed by HRP-labeled anti-human IgG secondary antibody (Jackson ImmunoResearch) at 1:5000 dilution for 1 hour at room temperature. Chemiluminescence was detected employing SuperSignal West Pico Chemiluminescent Substrate (Thermo Scientific Pierce).

10.- Cell-to-Cell fusion assays

Twenty-four hours post-transfecting HeLa and 293T cells with Env-expressing plasmids and pcTat, 3×10^4 Env⁺Tat⁺ HeLa/293T cells were cocultured with 3×10^4 TZM-bl cells for 6 hours or in kinetic experiments for 2, 4, 6, 12, 24 and 52 hours in 96-well plates in the presence or absence of the CXCR4 and the CCR5 coreceptor inhibitors JM-2987 and TAK-779 (1 μ g/ml). The fusion efficiency of each envelope clone was quantified by assessing the luminescence of the cocultures in each well (Britelite Luminescence Reporter Gene Assay System, Perkin Elmer Life Sciences) with a Luminoskan Ascent luminometer (Labsystems, Spain).

11.- Envelope-induced cytopathicity in CD4⁺ T cells: absolute cell loss and bystander apoptosis

Env-induced cytopathic effects on primary CD4⁺ T cells were evaluated after the coculture of these primary target cells with either Env-expressing HeLa cells or Env-expressing 293T cells, which acted as effector cells. The purified primary CD4⁺ T cells were stained with the far red cell tracker DDAO (10 μ g/ml) for 1 hour at 37°C, extensively washed with sterile PBS and maintained in R10 at 37°C in a 5% CO₂ incubator. The next day, 7.5×10^4 Env⁺ HeLa / 293T cells were cocultured with 5×10^4 CD4⁺ DDAO⁺ T cells on 96-well plates in the absence and presence of the inhibitor JM-2987 (1 μ g/ml). After 24 hours, cells were collected and stained with DiOC₆(3) (40 nM) and PI (5 μ g/mL) for 1 hour at 37 °C. Labeled MicroBeads (Perfect-Count Microspheres, Cytognos) were added to the stained coculture to quantify the absolute cell loss and samples were acquired in a FACS LSRII flow cytometer. The data were analyzed using the FACSdiva software (BD Biosciences).

12.- Hemifusion assay

Twenty-four hours post-transfection, 293T and HeLa effector cells expressing NL4-3, D589L and 41.2 envelopes were labeled with 1 μ l of the lipophilic probe DiI (1mM) and incubated for five minutes at 37°C prevented from light. Three washing steps with sterile Phosphate Buffered Saline (PBS) were performed to allow the clearance of the unbound probe prior a cellular suspension in complete medium. After 20 minutes of incubation at 37°C to completely remove the excess of dye, another two final washing steps were performed before a final cellular suspension in complete medium. CD4⁺/DDAO⁺ cells were used as target cells

for the hemifusion assay cocultures. 7.5×10^4 effector cells were cocultured with 5×10^4 target cells in the presence or absence of the fusion inhibitor peptide C34 (5 μ g/ml), which was used to avoid Env-mediated membrane lipid transfer. After 24 hours at 37°C, the cocultures were analyzed by flow cytometry and quantified by using the PE-labeled microbeads.

13.- Statistical analysis

The data were compared using non-parametric Mann-Whitney tests. All of the statistical analyses were performed using GraphPad Prism, version 5.01, for Windows (GraphPad Software, San Diego, California, USA). A P-value of 0.05 was considered to be significant for these studies.

RESULTS

*Chapter 1.- Predicted structures and functional evaluations of
patient-derived Rev responsive elements (RRE)*

The secondary structure of the genomic viral RNA has been shown to be important for the correct processing and folding of the viral proteins and also for regulatory functions [47,146]. The Rev responsive element (RRE) is one of the most studied secondary structures of HIV-1 because of its importance in viral pathogenesis and its role in the exportation of viral mRNAs, although the conformation of these stem-loop structures is mainly determined by bioinformatics predictions. It has been shown that alterations in the configuration of the high affinity binding site or deletions of any of the stems abrogate the functions of the RREs. However, little is known about the impact of nucleotide substitutions that are present *in vivo* in the RRE sequences and how these substitutions are affecting not only the predicted secondary structure but also the functionalities of these elements.

Previously it has been suggested that nucleotide substitutions that encode amino acid changes in gp41/RRE sequences were associated with resistance to T-20 and the improve of the viral replication capacity by increasing the structural stability of the RRE [150,151,159]. These data were based on analysis of viral replication kinetics; however, specific measurements of RRE functions were not analyzed. Another study also suggested that the conformation of the RRE was disrupted when single amino acid changes (Q40H or L45M) were selected under T-20 pressure but it was restored when both mutations were co-present[139], suggesting that this particular reestablishment in the secondary structure of this RRE was modulating the resistance pathways to T-20. Nevertheless, no data on the impact of these changes on the functionality of the RRE have been published.

The functionality of the RRE/Rev interaction of gp41/RRE sequence selected from patients receiving a T-20 containing salvage therapy was evaluated. Our results indicated that the predicted secondary structures of the RREs might not always reflect the real impact on the functionalities in the RRE suggesting that, the RRE has structural versatility and as long as the structural conformation is close to some consensus conformation the RRE is functional.

1.- Prediction of the patient-derived RRE secondary structures

Full-length Env-expressing plasmids were constructed from two previously characterized heavily treated HIV-1 infected patients receiving a T-20-containing salvage therapy. A patient that harbored amino acid changes at positions 36, 38 and 43 in gp41 (patient 10 in **Table 1**) and from another patient that harbored changes at positions 40 and 45 (patient 5 in **Table 1**). Interestingly, in the samples obtained from this latter patient we could only obtain plasmids with the Q40H change or with the double mutation Q40H-L45M, but none were found with the L45M present as a single substitution. In order to analyze both changes we created by site-directed mutagenesis from the full-length Env-expressing plasmid Q40H-L45M the plasmids encoding for the single Q40H, L45M and the wt 40Q-45L.

As all these changes were situated in the region where the RRE is located, two different bioinformatics programs, RNA fold (<http://rna.tbi.univie.ac.at/cgi-bin/RNAfold.cgi>, [158]) and Mfold (<http://mfold.rna.albany.edu/?q=mfold/RNA-Folding-Form>, [147]), were used to predict the secondary structures of the RREs present in some of our plasmids using their nucleotide sequences. The prediction of the RRE secondary structures obtained with those tools was based on the free energy minimization that was calculated using a loop-based energy model and a dynamic programming algorithm [157].

Figure 15: Alignment of the nucleotide sequences of the RRE fragments used for the prediction of the secondary structures. RREs from patient 5 were produced by site-directed mutagenesis and aligned to the clone which amino acid mutations were reverted (gray shading). RREs from patient 10 were aligned to a clone derived from the baseline sample (gray shading). Sequences corresponded to the HXB2 nucleotide fragment ranging 7815-8015 (201 nts), which encoded for the fragment in the gp41 protein between the amino acids 20th and 86th in this subunit. Boxes highlight the codons that encode for primary T-20 resistance mutations in the gp41 protein (36, 38 and 43 for patient 10; and 40 and 45 for patient 5). The nomenclature of the names of the clones mean: patient 5/10 (P5/P10), weeks 0, 4 or 24 of T-20 treatment (w0, w4 or w24), amino acid mutations harboring and a numeral corresponding to the individual number of the clone.

????? ? ? ? ?

```

* * * * *
HXB2      : GGCGCAGCCTCAATGACGCTGACGGTACAGGCCAGACAATTATTGTCTGGTATAGTGCAGCAGCAGAACAATTTGCTGAGGGCTATTGAGGCGCAACAGCA
P5_WT     : GGCGCAGCGTCAATAACGCTGACGGTACAGGCCAGACAATTACTGCTGGTATAGTGCAACAGCAAAACAACCTTGCTGAGGGCTATTGAGGCGCAACAACA
P5_Q40H   : .....A.....T.....
P5_L45M   : .....A.....
P5_Q40HL45M : .....A.....

P10_w0_WT : GGCGCAGTGTCAATGACACTGACGGTACAGGCCAGACAATTATTGTCTGGTATAGTGCAACAGCAGAATAATTTGCTGAGAGCTATTGAGGCGCAACAGCA
P10_w4_G36V_1 : .....T.....
P10_w4_G36V_2 : .....T.....
P10_w4_V38A_1 : .....C.....
P10_w4_V38A_2 : .....G.....
P10_w24_G36D : .....G.....G.....A.....
P10_w24_N43D_1 : .....G.....C.....
P10_w24_N43D_2 : .....G.....C.....

G36V/D V38A Q40H N43D L45M

```

```

* * * * *
HXB2      : TCTGTTGCAACTCACAGTCTGGGGCATCAAGCAGCTCCAGGCAAGAATCCTGGCTGTGGAAAGATACCTAAAGGATCAACAGCTCCTGGGGATTTGGGGT
P5_WT     : TCTGTTGCAACTCACAGTCTGGGGCATCAAGCAGCTCCAGGCGAGAGTCTGGCTGTGGAAAGATACCTAAAGGATCAACAGCTCCTAGGGATTTGGGGT
P5_Q40H   : .....
P5_L45M   : .....
P5_Q40HL45M : .....

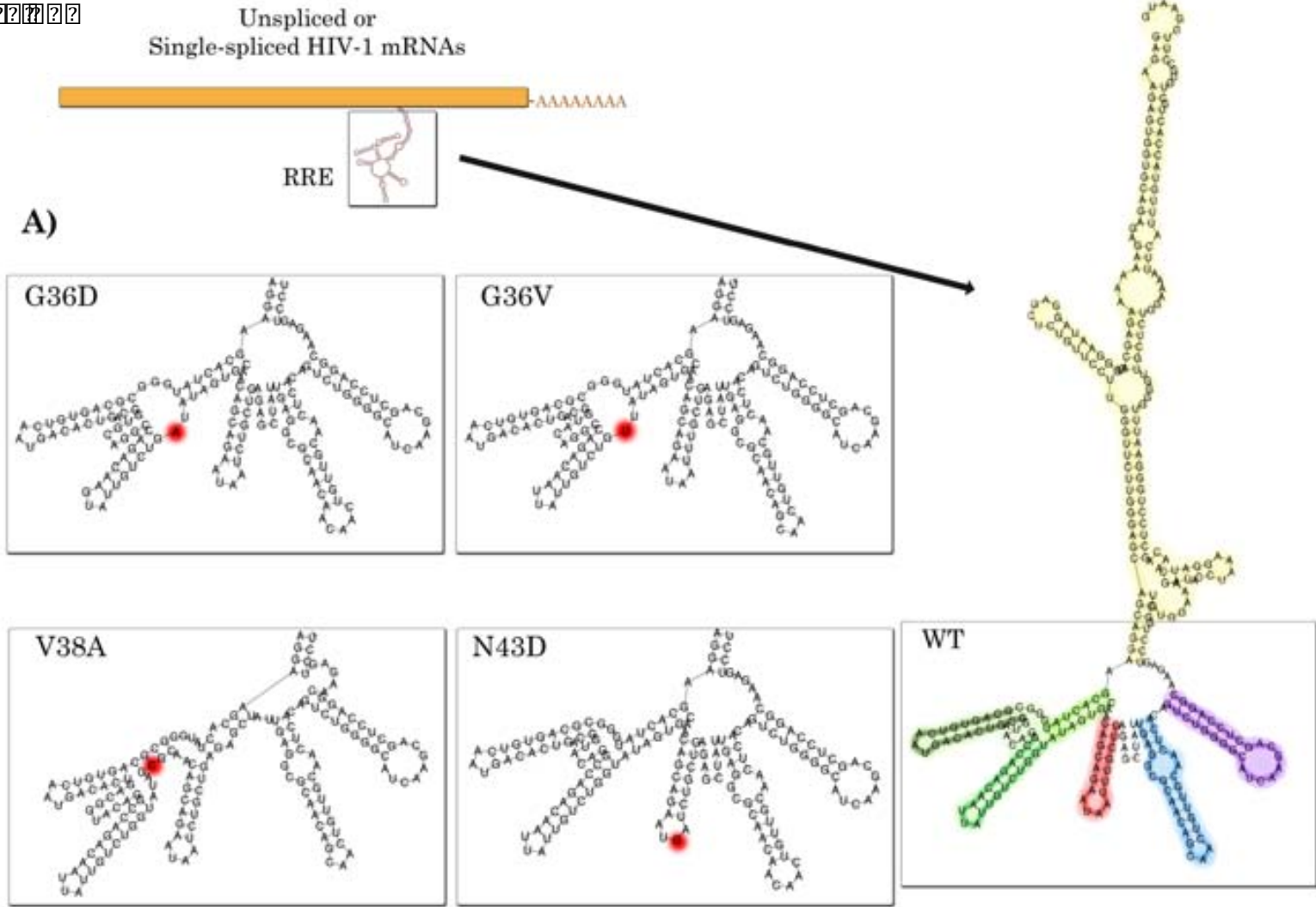
P10_w0_WT : ACTGTTGCAACTCACAGTCTGGGGCATCAAGCAGCTCCAGGCAAGAGTCTGGCTGTGGAAAGATACCTAAAGGATCAACAGCTCCTGGGAATTTGGGGT
P10_w4_G36V_1 : .....
P10_w4_G36V_2 : .....
P10_w4_V38A_1 : .....
P10_w4_V38A_2 : .....A.....
P10_w24_G36D : .....
P10_w24_N43D_1 : .....
P10_w24_N43D_2 : .....

```

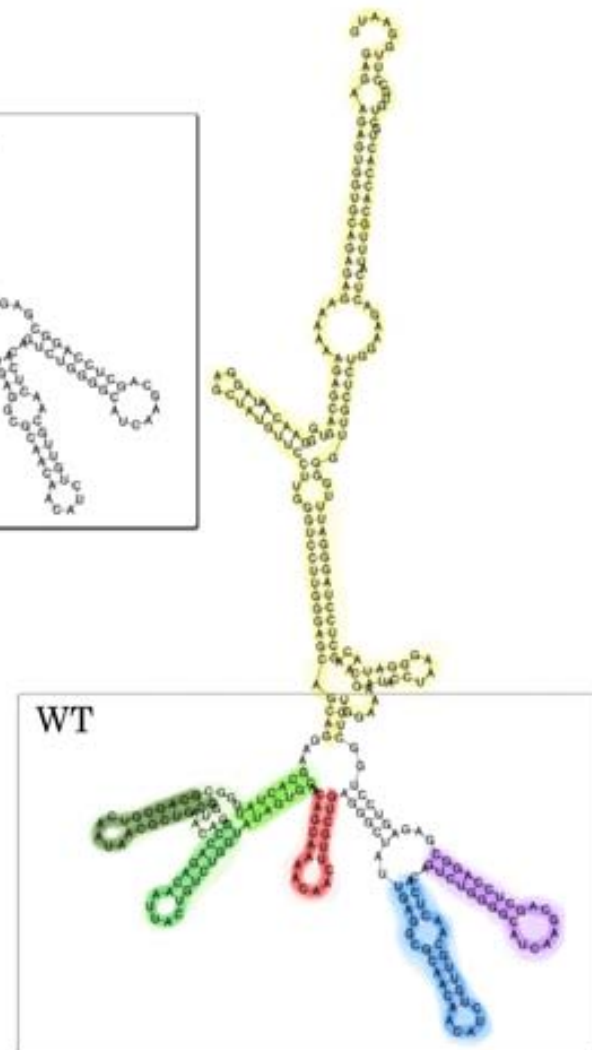
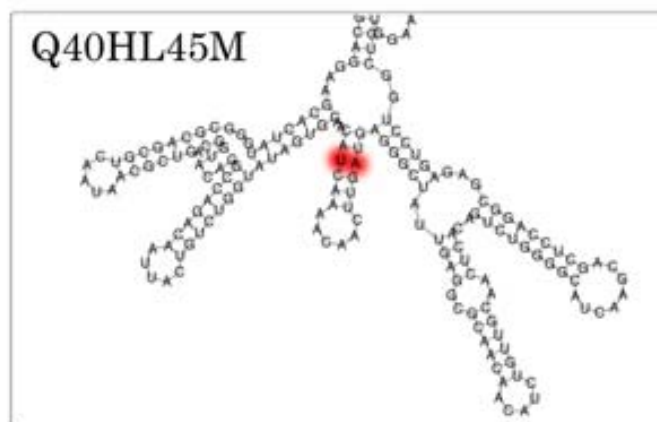
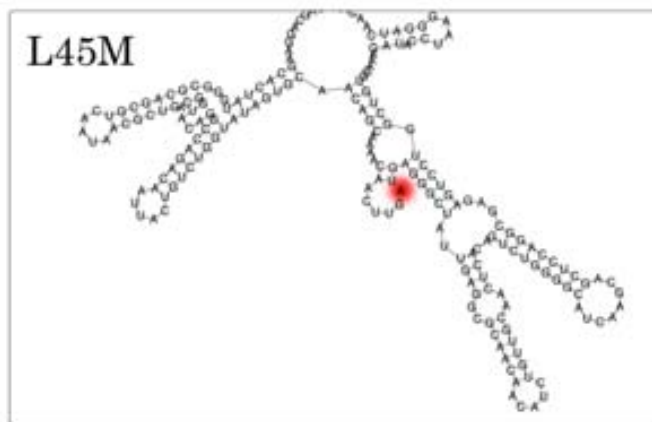
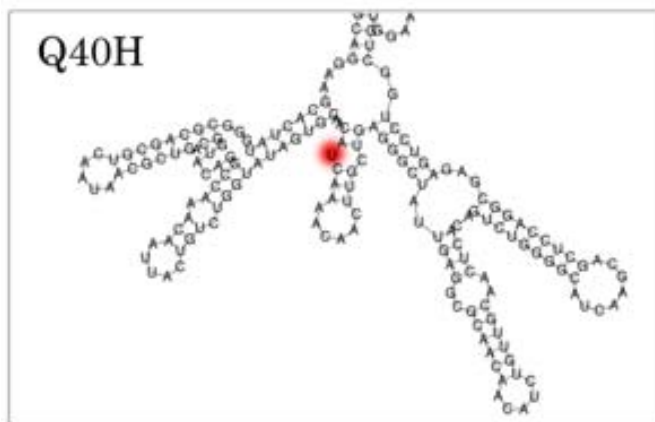
The secondary structures obtained from the RRE-expressing plasmids constructed from the patient 10 baseline samples (wt), displayed the characteristic 5 stem-loop subdomains that are extensively believed to be important for the correct interaction and function of the Rev protein (**Figure 16**). The G36V, G36D, V38A, and N43D amino acid mutations derive from the nucleotide substitutions (in boldface) GGT to GTT, GGT to GAT, GTG to GCG, and AAT to GAT, respectively. These nucleotide substitutions are placed at positions 135 (G36V/D), 141 (V38A) and 155 (N43D) of the RRE sequence fragments (329 nts) that were used to analyze the secondary structures, and are highlighted in red (**Figure 16A**).

Analyzing the different RREs derived from patient 10 (G36V, G36D, V38A and N43D), it was found that the sequences that were encoding for amino acid changes at positions 36 and 38 resulted in a change in the predicted secondary structure of the RRE (**Figure 16A**). G36D/V mutants showed an alteration of the secondary structure of the stem II (stem IIB and IIC) by disrupting a base pair located in the stem IIC. V38A mutants showed a more apparent impairment in the predicted secondary structure, with alterations in the stem II (stem IIA and IIB) and also in the stem III caused by a disruption of a base pair in the stem IIA. The RRE structures are altered in these clones because the change of nucleotides broke the conserved base pairs that were forming. However the RRE sequences that meant a change in the amino acid 43 did not modify the secondary structure of the RRE because the switched nucleotide lies in an external bulge of stem III and hence, the nucleotide substitution did not break any base pair. Although nucleotide substitutions that encode for G36D and G36V involve an alteration in the predicted structures of the RREs, these changes appear to be smaller than the ones induced by the V38A changes. Thus, it could be expected that RREs harboring the nucleotide substitutions encoding for the V38A mutation should be less functional than the RREs encoding for G36D/V changes, because of the difference in the magnitude of the predicted secondary structure alterations.

20220702



B)



Results

Figure 16: Minimum free energy secondary structure predictions of patient-derived RREs. A) A schematic representation of an unspliced or single-spliced mRNA is shown displaying the RRE with its wide-reported secondary structure, which allows the interaction with Rev for its shuttle to the cytoplasm. The five stem-loop secondary structure characteristic of the RRE is shown at the right side of the figure, which was predicted from a wt sequence of a baseline clone derived from patient 10. Each of the loops was colored in order to identify them. Stem I is colored in Yellow, stem II in green (different tonalities corresponded to Stem IIA, IIB and IIC), stem III in red, stem IV in blue and stem V in purple. The predictions were made using the RNA Fold Web Server (<http://rna.tbi.univie.ac.at/cgi-bin/RNAfold.cgi>, [158]) and the 329 nucleotide sequences of the RREs derived from patients treated with T-20. These fragments corresponded to the nucleotides ranging 7730-8058 of the HXB2 genome, which corresponded to the nucleotides 1506-1533 of the gp120 gene and 1-301 of the gp41 gene. Single nucleotides that implied the change of amino acids in gp41 to induce the primary resistance to T-20 are highlighted in red for each clone of **patient 10**. **B)** Secondary structures corresponding to the clones generated by site-directed mutagenesis from **patient 5** were also predicted.

In addition to changes at positions 36 and 38 of gp41, amino acid substitutions at positions 40 and 45 have previously also been associated with the modulation of the RRE structures. The secondary structure of the wt RRE (40Q-45L) generated by site-directed mutagenesis appeared to have the stems IV and V equal to the structure that was predicted for the wt of patient 10, although the bases of these stems did not attach directly to the central loop where the rest of the stems converge, but are attached to a new structure formed from the one that is normally lying between stems III and IV. Despite this visual alteration, this is consistent with a previous report that suggested that the base of the stem IV was not confined to a secondary structure [39] and that the nucleotides that were located at the base of the stem V appeared to be more flexible[47]. The predicted secondary structures of the RREs that harbored the nucleotide substitutions encoding for the single mutations Q40H and L45M showed an alteration in the stem III. This change was generated by a disruption of a base pair in this subdomain. The consequences of this base pair disruption are observed as a little bulge in the RREs characterized by having the Q40H alone and as a complete disruption of the stem III for the ones that have the L45M alone. However, RREs having both changes (Q40H-L45M) showed a restoration of the stem loop III and displayed a predicted RRE secondary structure identical to the one obtained with the wt plasmid 40Q-45L (**Figure**

16B). The nucleotides that are changed for the establishment of these particular mutations *in vivo* (CAG to CAT, for Q40H and CTG to ATG, for L45M) are forming a base pair in the stem III of the RRE structure. For this reason, the disruption of the base pair that is formed with the Q40H appeared to be restored in the presence of the L45M. The wt base pair is formed between **G-C**, while it is established between **T-A** when both Q40H-L45M are present. Analyzing the predicted secondary structures displayed from this sequences, it might be speculated that the Q40H mutants would have minimum functional impairments, while the L45M mutants might have the worst ability to develop its junctions accounting for the its huge disruption. In order to know the impact of all these changes in the RRE functions, Rev binding and Rev-dependent transport assays were performed.

Results

2.- Analyses of the RRE functions

2.1.- RRE-Rev binding assay

The ability of the Rev viral protein to interact with the different RREs harboring the selected nucleotide substitutions was analyzed. This capacity was examined by using a wt Rev protein and the RRE-expressing plasmids that were constructed into the pPCR Script Amp SK(+) vector (**Figure 13C**). Subsequently to the *in vitro* RNA production of the RRE fragments, these RNA molecules were tested for their binding capacity in increasing concentrations of Rev (**Figure 17**). The complexes $PROT_{Rev}-RNA_{RRE}$ were separated depending on their size and the discrimination of the complexes that had 3, 2, 1 or none Rev proteins attached to the RNA_{RRE} could be observed. The band shifts were analyzed by quantitative densitometry (Phosphorimager) of the gel. The quantification of the complexes RRE-Rev derived from patient 10 did not show any difference between the wt and the fragments harboring the G36V/D, V38A and N43D changes (**Figure 17A**). Thus, all of the RREs tested for patient 10 had the same ability to bind to Rev, irrespective of the nucleotide substitutions that they were harboring, and the predicted secondary structure they were displaying.

However, the bands observed in the gel and the % of shift of the complexes formed with the RREs with changes at positions 40 and 45 and the viral Rev protein showed differences (**Figure 17B**). The RREs that was harboring the L45M change showed an impairment in the ability to bind the viral Rev protein when the concentrations of Rev were low/intermediate, which was correlated with the alteration observed in the secondary structure. However, that RRE-Rev binding was mainly recovered when higher concentrations of Rev were used. Unexpectedly, the double-mutant Q40H-L45M showed the same RRE-Rev binding profile than the single L45M mutant despite the differences in the predicted structures, in which the double-mutant appeared to restore the alterations caused by the single mutant. The RREs that had a sequence that encoded for the single change Q40H, showed the same ability than the wt RRE to bind Rev, in concordance with the predicted structure.

Figure 17 A)

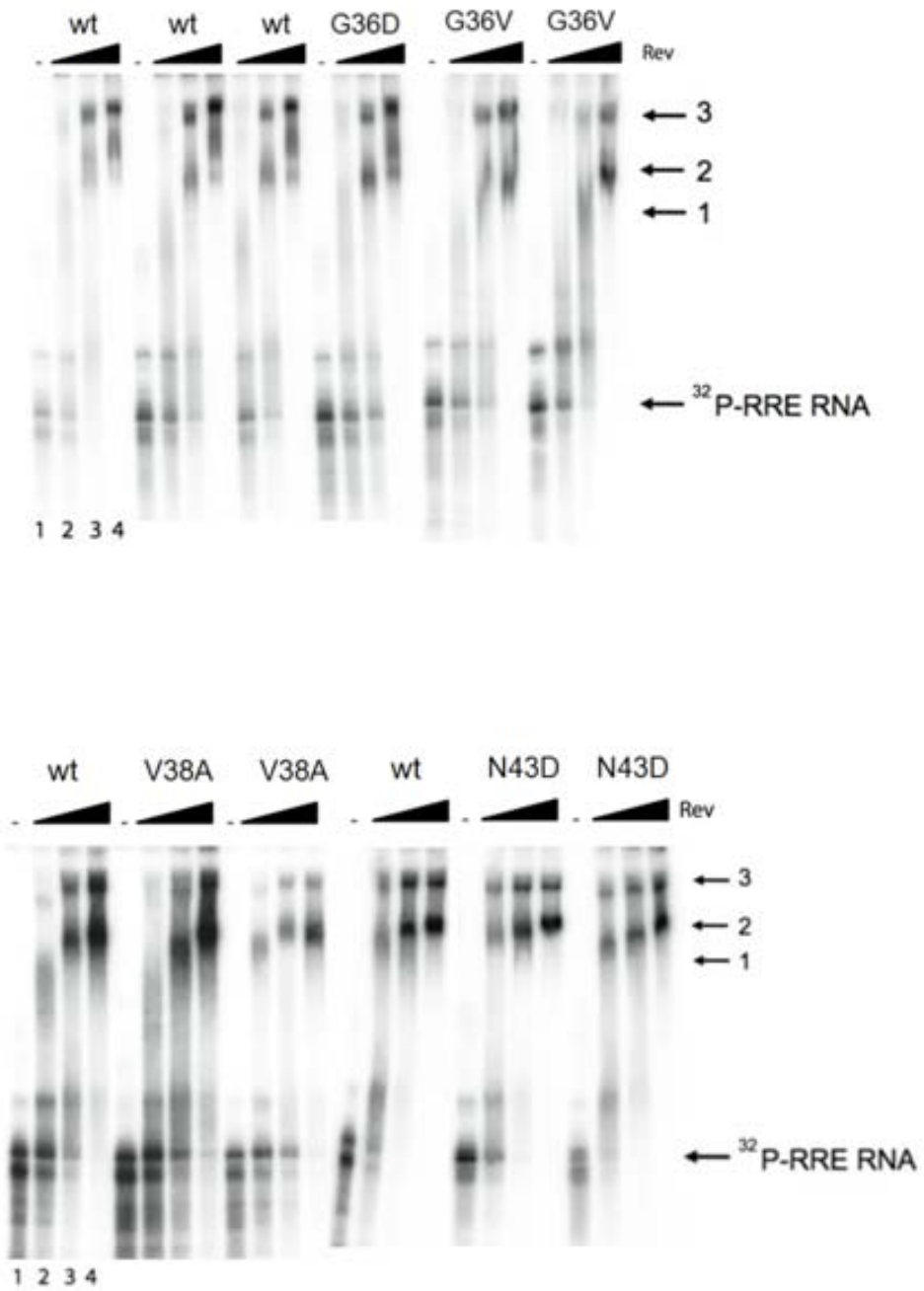


Figure 17 B)

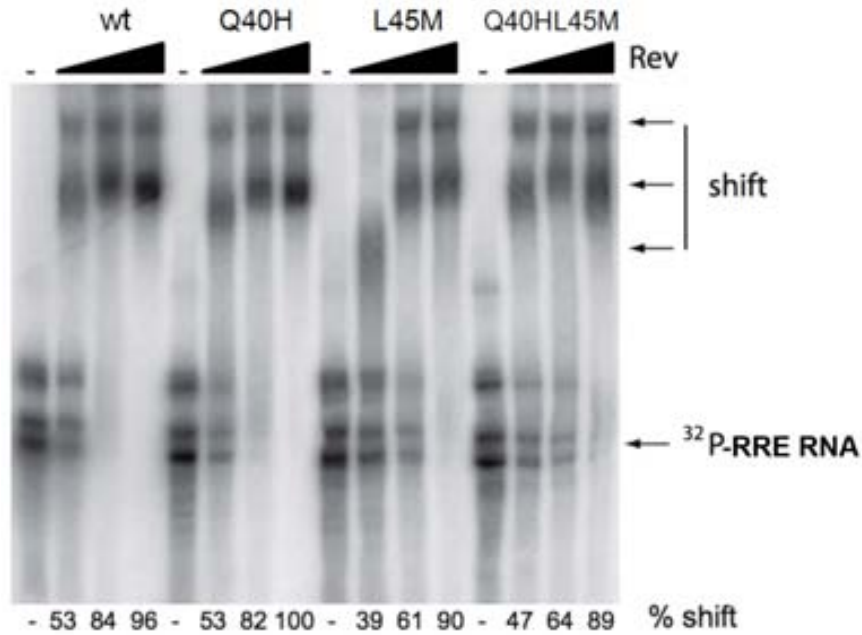


Figure 17: Band shifts corresponding to the Rev-binding assay with the RREs harboring different nucleotide changes selected under T-20 treatment. RREs derived from patient 1 with amino acid changes at positions 36, 38 and 43 (A). RREs with changes at positions 40 and 45 (B).The different RREs with nucleotide substitutions were tested for Rev-binding in increasing concentrations of the viral Rev protein. First lane of each RRE tested is without Rev, while lanes 2-4 are in increasing concentrations of Rev. Quantification of the band shifts were done in order to determine differences in their ability to bind Rev by phosphorimage. Bands showed complexes of the RRE bound to 3, 2, 1 or none viral Rev proteins, as noted by the arrows.

2.2.- Rev-dependent RNA transport assay

To examine if the capacity of Rev to shuttle the viral RNA to the cytoplasm was being affected by the nucleotide substitutions that were located in the gp41/RRE, a Rev-dependent RNA transport assay was performed. In this case, the different RREs were studied after cloning them into the reporter pDM628ΔRRE vector (**Figure 13D**). After the transfection of a Rev-expressing plasmid and the pDM628-RRE expressing plasmids, the transcripts produced upon transcription consisted in fragments encoding for the luciferase gene and the RRE and in which both elements were situated between a splicing donor and a splicing acceptor. If these transcripts are not exported by Rev, the

luciferase gene and the RRE would be splice out and hence, cultures would not produce light. However, if Rev is able to interact with the RRE and mediate the export of the transcript to the cytoplasm, the cultures will show the production of light. The efficiency in the shuttle mediated by Rev to the cytoplasmic compartment was analyzed of the different RREs. To determine our background light due to Rev-independent export, a negative plasmid control lacking the RRE was used (pDM628 Δ RRE). Analysis of the quantifications showed that there was not any Rev-dependent transport impairment, suggesting that the nucleotide substitutions tested, and therefore the different structural conformations observed, were not impacting the transport efficiency.

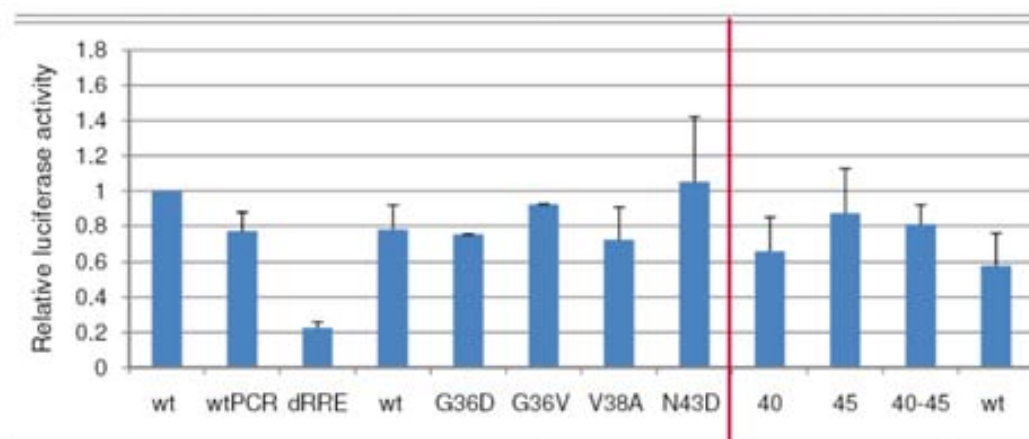


Figure 18: Rev-dependent RNA transport assay. Capacity of the RREs, with different nucleotide substitutions, to being shuttled by the Rev protein to the cytoplasm. Bars represent the ratio between the relative luciferase activity measured in patient-derived RREs and a wt. RRE. Bars represent the mean \pm SD of measurements from 3 independent experiments. Non-significant differences were found by non-parametric Mann-Whitney tests. wt: wild type; wtPCR: wild type (2); dRRE: pDM628 Δ RRE; 40: Q40H; 45: L45M; 40-45: Q40H-L45M.

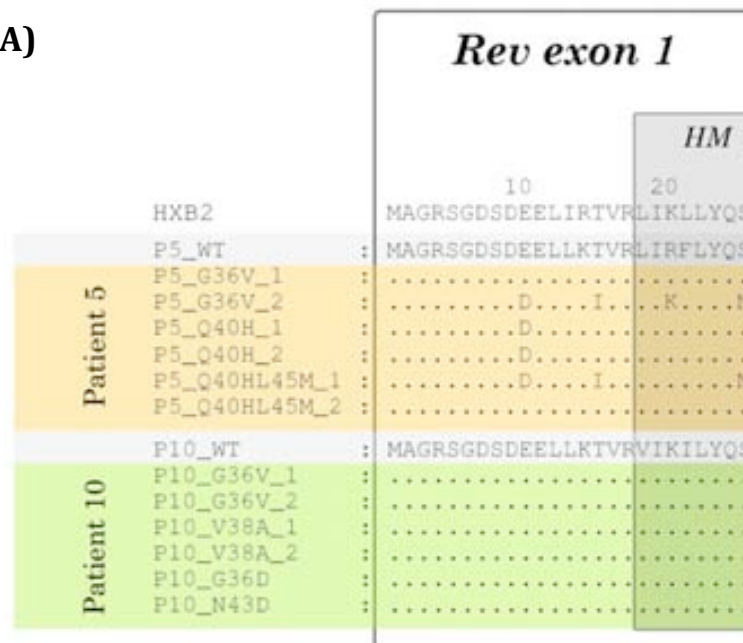
3.- Sequences of the Rev proteins

It has been suggested that changes in the RRE that appeared after T-20 treatment can be compensated by changes in the Rev protein [139]. Thus, in order to determine if any of our RREs were being associated with specific changes in the Rev protein that might regulate the functionality of the RREs, sequencing analyses of both exons of Rev were performed. Rev sequences obtained from full-length Env-expressing plasmids derived

Results

from patient 10 and patient 5 were aligned (**Figure 19**). Plasmids derived from patient 10 having the G36V, G36D, V38A or N43D mutations during the treatment were compared against the sequence at baseline treatment. Compensatory mutations in the *rev* gene in the sequences from patient 5 that harbored the G36V, Q40H and Q40HL45M mutants were also checked. The homomultimerization domains (HM; amino acids 18-26) of the Rev proteins were conserved between clones of the same patient, having only polymorphic changes that were not associated to specific resistance mutations located in the RRE (**Figure 19A** and **B**). At the Nuclear Localization Signal/RRE Binding site (NLS/RRE B; amino acids 34-50) only one change was present when comparing to the reference sequence of Rev, although this change was present in all the clones derived from both patients (**Figure 19B**). Finally, the Nuclear Export Signal (NES; amino acids 73-84) did not show any change in any of the clones derived from both patients (**Figure 19B**). The rest of the changes located outside these important domains were not associated neither to particular mutations. These data suggest that Rev is not exerting a role in the functionality of the RREs that were derived from the same virus and is not having a compensatory role.

Figure 19 A)



Chapter 2.- Methodological approach to study the cytopathicity of patient-derived HIV-1 envelope glycoproteins

Different strategies to study the cytopathicity of envelope glycoproteins have been developed by several groups until the date. However, most of the assays measure only fusion capacity and mainly laboratory-adapted or point mutant envelopes have been evaluated. Few efforts have been dedicated to measure clinically relevant envelopes, and no standard method is available to measure all the parameters involved in the envelope-induced cytopathicity.

Because of the central role of gp41 in mediating CD4 cell death, it is important to address the pathogenesis of primary, rather than laboratory-adapted, gp41 proteins to evaluate how changes in gp41 could modify the pathogenesis of the envelope protein. Moreover, because gp41 is involved in CD4⁺ cell loss by different mechanisms, it is important to evaluate absolute loss and bystander CD4⁺ cell apoptosis together with fusion capacity in order to fully characterize gp41-induced cytopathicity.

A methodological approach to study the biological properties of patient-derived Env/gp41 glycoproteins was evaluated using two envelope-expressing cell lines (293T and HeLa). The results showed a differential behavior when envelopes were expressed in each cell line, highlighting the relevance of the selection of the envelope-expressing cell line in *in vitro* assays and especially when the cytopathic properties of impaired or patient-derived gp41 glycoproteins are evaluated.

1.- Plasmids expressing hybrid Envs

The development of this functional assay was performed using 48 hybrid-Envelope expressing plasmids (**Figure 13B**), constructed as described in the methodology section. Briefly, envelopes that were encoded by these plasmids consisted in a gp120 subunit that was derived from a wild type (wt) HIV-1 strain (NL4-3) and 48 distinct gp41 subunits that were isolated from three different patients and which functionalities were unknown. All experiments were performed in parallel with two effector cell lines using the same hybrid-envelope expressing plasmids in each branch to compare the functional measurements in each condition.

2.- Cell lines used to transfect hybrid-Env expressing plasmids

The 293T [159] and, to a lesser extent, HeLa [135,136,160] cell lines have been previously used as effector cells in several cell-to-cell fusion assays, although an extensive comparison between both cellular models has never been made. The potential differences in transfection efficiency, Env processing, delivery of Env proteins to the cell-surface and other different cellular factors between these cell lines could turn one of them more suitable for the evaluation of the Env activity than the other one.

Subsequently to the optimization of the transfection and the cell surface staining procedures for each cell line, both cell lines were transiently transfected with the same 48 hybrid Env-expressing plasmids. Then, the cells were harvested and analyzed for Env expression.

3.- Cell surface expression of HIV-1 hybrid-Env glycoproteins

To analyze the expression of these hybrid Envs we benefit from their common gp120 subunit and we used the human monoclonal antibody 2G12, which binds to a glycosylation epitope in this region [161,162]. The binding capacity of the 2G12 antibody was expected to be equal for all hybrid proteins because all of them were having the same amino acid sequence in the gp120 subunits, and hence, all hybrid proteins had the glycosylation sites conserved. Furthermore, we used an anti-gp120

Results

antibody instead of an anti-gp41, to avoid problems in the recognition of the hybrid proteins because of the different changes in the patient-derived gp41 subunits.

The data obtained by flow cytometry showed that the percentage of Env-transfected cells that were positive for the expression of hybrid Env on their plasma membrane, was different between both cell lines. The percentage of Env-positive cells for the tested Envs was significantly higher in HeLa than in 293T cells ($P < 0.0001$) (**Figure 20A**). Similar statistically significant differences were observed when the Env expression levels were evaluated on these Env-positive populations, as measured by the geomean fluorescence intensity (**Figure 20B**) or by the relative fluorescence intensity, which is the measure of the total Env expression of the effector cells (**Figure 20C**). In addition, the presence of Env in both cell lines was further confirmed by Western blot analysis using the same 2G12 primary antibody that was used by flow cytometry (**Figure 21**).

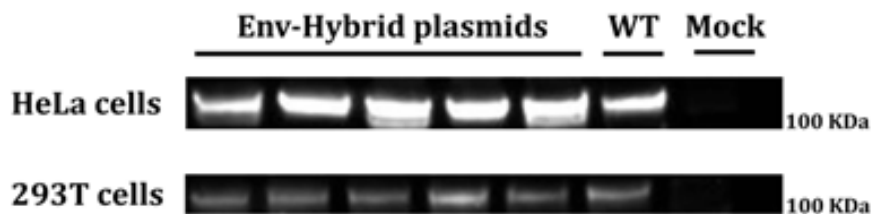


Figure 21: Envelope expression in Env-transfected HeLa/293T cells measured by Western Blot. Western Blot bands corresponding to HeLa and 293T cells transfected with 5 hybrid-Env expressing plasmids, a wild type (wt) Env control (NL4-3) or mock transfected, were obtained using the anti-gp120 primary antibody 2G12.

4.- Analysis of envelope fusogenicity

The function of the HIV Env glycoprotein is to facilitate the entry of the viral nucleocapsid into the target cell. This process has an important role in HIV pathogenesis, and the fusogenic activity of HIV Env has long been associated with cytopathic effects [148,163] both *in vitro* and *in vivo* [164-166].

In this methodological approach the fusion capacity was evaluated using an HIV-LTR-driven luciferase reporter gene assay using TZM-bl cells. Six hours after coculturing Env-expressing cells with reporter TZM-bl cells, luminescence was measured to quantify the fusion capacity of each hybrid envelope. This time point provides detectable levels of luciferase activity that are not influenced by the death of syncytia and are, hence, the direct result of fusion [159]. The capacity to mediate fusion of these Env was significantly different when they were expressed in the 293T cells or in the HeLa cells ($P=0.018$, **Figure 22A**, gray bars). The fusion values (RLU, relative luminescence units) were higher in the 293T cell subset and this finding was not due to a higher cell-surface expression because the expression in the 293T cells was significantly lower than in the HeLa cells (**Figure 20**). One possible explanation for the different values in absolute fusogenicities between both cell lines could be a difference in fusion kinetics. Thus, a faster fusion kinetic of the 293T cell subset expressing Env could have resulted in the observed higher luminescence values. However, when the fusion capacity was analyzed for two wild-type (wt) envelopes (NL4-3 and LaI) over time in a 52-hour coculture, the same kinetic was observed in both effector cell types. The fusion signal was detectable as early as 2 hours after beginning the cocultures of reporter and Env-expressing cells, and it reached a plateau at 12-24 hours (**Figure 22B**). Thus, despite displaying the same fusion kinetic as HeLa, Env-expressing 293T cells showed a higher ability to develop fusion during the entire 52-hour coculture.

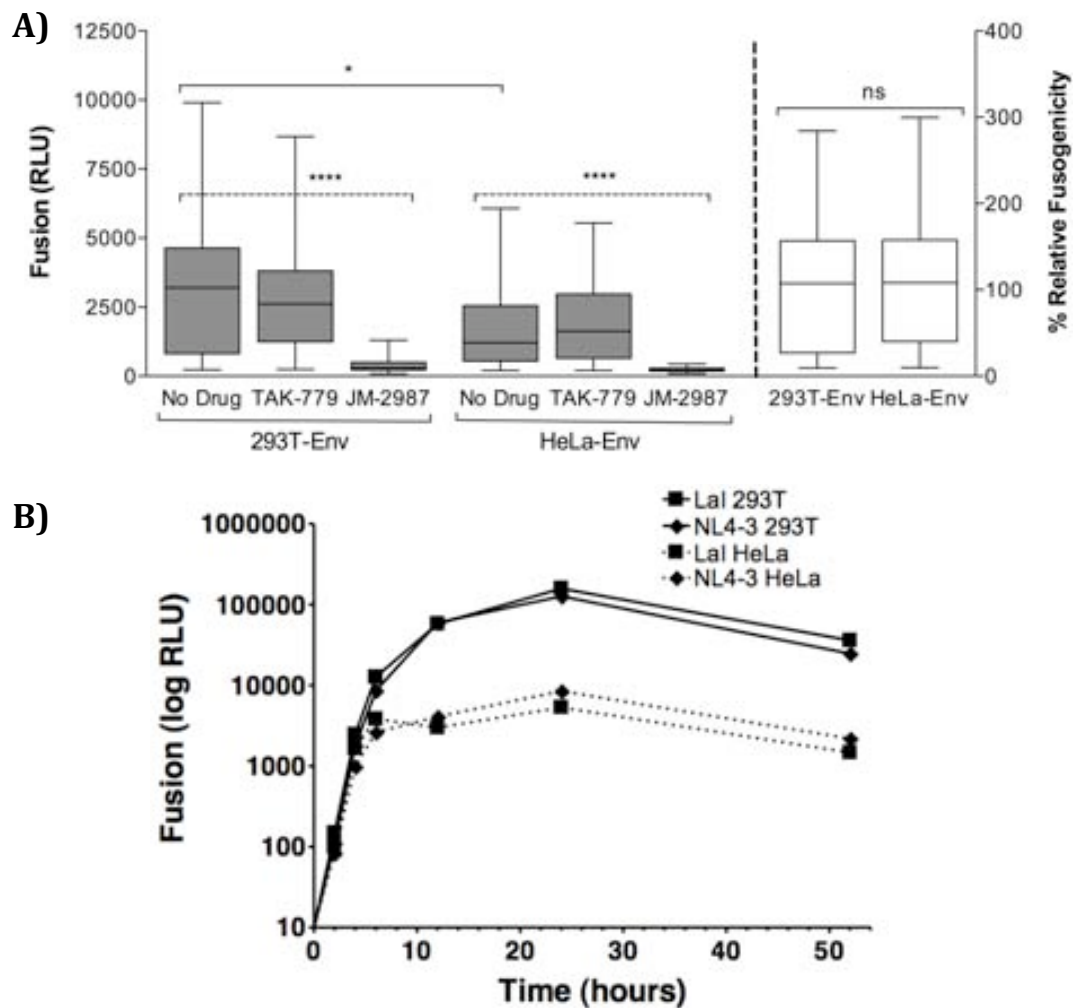


Figure 22: Fusion mediated by Env glycoproteins expressed in 293T and HeLa cells. (A) Fusion capacity was analyzed at 6 hours of coculture between 293T/HeLa cells expressing envelopes and TZM-bl-reporter cells. Cocultures were performed in the absence or the presence of either the CXCR4 or the CCR5 antagonists JM-2987 and TAK-779, respectively. Absolute fusion values obtained in absence or presence of the inhibitors are represented as gray boxes. The relative fusogenicity of each recombinant Env was calculated upon normalization against the fusogenicity of the recombinant envelope of NL4-3 (100%) for each experiment (white boxes). Median values obtained with 293T or HeLa cells without drugs or obtained in the presence or absence of the JM-2987 inhibitor in each cell type were compared using nonparametric MannWhitney tests. **(B) Kinetics of Env-mediated fusion with 293T/HeLa cells.** 293T cells (solid line) and HeLa cells (dotted line) were transiently transfected with NL4-3 (diamonds) and Lal (squares) envelopes and cocultivated with TZM-bl cells. Luminescence was measured at different time-points

Results

during the coculture. Ns, no significant differences; *Statistically significant differences ($p < 0.05$); RLU, relative light units.

The increased fusion efficiency in the 293T cells, as measured by luminometry, paralleled a higher syncytium formation in the culture, as determined by optical microscopy, with a destruction of most of the culture after 24 hours of coculture (**Figure 23**).

To monitor the reproducibility of the fusion assays that were being performed at 6 hours between effector and reporter cells, a control envelope (the NL4-3 wt) was transfected in each cell line and was included in each experiment. Importantly, when the data of the patient-derived envelopes were normalized to the control values obtained in each experiment (100%), the fusogenicities obtained by both cell lines become not significantly different ($P=0.915$) (**Figure 22A, white bars**). To monitor for the specificity of the fusion assay, coreceptor inhibitors were used. Accordingly to the design of the hybrid clones, which had a common X4-tropic gp120 subunit, the tropism of all Envs was X4-tropic. Thus, the fusion values displayed by all recombinant clones was inhibited when the CXCR4 inhibitor, JM-2987, was added to the cocultures, but not when it was used the CCR5 inhibitor, TAK-779 (**Figure 22A**).

The relevance of the differences in absolute fusion was evaluated using an Env mutant (D589L) described previously as defective in cell-to-cell fusion [135]. This mutation is located in the distal end of the HR1 and seems to affect the formation and dilation of fusion pores, being blocked the completion of the fusion process. To rule out the effect of other changes along the envelope sequence, this point mutation was introduced by site-directed mutagenesis into different backgrounds (NL4-3 and LaI) and complete fusion was evaluated in a 24-hour period when cocultured with reporter cells. At 6 hours of coculture, neither of the two D589L variants (D589L-NL43 and D589L-LaI) showed a clear ability to fuse when the envelopes were expressed in HeLa cells (9% and 14% when using the NL4-3 and the LaI variants, respectively), as was shown previously by another group [135] (**Figure 24**). At this time-point both variants (D589L-NL43 and D589L-LaI) showed fusion activities (43% and 27%, respectively) when 293T cells were used as effector cells. However, longer durations of the cocultures showed that the D589L mutants were fusogenic in both cell lines and that the fusion values of these

mutants were lower, but comparable, than their respective wt forms (**Figure 24**). Thus, these results highlight the importance of choosing the effector cell line in fusion readouts and suggest a higher sensitivity of the 293T-based fusion assay.

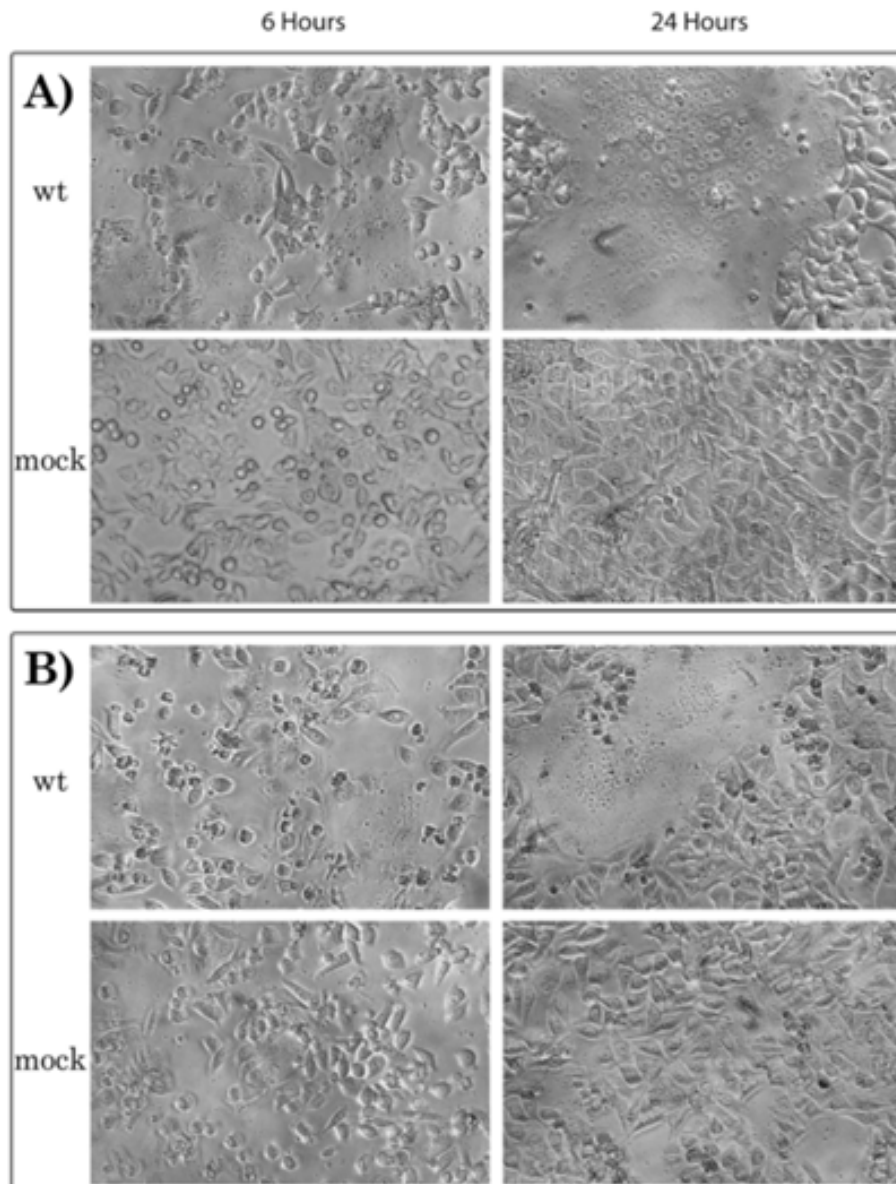


Figure 23: Cocultures at 6h and 24h between Env⁺ cells and TZM-bl cells. Appearance of the cocultures performed with Env-293T (A) or Env-HeLa cells (B). Syncytium formation in the cocultures done with effector 293T cells expressing wt NL4-3 envelopes were bigger and more numerous than when were used HeLa in the same conditions. Pictures used to assemble this figure were chosen to display the ability of both effector cells to develop fusion and may not show the real quantitative differences observed under the microscope due to the small optical field chosen. Negative controls were performed with mock-transfected 293T cells and HeLa.

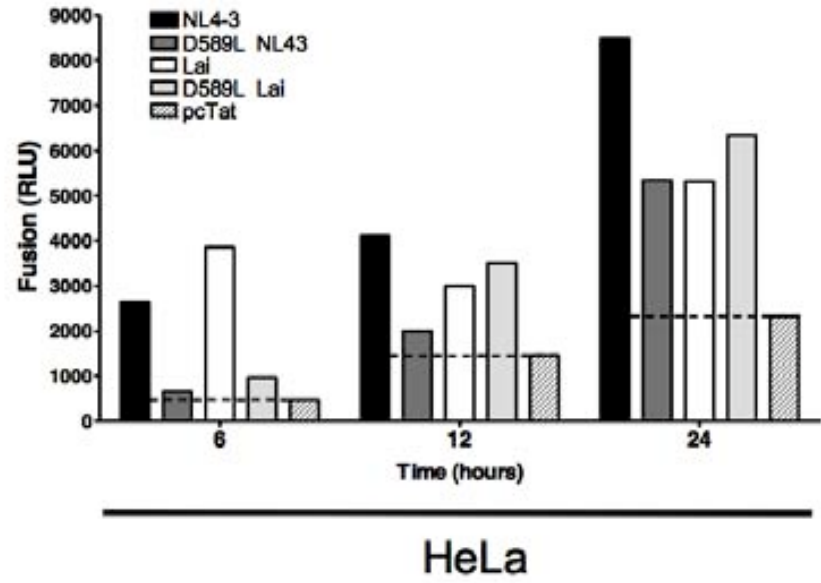
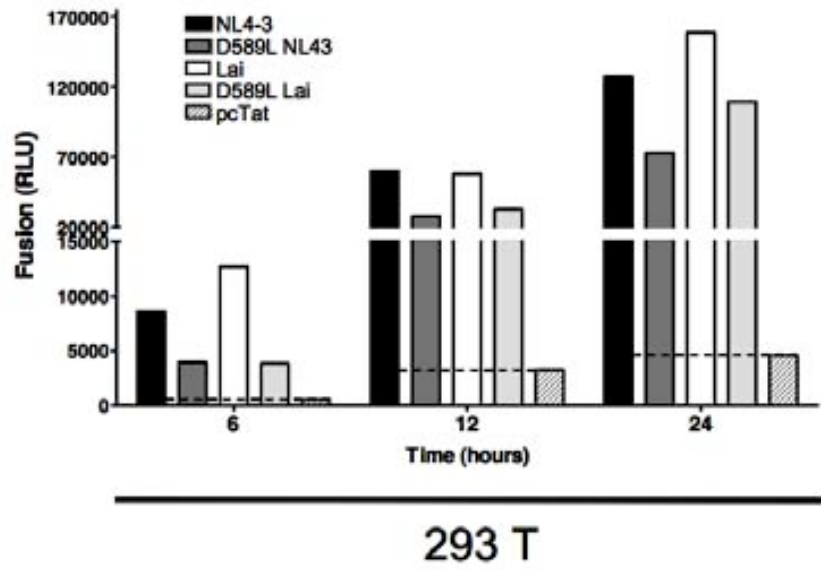


Figure 2. Fusion of NL4-3 and D589L NL43 with Lai and D589L Lai in 293 T and HeLa cells. Fusion was measured by RLU at 6, 12, and 24 hours post-transfection. pcTat is the control. Error bars represent standard deviation.

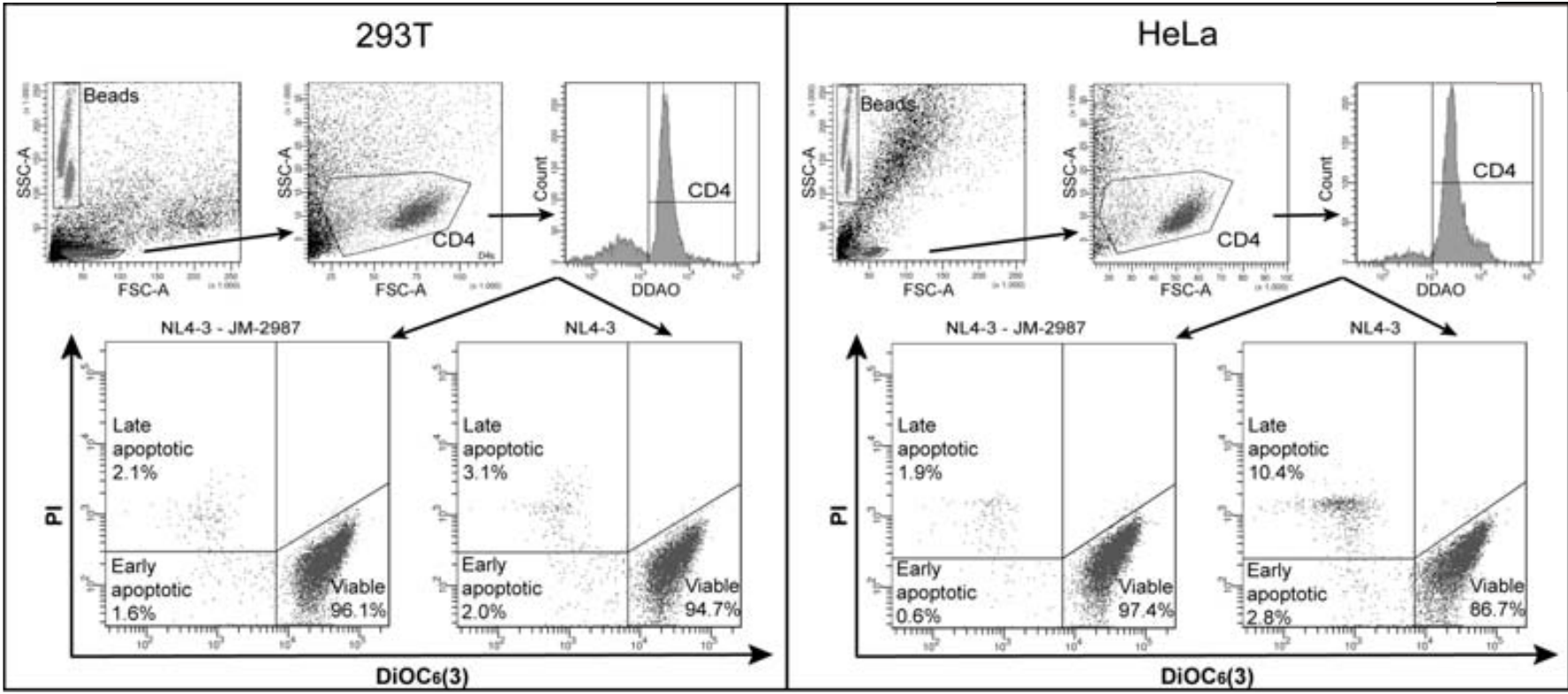
5.- Quantification of the Env-induced cytopathicity in CD4⁺ T cells

5.1.- Analysis of Env-induced bystander apoptosis

In addition to fusion, it has been shown that the Env glycoprotein plays an important role in the depletion of CD4⁺ T cells by inducing single bystander cell death [161]. The key role of the gp41 subunit in the induction of this bystander CD4⁺ cell death [68,135,167] established the basis for our experimental design of the hybrid Envelopes and the use of gp41 subunits that were fully derived from HIV infected patients let us discriminate the functional effects of specific gp41 subunits.

The cytopathic effects observed in primary CD4⁺ T cells by these patient-derived envelopes were evaluated by quantifying the Env-induced single cell death. Cocultures of both Env-transfected 293T and HeLa cells with purified CD4⁺ T cells were analyzed at 24 hours by flow cytometry after staining with Propidium Iodide and DiOC₆(3), to determine plasma membrane function and mitochondrial transmembrane potential, respectively. The CD4⁺ T cells that entered into the apoptotic pathway lose DiOC₆(3) staining and gained Propidium Iodide staining because of the loss of mitochondrial transmembrane potential and a progressive loss of plasma membrane integrity (**Figure 25A**) [164]. Apoptosis culminates in the development of secondary necrosis, which is characterized by Propidium Iodide-positivity and DiOC₆(3)-negativity, similar to primary necrotic cells (**Figure 25A**). Each hybrid Env was analyzed in both effector cell lines in the absence and presence of JM-2987. The use of this anti-CXCR4 inhibitor let us discriminate between the background death due to *in vitro* coculture conditions and the specific Env/gp41-mediated single cell death of primary CD4⁺ T cells [68,68,106,132,168]. Thus, the specific gp41-mediated apoptosis in CD4⁺ T cells for each Env was individually calculated by the subtraction of the background death obtained in the presence of the JM-2987 to the total death detected in the absence of the inhibitor (**Figure 25A**). The Env/gp41-mediated bystander apoptosis analyzed for 37 hybrid envelopes showed a significantly lower apoptosis induction when they were expressed on 293T cells than when they were expressed on HeLa cells (P<0.0001, **Figure 25B**).

Figure 5: *in vitro* ?



Results

5.2.- Analysis of the Env-induced absolute loss of CD4⁺ cells

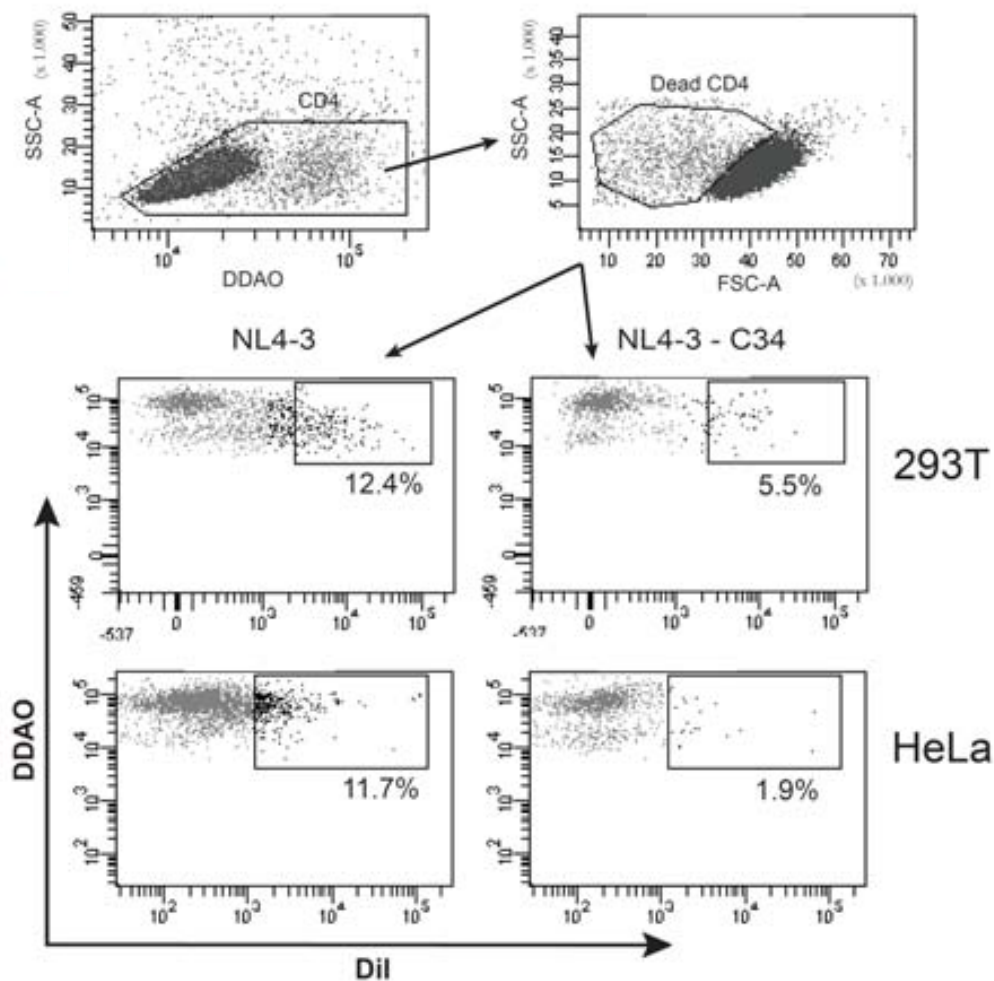
To fully characterize the Env-induced cytopathicity, in addition to the Env-induced single cell death, the total destruction of CD4⁺ T cells was evaluated by analyzing the disappearance of CD4⁺ cells from the coculture due to syncytium formation. In this experimental approach, we used both effector cell lines and the same gating strategy as in the analysis of the Env-induced single cell death (**Figure 25A**). The absolute count of viable CD4⁺ T cells remaining in the culture was quantified and the absolute cell loss was calculated by adding fluorescent-microbeads in each sample (**Figure 25A**). Contrary to the apoptosis induction but in correlation with the absolute fusion data, the absolute loss of CD4⁺ cells was significantly higher when the envelopes were expressed on 293T cells (P=0.037) (**Figure 25C**), again suggesting a difference in the hemifusion/fusion processes between both cell lines.

6.- Analysis of the Env-induced hemifusion activity

The envelope-induced single cell death has been associated with a specific gp41-mediated transfer of lipids from the membranes of Env-expressing cells to the membranes of target cells in the absence of detectable cell-to-cell fusion (hemifusion process) [68,135,148]. To further analyze the hemifusion processes mediated by the Env and to confirm the different observed behavior between these two processes depending on the effector cell line, the capacities to mediate hemifusion of different Envs were evaluated. Three Envs were used in this assay: the NL4-3 wt and two point mutant envelopes: the D589L Env-mutant, which was described previously as defective in cell-to-cell fusion but able to mediate hemifusion [135], and a 41.2 envelope, which could not fuse or hemifuse due to a mutation introduced at the second amino acid of gp41 (in FP) [169,170]. A lipophilic dye transfer assay was performed between each effector cell (Env-transfected 293T/HeLa cells), which were labeled with the cell tracker DiI, and primary CD4⁺ T cells, which acted as target cells and were stained with DDAO. Cocultures of both previously labeled cells were performed in the presence or absence of the fusion inhibitor, C34, which has been shown to inhibit hemifusion processes [68], and flow cytometry was used to analyze the transfer of lipids between cells. First, to determine this lipidic transfer, the primary CD4⁺ T cells that were

morphologically dead were identified and were specifically selected by their positive DDAO staining, which was their original cell tracker labeling. As expected, cocultures resulted in the appearance of double-labeled $CD4^+$ T cells ($DDAO^+DiI^+$) in the morphologically dead population, which were the primary cells that hemifused and that partially mixed their membrane lipids with the Env-expressing cells (**Figure 26A**). As shown in **Figures 26A** and **26B**, although both effector cells induced detectable levels of hemifusion, the dye's transfer was higher in the cocultures performed with HeLa as effector cells than in the cocultures where the 293T cells were the effectors. The higher signal-to-noise ratio that was obtained when the HeLa-Env cells were used as effectors allowed the quantification of hemifusion events induced by the D589L mutant, but not when 293T-Env cells were used. Overall, these data suggested that HeLa-Env cells provide higher sensitivity in hemifusion assays.

Figure 26B: **Quantification of hemifusion events.**



Results

B)

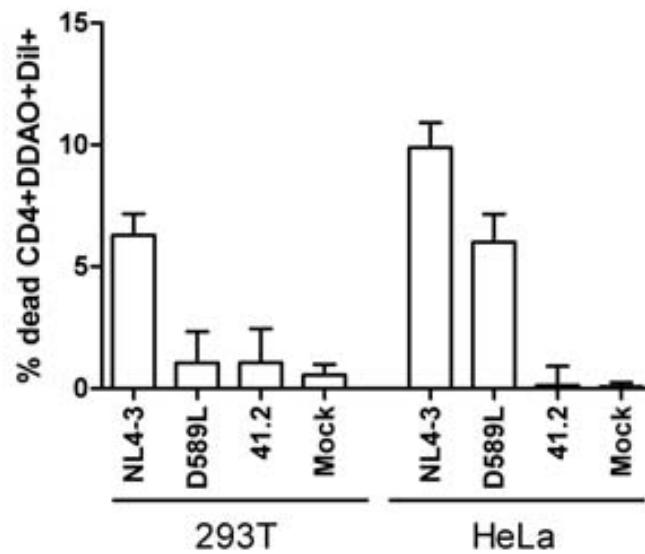


Figure 26: Hemifusion mediated by different HIV-1 envelopes with CD4⁺ T cells.

(A) Representative gating strategy used to characterize hemifusion. Cocultures of primary CD4⁺ T cells stained previously with a cell tracker (DDAO) and 293T/HeLa Env-positive cells labeled with the lipophilic DiI dye were performed and analyzed for dye transfer after 24 hours of coculture by flow cytometry. Single non-fused CD4⁺ T cells were gated by DDAO cell tracker staining and dead cells were identified in a forward- vs. side-scatter plot. **(B) Hemifusion data for the NL4-3, D589L and 41.2 mutant envelopes when expressed on 293T and HeLa cells.** Gp41-induced specific dye transfer to the dead CD4⁺ T cell populations is shown by subtracting the transfer detected in the presence of the fusion inhibitor, C34. Data shown are the median of 4 different donors. Data were expressed as means + SD.

Chapter 3.- Pathogenicity of patient-derived gp41 glycoproteins with specific changes in HR1 and HR2

The Env glycoprotein plays a crucial role in the depletion of CD4⁺ T cells by inducing the death of single bystander cells, which is mediated by gp41. Therefore, changes in gp41 that emerge under T-20 pressure could induce a change in the viral pathogenicity. Clinical findings have suggested that certain T-20-resistant mutants arising during salvage therapy, specifically those harboring the cluster V38A+N140I, are associated with an increase in CD4⁺ cell counts, even after virological failure [132,171]. Site-directed point mutations at position 38 in gp41 have been shown to exhibit deficiency in cell-to-cell fusion activity and apoptosis induction *in vitro*. However, it is important to note that the genetic background is relevant for functional evaluation of T-20 resistant Envs due to they may accumulate compensatory changes to restore the infectivity of the virus.

Using the methodological approach described in this thesis (*Chapter 2*), the pathogenicity of several patient-derived gp41 proteins isolated from highly experienced patients receiving a T-20-containing salvage therapy with changes at position 38 and 140 were evaluated.

Our results indicate that the primary gp41/Env proteins, with both V38A and N140I changes, induced lower levels of single cell death and depletion of CD4⁺ T cells, although they retained cell-to-cell fusion activity. However, the V38A mutation in context with a 140N or 140T change did not alter the Env functions, underscoring the importance of the Env genetic background in the modulation of the cytopathic effects of HIV-1 Env glycoproteins.

1.- Patients and plasmids expressing hybrid Envelopes

From our previously characterized heavily-pre-treated HIV-1 infected patients that received T-20 salvage regimens (**Table 1**), 48 hybrid-Env expressing plasmids were constructed. The constructions were made from three patients who had mutations associated with resistance to T-20 at position 38 of gp41 but differed in the amino acids found at position 140 (**Tables 1 and 3 and Figure 27**). Two plasma samples from each patient, which were collected at baseline and during treatment, were used to construct full-length Env-expressing plasmids. The selection of the plasmids expressing Env with the changes that were wanted to be test at positions 38 and 140 of gp41 was performed.

Table 3. Characteristics of the three patients receiving an enfuvirtide-containing salvage therapy when samples were collected.

Patient ^a	Sample	Weeks on ENF treatment	Plasma viral load (copies/mL)	CD4 ⁺ cell count (cells/ μ l)	No. of expression plasmids constructed
140N (9)	140N	0	366357	491	5
	V38A 140N	24	8536	700	8
N140T (10)	N140T	0	141497	13	10
	V38A N140T	4	332794	13	9
N140I (1)	N140I	0	33470	145	10
	V38A N140I	12	10806	150	6

^aThe patient IDs from a previous work [29] are indicated in parentheses.

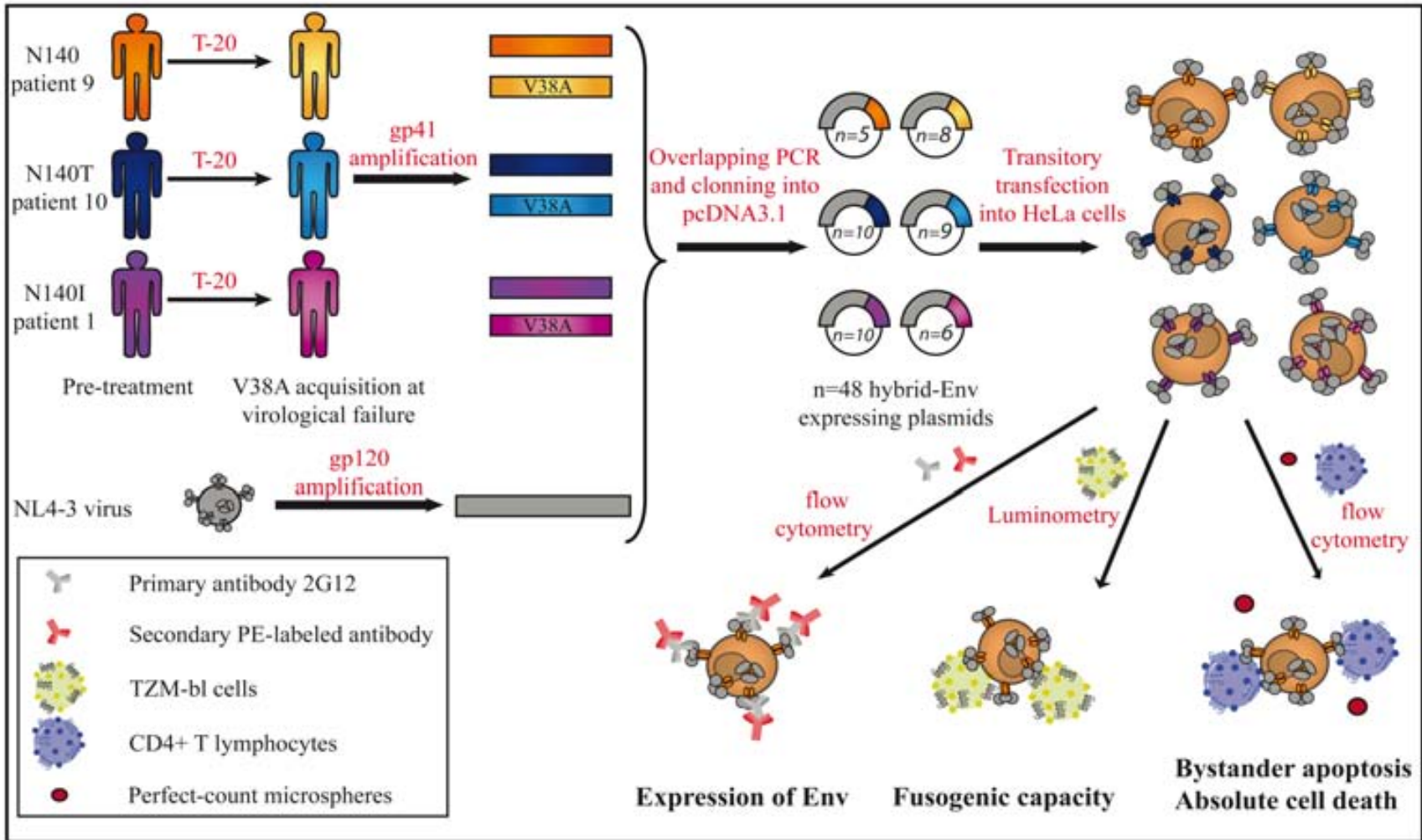
Then, plasmids expressing hybrid Envelopes were constructed (all bearing gp120 derived from an NL4-3 virus and gp41 derived from each of the patient's sample). All hybrids Env expressed in the selected plasmids were fully sequenced to verify that the gp120 subunit had a conserved sequence among all clones and that the NL4-3 wt fragment remained unchanged (**Figure 28A**). All the clonal sequences had a gp120 almost identical in all their nucleotides to the NL4-3's subunit. Importantly, no changes were observed in the region coding for the Env signal peptide, in any of the five variable loops or elsewhere in this gp120 subunit (**Figure 28A**). Among these plasmids, 13 clones were derived from patient 9, containing an asparagine at position 140 (140N) and the wild-type (wt) amino acid at position 38 (38V) or an alanine at position 38 (38A) (n=5 and n=8, respectively); 19 clones were derived from patient 10, who contained the substitution N140T and the wt 38V (n=10) or the V38A mutation (n=9); and finally, 16 clones were derived from patient 1, who had the polymorphism N140I and the wt amino acid at position 38 (n=10) or the V38A mutation (n=6, **Figure 28B**). Since we cloned the full gp41 protein found *in vivo*, we were able to identify other

Results

changes throughout the gp41 protein in addition to the changes at positions 38 and 140. Changes were found primarily in the HR2 domain, but also upstream and inside the HR1 domain and in the loop section. Most of the hybrid-Env expressing plasmids constructed from sequences obtained during T-20 treatment carried the V38A mutation as the only change associated with T-20 resistance, although four clones derived from the 140N patient carried the N42T mutation and three others showed the N126K mutation. The analysis of a caveolin-1 binding motif in the gp41 protein, which has been recently reported to affect HIV-1 pathogenesis [168,172], showed that only one plasmid from the patient harboring the 140N background carried an M to V substitution at position 115. The remaining plasmids constructed with sequences from this patient and all of the hybrid constructs from the other two patients showed no changes in this region before or after treatment (**Figure 28B**).

Figure 27: Methodological approach to study the cytopathicity of patient-derived HIV-1 Env glycoproteins. Plasma samples from patients 9, 10 and 1 were used to construct hybrid-Env expressing plasmids to study the capacity of their Envs to being expressed, to fuse and to develop bystander apoptosis and absolute cell death to target cells.

2222222222



2

2222222222

	Env Signal Peptide																
	* 10	* 20	* 30	* 40	* 50	* 60	* 70	* 80	* 90	* 100							
NL4-3	MRVKEKYQHLNRWGWKWTMLLGI	MLICSA	TEKLWVT	VYVYGV	PVWKEAT	TLFCASDA	KAYDTEV	HNVWATH	ACVPTDP	HPQEVV	LVNVTE	HFNMKN	DMVEQ	MH			
140N-WT			
140N-38A			
140T-WT			
140T-38A			
140I-WT			
140I-38A			
	V1 Loop					V2 Loop											
	110	* 120	* 130	* 140	* 150	* 160	* 170	* 180	* 190	* 200	* 210						
NL4-3	EDIISLWDQSLKPCVKLTPL	CVSLKCTDLKND	TNTNSSSGRM	IMEKGEIK	NCFSNIST	SIRDKVQ	KEYAFFY	KLDIVP	IDNTSYRL	IS	CNTSVITQACPKVSEFEP						
140N-WT						
140N-38A						
140T-WT						
140T-38A						
140I-WT						
140I-38A						
	V3 Loop																
	* 220	* 230	* 240	* 250	* 260	* 270	* 280	* 290	* 300	* 310							
NL4-3	IPIHYCAPAGFAILKCN	KTIPNGTGPCT	INVSTVQCT	HGIRPVV	STQLLNGSL	AEEDVVIR	SANFTD	NAKTIIV	QLNTS	VEINCT	RPNNTR	KSIRIQ	RGPGRAF				
140N-WT				
140N-38A				
140T-WT				
140T-38A				
140I-WT				
140I-38A				
	V4 Loop																
	320	* 330	* 340	* 350	* 360	* 370	* 380	* 390	* 400	* 410	* 420						
NL4-3	VTIGKIGNMRQAH	CNISRAK	WNATLKQI	ASKLREQ	FGNNKTI	IFKQSSGG	DPEIVT	HSFNC	GGEFFY	CNSTQL	FNSTWF	NSTW	STEGSN	TEGSDTITLPCR			
140N-WT			
140N-38A			
140T-WT			
140T-38A			
140I-WT			
140I-38A			
	V5 Loop																
	* 430	* 440	* 450	* 460	* 470	* 480	* 490	* 500									
NL4-3	FINMQE	VGRAMY	APPISGQ	IRCSS	NITG	LLLRD	GGNN	NGSEIF	RPGGG	DMRD	NWRSE	LYKY	VVKIE	PLGV	APTAK	RRVVQ	REKR
140N-WT
140N-38A
140T-WT
140T-38A
140I-WT
140I-38A

2222222222

	HR1										HR2														
HEB2	LTVQARQLLSQTVQCCSNLLRAIEAQQHLLQLTVWGIKQLQARILAVERYLKDQQLLGINGCSGKLICTTAVFPHASWENKSLG										MSNTWQWQREISNYTSLINSLIERSQDQEQNKQELLELDKQASLAGMNFYITM														
HL4-3	LTVQARQLLEDVQCCSNLLRAIEAQQHLLQLTVWGIKQLQARILAVERYLKDQQLLGINGCSGKLICTTAVFPHASWENKSLG										MSNTWQWQREISNYTSLINSLIERSQDQEQNKQELLELDKQASLAGMNFYITM														
	LTVQARQLLSQTVQCCSNLLRAIEAQQHLLQLTVWGIKQLQARVLAVERYLKDQQLLGINGCSGKLICTTAVFPHASWENKSLG										MSNTWQWQREISNYTGLIYTLIERSQDQEQNKQELLELDKQASLAGMNFYITM														
N140	140N-WT.01													
	140N-WT.03													
	140N-WT.05													
	140N-WT.06													
	140N-WT.13													
	140N-38A.01	A									K												
	140N-38A.03	A									K												
	140N-38A.07	A									A												
	140N-38A.09	A									S												
	140N-38A.13	A									K												
	140N-38A.14	A									K												
	140N-38A.15	A									K												
	140N-38A.19	A									V												
	140T-WT.03	R	Q							F	A	RS	D	K	I	LT	Q	E	W	K	H	N	N	TH
	140T-WT.04		Q							F	A	RS	D	K		LT	Q	E	W	K	H	N	N	TH
	140T-WT.07		Q							F	A	RS	D	K		LT	Q	E	W	K	H	N	N	TH
	140T-WT.08		Q							F	A	RS	D	K		LT	Q	E	W	K	H	N	N	TH
	140T-WT.10		Q							F	A	RS	D	K	I	LT	Q	E	W	K	H	N	N	TH
	140T-WT.13		Q							F	A	RS	D	K	I	LT	Q	E	W	K	H	N	N	TH
	140T-WT.18		Q							F	A	RS	D	K	I	LT	Q	E	W	K	H	N	N	TH
	140T-WT.20		Q							F	A	RS	D	K	I	LT	Q	E	W	K	H	N	N	TH
	140T-WT.21		Q							F	A	RS	D	K		LT	Q	E	W	K	H	N	N	TH
	140T-WT.22		Q							F	A	RS	D	K		LT	Q	E	W	K	H	N	N	TH
N140T	140T-38A.13	A	Q							F	A	RS	D	K	I	LT	Q	E	W	K	H	N	N	TH
	140T-38A.20	A	Q							F	A	RS	D	K	I	LT	Q	E	W	K	H	N	N	TH
	140T-38A.22	A	Q							F	A	RS	D	K	I	LT	Q	E	W	K	H	N	N	TH
	140T-38A.26	A	Q							F	A	RS	D	K	I	LT	Q	E	W	K	H	N	N	TH
	140T-38A.27	A	Q							F	A	RS	D	K		LT	Q	E	W	K	H	N	N	TH
	140T-38A.28	A	Q							F	A	RS	D	K		LTK	Q	E	W	K	H	N	N	TH
	140T-38A.29	A	Q							F	A	RS	D	K	I	LT	Q	E	W	K	H	N	N	TH
	140T-38A.30	A	Q							F	A	RS	D	K	I	LT	Q	E	W	K	H	N	N	TH
	140T-38A.32	A	Q							F	A	RS	D	K	I	LT	Q	E	W	K	H	N	N	TH
	140I-WT.1			T	A	G	SYDH	N	D	ST	T	Q	E	N	K	D	N								
	140I-WT.2			T	A	SYDH	N	D	ST	T	Q	E	N	K	D	N									
	140I-WT.6			T	A	SYDH	N	D	ST	T	Q	E	N	K	D	N									
	140I-WT.7	F		T	A	TYDH	N	D	K	SA	T	H	M	K	D	N									
	140I-WT.8			T	A	SYDH	N	D	ST	T	Q	E	N	K	D	N									
	140I-WT.17			T	A	SYDH	N	D	NV	T	Q	AH	M	K	D	N									
	140I-WT.18	A		T	A	SYDH	N	D	NV	T	Q	AH	M	K	D	N									
	140I-WT.20			T	A	SYDH	N	D	ST	T	Q	E	N	K	D	N									
N140I	140I-WT.21			T	A	SYDH	N	D	ST	T	Q	E	N	K	D	N									
	140I-WT.22			T	A	SYDH	N	D	ST	T	Q	E	N	K	D	N									
	140I-38A.4			T	A	SYDH	N	D	NV	T	Q	AH	M	K	D	N									
	140I-38A.8			T	A	SYDH	N	D	NV	T	Q	E	N	K	D	N									
	140I-38A.16			T	A	SYDH	N	D	NV	T	Q	AH	M	K	D	N									
	140I-38A.19			T	A	TYDH	N	D	K	SV	C	T	H	M	K	D	N								
	140I-38A.34			T	A	SYDH	N	D	NV	T	Q	AH	M	K	D	N									
	140I-38A.35			T	A	SYDH	N	D	NV	T	Q	AH	M	K	D	N									

Position 38

Cav-1 Binding Domain Position 140

Results

Figure 28: Sequences alignment of the hybrid Envelopes constructed from patient samples. (A) Sequence alignment of gp120 clonal subunits. The fragments were aligned to the NL4-3 strain, from which were derived. The env signal peptide, and the five variable loops of this subunit are highlighted. Fragments corresponded to the nucleotides ranging from 6225 to 7757 of the HXB2 genome and were numbered as the relative positions that were corresponding to the gp120 protein's start. **(B) Alignment of gp41 ectodomain sequences (HR1 and HR2 domains)** from the selected hybrid-Env expressing plasmids that carried a V38A mutation (HR1 box) with the amino acid I, N or T at position 140 (HR2 box). The Cav-1 binding domain in the HR2 region is highlighted.

2.- Cell surface expression of HIV-1 hybrid-Env glycoproteins.

As HeLa cells provide higher sensitivity for the evaluation of cell death parameters, we chose this cell line to study the different behavior of all our constructed Env glycoproteins. Cells were transiently transfected with the 48 plasmids expressing the hybrid Env and 24 hours post-transfection, the cell surface expression of Env was analyzed using an anti-gp120 antibody (2G12). All tested Envs were expressed on the cell surface with expression levels ranging from 2.7% to 29.9% of positive cells (**Figure 29A and 29B**). An inter-patient comparison between the grouped Envs derived from each patient irrespective of the sample's time point, showed a percentage significantly different of positive Env-expressing cells between the two groups conformed by the plasmids derived from the 140N patient and the ones derived from the N140T patient (**Figure 29A**). The lowest percentage of Env-positive cells was observed for the 140N constructs (mean= 11.40 +/- 3.9), whereas the highest percentage of Env-expressing cells was observed for the N140T clones (mean= 15.91 +/- 4.4). However, when we analyzed the percentage of cells expressing the Env constructs obtained from the same patient by comparing clones displaying or not the V38A mutation (an intra-patient comparison between the pre- and post-treatment samples, respectively), the Env expression was shown to be similar in all cases (**Figure 29B**). In addition to determine the percentage of positive cells, the Env expression levels, which could play an important role in Env pathogenesis, were evaluated. However, there were no differences in the levels of Env expression in intra-patient comparisons between constructs containing a 38V gp41 and those containing a V38A mutation, as determined by the geometric mean fluorescence intensities (**Figure 29C**), or the relative fluorescence intensities [38,148] (**Figure 29D**). Thus, the intra-patient comparisons suggest that the expression of Env does not change upon acquisition of the V38A mutation, and hence, the levels of Env expression is an intrinsic characteristic of

the particular Env that carried each infected patient. Overall, these results allowed us to analyze the cytopathic effects of Env without correcting for the cell surface expression of each Env.

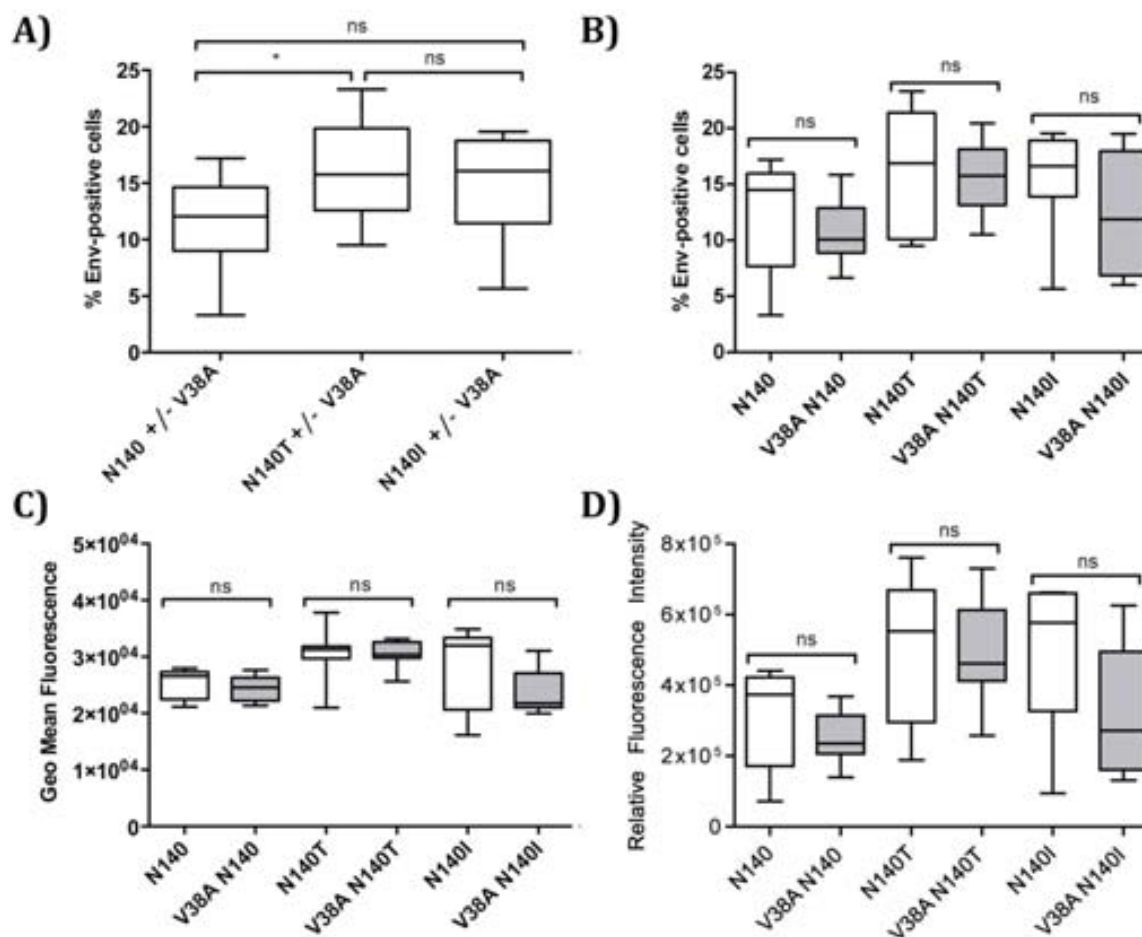


Figure 29: Expression levels of hybrid envelopes on the surface of HeLa effector cells.

Hybrid Envs were transfected into HeLa cells and their expression on the cell surface was analyzed 24 hours later using the 2G12 antibody. **Inter-patient (A) and intra-patient (B) analyses of the Env expression determined by the percentage of Env-positive cells. C) Intra-patient analysis of the Env expression levels expressed in their geometric mean fluorescence. D) Intra-patient analysis of the total levels of Env expression determined by the relative fluorescence intensities (RFI= % of Env-positive cells x geometric mean fluorescence of Env-positive cells).** Baseline samples (white boxes) and V38A samples (gray boxes) for intra-patient analysis, or all grouped samples of each patient (white boxes shown in A)) for inter-patient analysis represent the median and interquartile range of the values. The median values were compared using a nonparametric Mann Whitney test. * $p < 0.05$, *** $p = 0.0006$, and ns denotes non-significant differences.

3.- Analysis of the Env protein fusogenicity

It has been described that single amino acid mutations in the ectodomain (V38A/E) or in the transmembrane region of gp41 reduce cell-to-cell fusion activity of the virus [136,173]. In order to characterize the fusion capacity of our hybrid-Env proteins, all the constructed Envs were first assayed for fusion activity in 293T cells, because as we have demonstrated, they are more sensitive for this evaluation than HeLa. Detectable fusion was observed in all of the Env, showing fusion levels over the 50% when compared with an NL4-3 wt Env. Given that all of our Env were functional, we used HeLa as the effector cell line for the cytopathicity evaluation of our constructs. Thus, these cells were transiently co-transfected with the Env- and the pcTat-expressing plasmids and cocultured with the reporter TZM-bl cells. After six hours of coculture, the luminescence of the samples was measured, and the relative fusion capacity of each hybrid Env was calculated in comparison to the fusion values obtained using the NL4-3 wt Env (100%). The levels of fusion of the Envs obtained from the different patients (inter-patient analysis) showed significant differences when compared between them, underscoring that the virus each patient carries may have an Env with a distinct fusogenic capacity, which in this case, is only determined by gp41 (**Figure 30A**). Differences in fusion were not correlated with the Env expression levels on the cell surface, because higher Env expression levels did not result in an increased fusion capacity (**Figures 29 and 30**). However, in contrast to previously published data [136,137], when intra-patient analyzes were performed, the fusogenic activities of the hybrid Envs from each patient were similar, indicating that in a full-length gp41 background, the V38A mutation did not impair the cell-to-cell fusion activity of Env in the presence of the amino acids N, T or I at position 140 (**Figure 30B**).

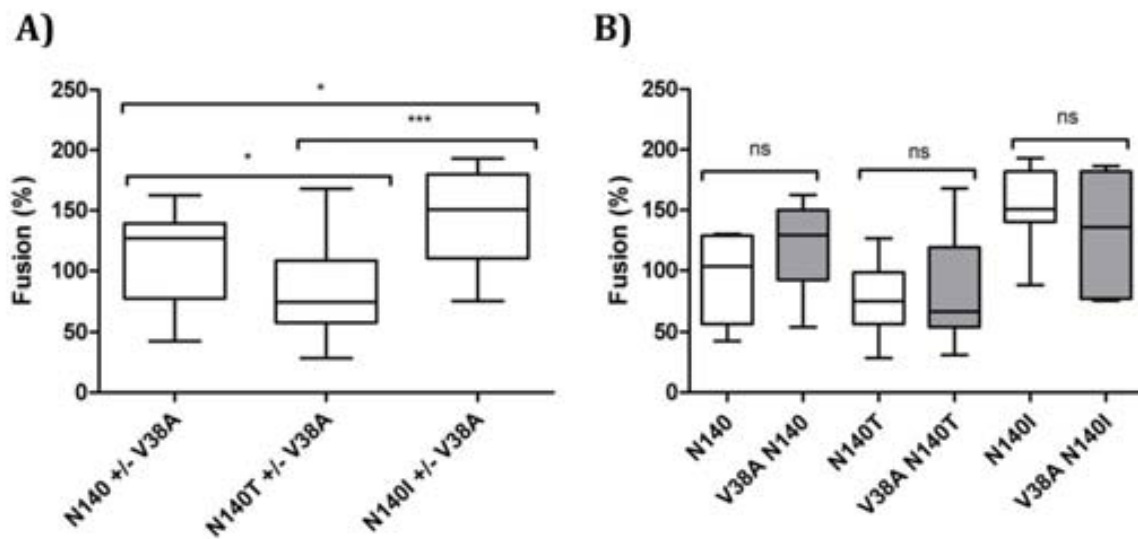


Figure 30: Inter-patient (A) and intra-patient (B) analysis of cell-to-cell fusion values obtained with HeLa cells expressing the different patient-derived Envs with changes at positions 38 and 140 in gp41. Cocultures of Env⁺ HeLa cells with TZM-bl cells were performed for 6 h, and fusion activity was determined by measuring the luciferase activity. The relative fusogenicity of each hybrid Env was calculated by normalization against the luminescence obtained using the hybrid Env of NL4-3 (100%) for each experiment. The boxes represent the median and interquartile range of the values. The median values obtained from the clones constructed from samples from each patient were compared in an inter-patient analysis, and those obtained from baseline (white boxes) and after treatment samples with the change V38A (gray boxes) clones were also compared in an intra-patient analysis using a nonparametric Mann Whitney test. * $p < 0.05$ *** $p = 0.001$ ns, not significant differences.

4.- Quantification of Env-induced absolute loss of CD4⁺ T cells.

In addition to fusion activity, the cytopathic effects of our hybrid Envs were evaluated by quantifying the absolute loss of the purified primary CD4⁺ T cells that were cocultured with HeLa cells that expressed these Envs. Despite the similar observed fusogenic capacity of the wt Envs to those bearing mutations at position 38, the absolute loss of CD4⁺ T cells was significantly lower after their exposure to Envs containing the V38A mutation in a N140I background than after their exposure to 38V Env in that N140I background (18.1% and 31.3%, respectively. $P=0.022$) (**Figure 31A**). In contrast, Env proteins containing either an N or a T at position 140 induced comparable levels of absolute CD4⁺ T cell loss, irrespective of the amino acid present at position 38 (33.4% 38V and 25.6% 38A in an 140N background and 15.8% and 17.0%, respectively, with a N140T change, **Figure 31A**).

5.- Analysis of Env-induced bystander apoptosis.

HeLa cells expressing hybrid Envs were cocultured with primary CD4⁺ T cells. After 24 hours, the culture was stained with propidium iodide (PI) and DiOC₆(3). In an intra-patient analysis of this Env-mediated single cell death, only differences between the N140I recombinant clones were observed when they carried the V38A mutation or the wt form 38V. The clones bearing the amino acids N or T at position 140 showed similar apoptosis-inducing capacity when wt or V38A clones were compared (**Figure 31B**). Thus, the impaired ability to deplete CD4⁺ T cells by the recombinant Envs that contained the cluster of mutations V38A+N140I in the gp41 protein was associated with a significant reduction in apoptosis induction on primary cells (13.4% and 7.4% for baseline and with the cluster of mutation samples, respectively; $P=0.031$).

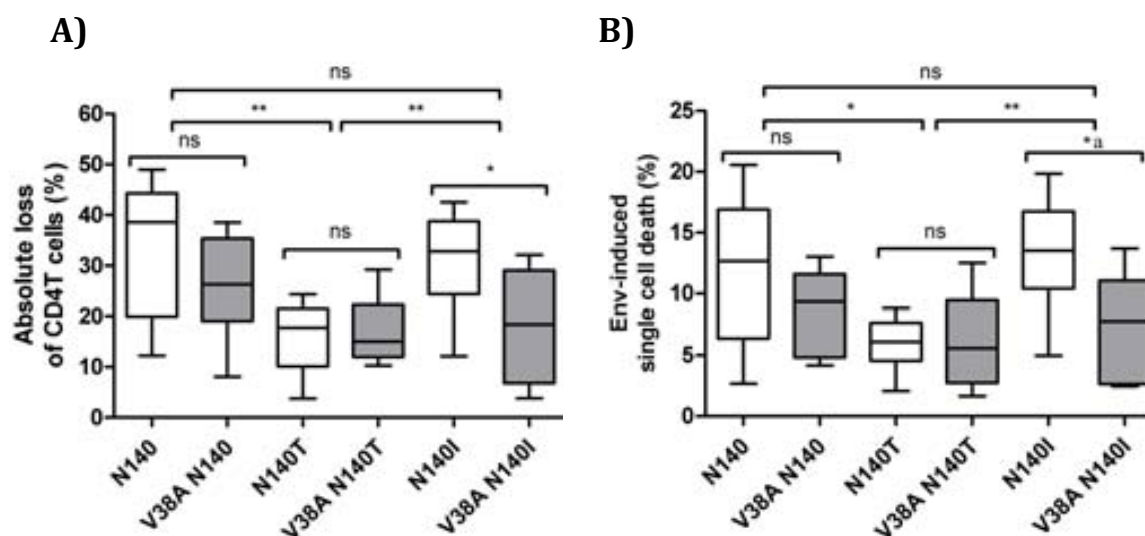


Figure 31: Envelope-induced cytopathicity in CD4⁺ T cells. (A) Envelope-mediated absolute CD4⁺ T cell depletion. Absolute loss of CD4⁺ T cells in cocultures of HeLa-expressing Envs and purified CD4⁺ T cells was determined. Single living CD4⁺ T cells were morphologically gated, and the absolute loss of CD4⁺ T cells in the coculture was quantified by the addition of PE-labeled microbeads. * p=0.022, **<0.007. **(B) Bystander apoptosis induced by envelopes harboring changes at position 38 and 140 in gp41.** Cocultures of primary CD4⁺ T cells, previously stained with the DDAO cell tracker, and HeLa Env⁺ cells were performed and analyzed after 24 hours by flow cytometry. Single, nonfused CD4⁺ T cells were gated by the forward- vs. side-scatter characteristics and by being positives for the cell tracker. Detection of early (PI⁻DIOC⁻) and late apoptotic (PI⁺DIOC⁻) populations were determined in this gated population for each hybrid Env in the presence or absence of the coreceptor inhibitor JM-2987. Boxes represent median and interquartile range of values. Median values were compared in an inter-patient and in an intra-patient assay, using a Mann-Whitney test. Baseline samples (white boxes) and V38A mutant clones (gray boxes). *_ap=0.031, *p=0.0213, ** p=0.0038 and ns non-significant differences.

DISCUSSION & PERSPECTIVES

The HIV-1 Envelope (Env) glycoprotein is the most external viral protein in the virions and it plays a central role in HIV pathogenesis and in the primary steps of the viral life cycle. However, the *envelope* gene is not only important for the protein that is encoding, but also for the secondary structure that displays in the RNA transcripts where is present. This secondary structure is called the Rev responsive element (RRE) and is crucial for the proper translation of the viral proteins, the incorporation of the full-length genome into nascent virions and for the correct assembly of infectious virions.

The RRE has a highly conserved stem-loop structure that is important for Rev binding [39,150] and that allows the development of its function [151,171]. Although this secondary structure is governed at the nucleotide level [132,172], the structure, rather than the sequence, appear to be necessary for Rev-RRE interactions [38,174]. Single nucleotide changes within this region could impair its functionality by disrupting conserved base pairs and hence, the secondary structure of the RRE. All the codons encoding the gp41 residues associated with T-20 primary resistance are localized within the RRE. Thus, changes selected upon T-20 treatment could be affecting the structure and the functions of this conserved region. Functional impairments may impact the Rev-RRE interaction, the multimerization of Rev proteins [39,47,48,51,52], the transport of non-completely spliced viral mRNAs to the cytoplasm and the viral replication capacity.

Few reports have characterized the effects of T-20 treatment to the RRE functions. Nameki and colleagues [150] showed that changes developed after T-20 treatment at amino acid positions 36 and 38 of gp41 were predicted to alter the stability of the stem II, and substitutions at position 43 did not affect the overall structure. If the RRE functions were being affected by these secondary structure alterations, compensatory changes could appear in order to restore them. However, these nucleotide changes may not be noticed at the amino acid level because synonymous mutations could be promoting these compensatory effects. In fact, the importance of these changes was specifically demonstrated in the gp41/RRE sequences corresponding to the stem III, showing improvements in *in vitro* viral replication when were present together with changes that were developed after T-20 treatment [151]. The nucleotide substitution encoding for the T18A was suggested to compensate the V38A and to increase its

Discussion & Perspectives

replication capacity by a restoration of the stem IIA; and hence, a possible stabilization of the interaction between RRE-Rev [132]. These suggestions were further confirmed after finding a compensatory evolution between both nucleotide changes in samples obtained from T-20 treated patients [174]. However, the functionalities of all these patient-derived RREs were not specifically tested and all the speculations were based mainly on models of the RRE structure. Therefore, in order to study the effect of different nucleotide substitutions associated with T-20 treatment to the functionalities of the RRE, we purposed to measure them experimentally. To analyze if the predictions of secondary structures were mimicking the functionalities of the RREs we also modeled their structure. For the RRE functional analysis we measured: their capacity to interact with Rev and their ability to being shuttled to the cytoplasm.

The analyses showed that the nucleotide substitutions that encoded the G36V/D (GGT to GTT/GGT to GAT), V38A (GTG to GCG) and N43D (AAT to GAT) amino acid changes do not affect specifically the RRE functions. These RREs displayed the same ability to bind Rev and this protein had the same capacity to shuttle them to the cytoplasm despite the alterations in the predicted secondary structures that were observed in the changes at positions 36 and 38 of gp41. Thus, changes in the predicted secondary structures do not always imply functional impairments. Taking into account the conserved secondary structure that was predicted for the N43D variant, it was expected a functional RRE. However, the alterations in the V38A and the G36D/V structural models suggested functional impairments that were surprisingly not reached in our experiments. The secondary structure alterations observed in the V38A variants were localized in the stems II and III, which had been shown to be important for Rev-binding and function [31,39,44,45,139,151]; and for variants encoding G36D/V changes, the altered stems were the IIB and IIC, which are mainly important for Rev-binding. Specifically, the RRE that encoded the V38A change was expected to have a more impacted function than the G36D/V RREs due to the degree of alteration that was observed in the predicted structure. However, these speculations did not fit with the functional data, as none of these RREs were functionally impaired. Thus, the properties accounting for the new amino acids might govern the impairment in replication kinetics that had been reported for these RRE variants [175,176].

It has been extensively described that in patients treated with T-20, the L45M substitution appears mainly co-selected with other changes associated with resistance to that fusion inhibitor (Q40H, N42S, N42T) [132,133,175,177,178]. Besides, it has been suggested that the L45M change was co-selected with the Q40H in T-20 treated patients to restore its impaired RRE secondary structure and functions [139]. To functionally test these hypotheses, we analyzed RREs derived from gp41 that harbored the changes Q40H, L45M or Q40H-L45M.

The nucleotide substitutions that encode for Q40H (CAG to CAU) and L45M (CTG to AUG) amino acid changes are located in the stem-loop III of the RRE. The positions of these nucleotides originally form a base pair, but with either of these substitutions this base pair is disrupted and consequently the predicted secondary structures of these single mutants are altered. The RRE structures that harbored the nucleotides encoding for the Q40H substitution were less impacted than the ones encoding for the L45M change. The Q40H mutation created a small bulge in the stem III of the RRE, but the nucleotide encoding for the L45M disrupted completely the whole stem III in our predictions. Therefore, from these structure models it was expected a bigger impact in the functions of L45M variants due to the marked alterations that were observed in the structure. However, when both changes were co-present in the same RRE this base pair was restored and the overall structure assembled as it was predicted in the wt sequence. Thus, as suggested previously [139], it was expected a restoration of the RRE functions when both changes were co-present in the same fragment.

The functional data revealed impairments in Rev binding to RREs that were derived from L45M-containing variants (L45M and Q40H-L45M), but not in the RREs that harbored nucleotide substitutions encoding for the single Q40H change. These results suggested a specific influence of the L45M change in the RRE-Rev interactions; especially at low levels of Rev due to the impact at high levels was not that remarkable. However, despite these differential phenotypes in Rev binding, it was not observed any impact in the Rev-dependent RNA transport, which showed comparable values between all RREs. Therefore, consistent with the results obtained with the

Discussion & Perspectives

other RRE variants, assays analyzing the specific functions of the RREs are necessary to determine impairments in the RREs.

Our data suggest that the nucleotides encoding for the L45M change in gp41 is impacting the Rev binding only when this protein is in low concentrations and hence, might not have a relevant impact *in vivo*. The accumulation of Rev proteins during the late phase of the mRNA transcription into the nucleus might increase the levels of Rev over the threshold that is needed for the Rev-dependent transport of L45M RRE variants. Thus, it could be suggested that with high amounts of Rev inside the nucleus, the binding capacity might be specific but less restricted than in relatively low amounts of Rev. Therefore, the overall RRE secondary structure might be important and needed to develop its function [36,149], but little changes outside the high-affinity binding site might be overcome in high levels of Rev proteins, which may imply certain plasticity that has not been suggested yet. This ability to overcome little impairments, may allow viruses to accumulate new changes, replicate and develop resistance to the antiretroviral drugs.

Therefore, other reasons, rather than restoration of the functions of the RREs, appear to select together these Q40H and L45M changes. Properties of the new encoded amino acids could improve the functionality of the Env when co-present in the same glycoprotein after prolonged treatment with T-20. A selection of these double-mutants due to an increase in the T-20 resistance could also be applied due to the single mutants conferred moderate resistance and the double-mutants had strong resistance [151,179,180].

However, as the exportation process are interacting two elements from the virus (RRE and Rev), it could be possible to have a compensatory evolution between them [139]. The RREs that were harboring nucleotide substitutions encoding for the L45M and that were having an impairment at low concentrations of Rev, could be compensated by changes in Rev in order to restore them. The E57A change in the Rev protein was associated with the Q40H-L45M substitutions [139]; however, none of the Rev sequences were having this previously reported compensatory change or any other one.

Further functional approaches should be done in order to understand the limitations of mutated RRE or Rev proteins and in order to develop novel compounds to avoid viral replication by targeting their interactions or their functions [181,182]. As the accuracy of SHAPE analyses are thought to be greater than the bioinformatics tools used to analyze the secondary structures of the RREs, it would be interesting to study these or other nucleotide changes and compare the data between both techniques. Comparative data with functional analyzes, may determine if SHAPE is a good technique to analyze functions, although we might be skeptical taking into account our results.

The main function of the *env* gene apart from the fact that is encoding for this secondary structure important for viral mRNA exportation, and hence, viral replication, is the encoding of the Env glycoprotein. This Env glycoprotein has been widely studied by numerous studies since the discovery of the virus due to its importance in viral entry into target host cells. However, the vast majority of the *in vitro* assays that have been performed to study the cytopathic mechanisms of the HIV-1 Env glycoprotein used point mutant or whole laboratory-adapted HIV strains. In fact, few efforts have been dedicated to measure biological properties of the Envs that might be clinically relevant for physicians [183-185], which might be the ones derived from HIV infected patients. Moreover, until the date is lacking a standard methodology to follow in a single assay the measurements of all cytopathic-related properties of the Env. Therefore, in order to have a well-established methodology to functionally evaluate the Envs expressed in *in vivo*-circulating virions and in HIV infected cells, we developed an *in vitro* assay to measure the expression capacity of the Envs derived from patient samples and their ability to induce single cell death and fusion to target cells [186].

The experiments were based on the construction of hybrid envelopes (Envs) that were partially derived from viruses isolated from plasma samples. The strategy to use a wild type (wt), instead of a homologous gp120, was devised to avoid gp120 interferences in the functional evaluations of patient-derived gp41 due to polymorphisms or distinct genetic contexts in these subunits between the patients. Our experiments were based on the functional study of the gp41 subunit due to this glycoprotein has been extensively proven to have an indispensable role in the pathogenesis of the Env [187] via its essential role in the development of single cell

Discussion & Perspectives

death [68,69,106,161,167,188] and fusion [189,190] *to target cells*. Therefore, in order to avoid gp120-masking effects in these gp41 functional evaluations and to be able to associate clearly specific gp41 mutant subunits with their related biological properties, it was crucial the wt gp120 subunits in these hybrid Envs.

Once we had the hybrid Envs, we wanted to check if the effector cell line affected the assay's sensitivity. Thus, we decided to express the hybrid Envs in two cell lines that had already been used in the analysis of the HIV Env function, the 293T [159,191] and the HeLa [135,136,190,192]. Comparative analyses between the data obtained using each of the effector cells might uncover if the selection of the effector cell line is an important variable to take into account when designing this experiment.

In the last decade, a number of different **fusion** assay systems have been described. The methods used in these reports include the evaluation of the syncytium formation by light microscopy [193] the analysis by flow cytometry of cell-to-cell cytoplasmic transference of fluorescent dyes [194-196] and the use of assays based on resonance energy transfer [197,198]. However, the light microscopy evaluations are prone to subjectivity and the rest of the mentioned assays are really time-consuming. These reasons led us to select the currently wide-used reporter genes for our assay, which are sensitive and quantitative [159,192,199], although do not permit a direct enumeration of the fusion events.

Thus, the fusion capacity was chosen to be evaluated with the TZM-bl reporter cell line, which had a Tat transactivable reporter system that showed high sensitivities to infection with a wide dynamic range [159]. Consistently, in our assay, the fusion was detected after 2 hours of cell mixing and increased over time until a plateau was reached at 12-24 hours in both Env-expressing cell lines. Despite the lower **levels of Env expression** in the Env-293T, these effector cells were still able to display higher absolute fusion values (in relative luminescence units) than Env-HeLa. However, when fusogenic values were normalized to a NL4-3 reference envelope, which was used in each assay as an experimental control, the fusion values obtained by both types of Env-expressing cells became comparable, suggesting that there was an

equivalent Env fusion behavior in both cell lines although the observed differences in absolute values.

To evaluate if the differences observed in fusion between both effector cell lines were relevant for the characterization of this function in primary Envs we used a previously characterized Env point mutant that was described as defective in cell-to-cell fusion [73,135,190], the D589L envelope. This Env when was expressed in the HeLa cell line showed a highly impaired fusion in the standard 6-hours coculture, but was able to fuse when expressed in 293T cells. To further evaluate its ability to develop fusion, these cocultures were maintained for a long period of time and then, it was clearly demonstrated that the D589L mutant was able to fuse when expressed in both tested cell lines. Thus, these data suggested that in standard 6-hours cocultures the fusogenicities measured with HeLa cells as effector might miss-categorize fusion-impaired Envs. Therefore, it should be more appropriate to study the fusion capacity with the 293T cell line due to it showed, for the same conditions, greater efficiencies than HeLa. Alternatively, fusion kinetic assays, although time consuming, may also be useful to accurately evaluate the fusion capacity of impaired Env glycoproteins or Envs derived from patients infected with HIV, which were not previously tested in a fusion assay.

In addition to the fusion capacity, the Env-mediated **cytopathicity** induced in primary cells was also evaluated with each effector cell. To analyze this functionality, cocultures of Env-expressing cells and labeled primary CD4⁺ T cells were performed to evaluate the single cell death induction and the absolute cell loss of target cells.

The analysis of the Env-mediated **single cell death** showed, unexpectedly, lower values when the cocultures were performed with Env-293T cells. This observation seemed to contradict the values obtained in the fusion assay, due to the single cell death had been widely associated with hemifusion processes, which is an intermediate step of the fusion procedure [200]. Thus, our data showed higher fusion levels using Env-293T cells despite displaying lower abilities to induce single cell death, presumably due to hemifusion processes. To further study this fusion intermediate step, it was performed a lipophilic dye transfer assay to quantify the amount of lipid mixing between the outer leaflets of the target and the effector cell membranes due to

Discussion & Perspectives

hemifusion processes. Cells that underwent complete fusion were discarded morphologically by flow cytometry and only single nucleated cells were analyzed, which might be the cells that would die through single cell death if hemifused [68]. The results of our experiment showed lower quantities of lipid mixing between target cells and Env-293T cells, which correlated with the single cell death data. Therefore, Env-293T cells had a lower ability to induce single cell death due to a lower capacity to hemifuse with target cells, although having a huge capacity to undergo complete fusion.

Complete fusion is not always reached when the fusion process is initiated and sometimes is interrupted at the hemifusion step. This situation could occur often, especially *in vivo*, where Env-induced syncytias are rarely seen [99-102]. In agreement with this, Env-293T cells seem to follow a major direct pathway [201], developing a direct transition to the formation of the fusion pore by generating high levels of fusion and lower levels of hemifusion, and hence, single cell death. And in contrast, Env-HeLa cells may mainly follow a slow indirect pathway and might fuse their external leaflets with target cells through a large contact area by inducing greater extents of hemifusion and single cell death while having a low capacity to develop complete fusion.

The **absolute cell loss** of the target cells corresponds to the total death experienced in the cocultures, including the Env-mediated deaths promoted by both fusion and hemifusion processes. Despite the discrepancies between the fusion and the single cell death values, the Env-293T cells were able to kill globally more target cells, suggesting that the huge ability to promote complete fusion masked the lower ability to induce single cell death by this cell line.

It has been described that the gp41-mediated hemifusion that do not progress to the formation of the fusion pore is both required and sufficient to induce apoptosis in bystander cells [68,106]. Furthermore, bystander cell death has been linked to the great depletion of uninfected CD4⁺ cells observed in HIV infected individuals, because of the low levels of productively infected CD4⁺ cells observed *in vivo*, which can not account for the massive target cell depletion observed [107]. Consequently, considering the importance of the single cell death in *in vivo* HIV pathogenesis, the

HeLa (or another cell line that would follow the same functional effector patterns) should be the **preferred Env-expressing** cell line to use in complete functional analyses of patient-derived Envs. Special attention on fusogenic assays must be paid if HeLa cells are used as effector in order to avoid the miss-categorization of impaired fusogenic envelopes into non-fusogenic. Thus, kinetic experiments could be performed when negative fusogenic results were acquired in the standard fusion experiment, to avoid false-negative results because of a lack of sensitivity at shorter times. If the experiments are performed only to analyze the development of fusion, the preferred cell line might be the 293T due to its higher sensitivity in fusion assays. However, a combination of assays should be the perfect recommendation to achieve a global characterization of Env-mediated cytotoxic events, especially when Envs with low fusogenic capacity or Envs derived from patients and that are not previously tested for fusogenicity are tested. Patient-derived and mutant Envs are thought to be less fusogenic than Envs derived from laboratory-adapted strain viruses, so the ability to accurately define the phenotype of these Envs should be of great importance.

Based on our results, comparisons between experiments that use different effector cell lines might incorporate possible alterations in the ratio between hemifusion and fusion if the data are expressed in absolute values, so normalized data against the same Env control must be always necessary in order to be able to compare with other experiments.

HeLa cells **expressed** higher levels of Env glycoproteins on their plasma membranes, but this fact did not affect the different biological properties measured in the assays. Although it has been previously associated higher surface densities of Env glycoproteins with an easy way to reach the threshold number needed to form of fusion-active complexes [202], our results did not reflect that. The higher levels of Env expression in HeLa did not result in higher fusogenicities, but only in higher single cell death induction. Thus, the distinct sensibilities showed in the assays with each effector cell line may account for the particular **cellular properties**.

The trend of lipid bilayers to hemifuse and develop fusion pores has been reported to be highly dependent on lipid composition, cytoskeleton components and transmembrane osmotic pressures [89]. In addition to the necessary microclustering

Discussion & Perspectives

recruitment of the CD4-CCR5 receptors in the target cell membrane to develop HIV fusion and infection [203-205], the Env mobility in the effector cells might also have severe consequences in fusion. It has been shown that cholesterol and sphingomyelin play a main role in HIV fusion by promoting the aggregation of the Env into ordered structures [206], and consistently, gp41 has been found to bind directly to cholesterol molecules [207]. After the establishment of the gp41 six-helix bundles, the target and the Env-expressing membranes become into close proximity. However, subsequent formation of highly ordered clusters of these six-helix bundles might be necessary to create the fusion pore that leads to the complete fusion between both membranes. The organization process of these structures depends on the lipid composition of the membrane [88]. Therefore, the lipid composition of the plasma membrane of the effector cells could be one of the factors that could be affecting to the Hemifusion:Fusion ratio. In fact, it has been shown that lipids that promote the hemifusion process, inhibits the pore formation, and vice versa, due to they induce different spontaneous curvatures to the membranes [89]. Consequently, we might speculate that the cell lines whose plasma membranes are enriched in phospholipids that preferentially promote fusion, may low the sensitivity for Env-mediated hemifusion processes, and vice versa. Thus, in an *in vivo* scenario where the target cells are distributed in different tissues and compartments and possibly having different cellular properties, it could be hypothesized that when become infected by HIV, these cells may also be preferentially prone to either induce single cell death or form multinucleated cells.

Multinucleated giant cell formation has already been reported in *in vivo* samples of lymph nodes [99], spinal cord [100,101] and lymphoid tissues [102]. However, bystander cell death, and hence, hemifusion processes, would be the representative of the main death of target cells due to HIV pathogenesis *in vivo*, because multinucleated cells are rarely obtained from patients' samples. It must be noted as well, that in an *in vivo* scenario several other factors like cell activation and cell densities of the target populations might also introduce variability to this ratio between hemifusion and fusion tendencies.

Overall, the possibility to use this strategy in high-throughput screening assays for drug testing or to identify other low pathogenic Env variants uncover the potential

power of this assay in HIV research. Our assay is useful to analyze the cytopathicity of the viral Envs that are currently circulating *in vivo* in patients infected with HIV and, hence, to identify anti-retroviral treatments that induce the appearance of low pathogenic Env variants. Currently, it has been extensively suggested that the treatment of patients infected with HIV with the fusion inhibitor Enfuvirtide (T-20) can promote the appearance of low pathogenic resistance variants [132-134,178,180,208,209]. One of the last clinical associations between certain T-20 resistance mutants and low pathogenesis was requiring *in vitro* studies to evaluate at a clonal level this correlation [132], so we decided to functionally characterize these mutant Envs using our methodology in HeLa cells.

The statistical analyses of that clinical trial showed that the *in vivo* CD4⁺ T cell counts benefit was associated with the concrete appearance of V38A mutants that had the N140I viral polymorphism. To test this correlation at a clonal level, we constructed the hybrid envelopes with the gp41 subunits that were derived from the patients that developed the V38A mutation and that were harboring different changes at the position 140. The comparisons of the functional data obtained with the hybrid envelopes that were constructed from baseline samples and after failing the treatment with T-20 (which selected the V38A resistance mutation), allowed us to measure the differences in the cytopathic ability specifically derived from the acquisition of the V38A primary mutation in each of the gp41 contexts (140N, N140T, N140I).

The results of our *in vitro* study [210] were correlated with the previously reported *in vivo* clinical associations [132] and showed that the Envs harboring the V38A mutation in a N140I background were low pathogenic, because they killed less CD4⁺ T cells than the rest of the variants tested. These V38A-N140I resistant viruses were demonstrated to be less pathogenic because they were less efficient to induce bystander cell death to target cells than wild-type viruses (38V-140N, 38V-140T, 38V-140I). V38A mutants with other polymorphisms in the amino acid position 140 (V38A-140N, V38A-140T) did not show any functional impairment in the ability to induce bystander cell death when compared to their respective wild-type variants. This low ability to induce apoptosis by the V38A-N140I mutants was not due to a low ability to fuse with target cells or a low capacity to express the Env glycoproteins,

Discussion & Perspectives

because both abilities were shown to be similar in all the Env variants tested in the assay. Therefore, the pathway that is impaired by the V38A-N140I mutants and that account for an *in vivo* low ability to kill CD4⁺ T cells, is the bystander cell death, which is dependent on the gp41-governed hemifusion processes and is culminated in a single cell death. Previous studies performed by site-directed mutagenesis of HIV at position 38 of gp41 suggested that the low ability to kill of V38A and V38E mutants was due to a lower ability to induce fusion [136]. However, these studies used site-directed mutants, and they did not consider different polymorphisms or contexts where the mutations arise *in vivo*. Therefore, possible compensations or changes in the phenotype were not taken into account. In our studies, however, we could test for those native changes, and we saw that these mutants were not defective in fusion, but only in hemifusion processes and their ability to kill target cells by single cell death. These discrepancies between the results obtained in studies made with real contexts and site-directed mutants constructed in laboratory-adapted strains, underscores again, the importance of the context when analyzing the functionalities of the Env glycoprotein. Thus, our data demonstrates that polymorphisms in HR2 have an important role in the HIV pathogenesis. Nevertheless, a methodological limitation of our study was the relative small number of clones analyzed, which gave us a low statistical power. Therefore, further *in vitro* studies with larger sample sizes and Env variants, may complement our results to have a more accurate vision of the importance of viral polymorphisms in the HIV pathogenesis.

The apoptosis of bystander CD4⁺ T cells is believed to be induced by soluble gp120 [97,98] and due to membrane-expressed envelopes [104]. However, in our assay we only measured the functional differences that accounted for the Envs that were expressed on the plasma membrane of the effector cells. The trivial amount of soluble gp120 that could be in the medium of the cultures and that could be inducing apoptosis to target cells was subtracted from the apoptotic single cell death data by removing the background death obtained when cultured in the presence of a CXCR4 inhibitor. Anyways, in our system, the gp120 subunit is not exerting a differential phenotype among the clones; due to all the hybrid Envs have a common NL4-3-derived wild-type fragment. This characteristic is also useful to avoid functional

interferences due to different coreceptor usage of the patient-derived Envs, which is a major determinant of the Env pathogenicity both *in vivo* [168] and *in vitro* [69].

Furthermore, the analysis of the patient-derived gp41 sequences ensured that none of the hybrid-Env expressing plasmids obtained from the patient carrying the N140I mutation accumulated changes in the caveolin-1 binding region, which has been reported to modulate the gp41-induced bystander cell death [94].

Previous *in vivo* studies have also showed an association between the appearance of V38A mutants and immunological benefits, although in these reports they did not associate the phenotypic changes with specific viral polymorphisms outside the HR1 region [133,134]. Taking into account our results and associations made by other groups of other specific primary mutations within HR1 and fitness compensatory mutations or polymorphisms in HR2 region [126,128,129,178,211-213], we strongly believe that the gp41 viral context is a really important factor that can affect the cytopathicity of this subunit. Therefore, we encourage other groups to perform future genotype-phenotype associations by focusing also in other regions outside HR1, although being this latter fragment the main responsible for the acquisition of resistance.

The susceptibility to T-20 has been shown to be quite variable in T-20 naïve patients [214,215]. And this can be associated with the different envelope contexts of the patients due to the fragment of gp41 that represents the 90% [216] of the primary resistance mutations to T-20 (amino acids 36-45) has been shown to be highly conserved in non-treated patients. Mink and colleagues [177] also reported the importance of the viral context by showing that the T-20 susceptibility varied depending on the viral context where the primary resistance mutations were tested, being higher if the specific mutations were introduced into a NL4-3 background than if they were tested in their original context in clinical isolates. Despite these reports highlighting the importance of the envelope context, no clinical studies have been done examining the rate of emergence of specific resistance-associated mutations to T-20 depending on the specific viral genetic forms that were in the patients. These kinds of studies may help to evaluate the envelope background effects on the efficacy of the treatment with this fusion inhibitor.

Discussion & Perspectives

As we have shown, the functionality of the HIV envelope is influenced by viral polymorphisms and the subunit context where the T-20 resistance mutations arise. The T-20-associated secondary mutations are amino acid compensations that are mainly selected in mutants because they restore interactions between HR1 and HR2 in the six-helix bundle formation [130,217], which is important for the development of fusion and hemifusion. As not all the associations between primary mutations in HR1 and viral polymorphisms or changes in HR2 are reported to develop immunological benefits after a viraemia rebound as the V38A-N140I mutants, it could be important to previously sequence the viral bulk population of the patient in order to help the physician to make a decision about giving a salvage treatment with T-20 or not. Patients harboring viral populations with polymorphisms that have been shown to be beneficial for the immunological recovery, like N140I when is associated with the V38A mutations or N126K for G36V [132], should be preferentially treated with T-20 before than patients harboring polymorphisms with bad prognosis or decrease in the CD4⁺ T cell counts after the virological failure, like T268A for Q40H-L45M mutants [132]. However, both types of patients might be more risky to develop an earlier T-20 resistant phenotype with a good fitness than patients that do not have a viral polymorphism that could act as compensatory. Further analysis of clinical data must be performed in order to establish the perceptual risk of failure of each group of patients. However, we could speculate that the better candidates for a T-20 salvage treatment would be the ones that did not have any viral polymorphism in HR2 that may favor the fitness of T-20 resistance mutants. The next group of patients to be preferentially treated with T-20 would be the ones that have polymorphisms associated with CD4⁺ T cell count benefits despite showing a restoration of the viral fitness, and hence, virological failure. And finally, the last option would be the group of patients that harbors viral populations with polymorphisms associated with a rapid depletion of the target cells after acquiring a virological failure phenotype. However, these are speculations based on reasonable thinking that have to be checked by *in vivo* data and a big cohort of patients. Thus, further research in the envelope context must be performed to understand, or even be able to predict at some extent, the rates of *in vivo* resistance and pathogenicity depending on certain viral populations. Also, it must be noted that the administration of T-20 is made intravenously, is very expensive and also that resistance mutations arise quickly after beginning the treatment, turning this

drug as one of the last options that the physician might give to the patient. However, this FDA-approved drug might be useful in cases where all the rest of the drugs are failing due to multi-resistant viruses. Other peptides with a higher genetic barrier than T-20, cheaper and with the possibility to being administered orally may turn this pathway one of the best candidates to efficiently block *de novo* infection.

CONCLUSIONS

1. Modeling secondary structures of RREs from nucleotide sequences does not reflect the real impact on their functionalities.
2. Nucleotides that encode for the amino acid 45 in gp41 play a role in the RRE-Rev binding.
3. RREs harboring the nucleotide substitutions that encode for the L45M change in gp41 have an impact in Rev binding at low concentrations of this viral protein.
4. Rev might perform exportation of RNA viral transcripts despite small impairments in its binding capacity to their RREs.
5. The co-expression of the mutations Q40H and L45M is not acquired due to a restoration of the RRE functions.
6. The sensitivity of *in vitro* assays used to measure the cytopathic capacities of Env glycoproteins is affected by the selection of the effector cell line.
7. 293T cells used to express Env glycoproteins might be preferentially selected in order to perform fusogenic evaluations, while HeLa cells should be selected for the evaluation of cell death parameters.
8. Patient-derived gp41 proteins with both V38A and N140I changes showed a reduced ability to induce single cell death and deplete CD4⁺ T cells despite maintaining fusion activity.
9. The specificity of the phenotype associated with the changes V38A and N140I highlights the relevance of the genetic context in the cytopathic capacity of the Env.
10. T-20-resistance mutations modulate the viral pathogenicity *in vivo*, further supporting the hypothesis that gp41 is a critical mediator of HIV pathogenesis.

PUBLISHED ARTICLES

- **Cunyat F**, Curriu M, Marfil S, García E, Clotet B, et al. **(2012)** *Evaluation of the Cytopathicity (Fusion/Hemifusion) of Patient-Derived HIV-1 Envelope Glycoproteins Comparing Two Effector Cell Lines.* J Biomol Screen. doi:10.1177/1087057112439890.
- **Cunyat F**, Marfil S, García E, Svicher V, Pérez-Alvárez N, et al. **(2012)** *The HR2 polymorphism N140I in the HIV-1 gp41 combined with the HR1 V38A mutation is associated with a less cytopathic phenotype.* Retrovirology 9: 15. doi:10.1186/1742-4690-9-15.
- **Cunyat F**, Ruiz L, Marfil S, Puig T, Bofill M, et al. **(2010)** *Genotypic and phenotypic evolution of HIV type-1 protease during in vitro sequential or concomitant combination of atazanavir and amprenavir.* Antivir Ther (Lond) 15: 431–436. doi:10.3851/IMP1543.
- Curriu M, Carrillo J, Massanella M, García E, **Cunyat F**, et al. **(2012)** *Susceptibility of Human Lymphoid Tissue Cultured ex vivo to Xenotropic Murine Leukemia Virus-Related Virus (XMRV) Infection.* PLoS ONE 7: e37415. doi:10.1371/journal.pone.0037415.

REFERENCES

1. Malim MH, Hauber J, Le SY, Maizel JV, Cullen BR (1989) **The HIV-1 rev trans-activator acts through a structured target sequence to activate nuclear export of unspliced viral mRNA.** *Nature* 338: 254–257. doi:10.1038/338254a0.
2. Pneumocystis Pneumonia in Los Angeles (1981) **Pneumocystis Pneumonia in Los Angeles.** *Centers for Diseases Control and Prevention* 30: 1–3. Available: http://www.cdc.gov/mmwr/preview/mmwrhtml/june_5.htm.
3. Barré-Sinoussi F, Chermann JC, Rey F, Nugeyre MT, Chamaret S, et al. (1983) **Isolation of a T-lymphotropic retrovirus from a patient at risk for acquired immune deficiency syndrome (AIDS).** *Science* 220: 868–871.
4. Levy JA, Hoffman AD, Kramer SM, Landis JA, Shimabukuro JM, et al. (1984) **Isolation of lymphocytopathic retroviruses from San Francisco patients with AIDS.** *Science* 225: 840–842.
5. Gallo R, Salahuddin S, Popovic M, Shearer G (1984) **Frequent detection and isolation of cytopathic retroviruses (HTLV-III) from patients with AIDS and at risk for AIDS.** *Science*.
6. Coffin J, Haase A, Levy JA, Montagnier L, Oroszlan S, et al. (1986) **Human immunodeficiency viruses.** *Science* 232: 697.
7. UNAIDS Report on the global AIDS epidemic 2010 (2010) **UNAIDS Report on the global AIDS epidemic 2010.** *UNAIDS* Geneva. pp.
8. Clavel F, Guétard D, Brun-Vézinet F, Chamaret S, Rey MA, et al. (1986) **Isolation of a new human retrovirus from West African patients with AIDS.** *Science* 233: 343–346.
9. Teixeira C, Gomes JRB, Gomes P, Maurel F (2011) **Viral surface glycoproteins, gp120 and gp41, as potential drug targets against HIV-1: Brief overview one quarter of a century past the approval of zidovudine, the first anti-retroviral drug.** *European Journal of Medicinal Chemistry* 46: 979–992. doi:10.1016/j.ejmech.2011.01.046.
10. Gao F, Bailes E, Robertson DL, Chen Y, Rodenburg CM, et al. (1999) **Origin of HIV-1 in the chimpanzee *Pan troglodytes troglodytes*.** *Nature* 397: 436–441. doi:10.1038/17130.
11. Korber B, Muldoon M, Theiler J, Gao F, Gupta R, et al. (2000) **Timing the ancestor of the HIV-1 pandemic strains.** *Science* 288: 1789–1796.
12. Hirsch VM, Olmsted RA, Murphey-Corb M, Purcell RH, Johnson PR (1989) **An African primate lentivirus (SIVsm) closely related to HIV-2.** *Nature* 339: 389–392. doi:10.1038/339389a0.
13. Alimonti JB, Ball TB, Fowke KR (2003) **Mechanisms of CD4+ T lymphocyte cell death in human immunodeficiency virus infection and AIDS.** *J Gen Virol* 84: 1649–1661.
14. Zhu P, Liu J, Bess J, Chertova E, Lifson JD, et al. (2006) **Distribution and three-dimensional structure of AIDS virus envelope spikes.** *Nat Cell Biol* 441: 847–852. doi:10.1038/nature04817.
15. Turner BG, Summers MF (1999) **Structural biology of HIV.** *Journal of Molecular Biology* 285: 1–32. doi:10.1006/jmbi.1998.2354.
16. Costin JM (2007) **Cytopathic mechanisms of HIV-1.** *Virol J* 4: 100. doi:10.1186/1743-422X-4-100.
17. Popov S, Rexach M, Ratner L, Blobel G, Bukrinsky M (1998) **Viral protein R regulates docking of the HIV-1 preintegration complex to the nuclear pore complex.** *J Biol Chem* 273: 13347–13352.
18. Ganser-Pornillos BK, Yeager M, Sundquist WI (2008) **The structural biology of HIV assembly.** *Current Opinion in Structural Biology* 18: 203–217. doi:10.1016/j.sbi.2008.02.001.
19. Nabel GJ, Rice SA, Knipe DM, Baltimore D (1988) **Alternative mechanisms for activation of**

References

- human immunodeficiency virus enhancer in T cells.** *Science* 239: 1299–1302.
20. Hill M, Tachedjian G, Mak J (2005) **The packaging and maturation of the HIV-1 Pol proteins.** *Curr HIV Res* 3: 73–85.
 21. Ammaranond P, Sanguansittianan S (2011) **Mechanism of HIV antiretroviral drugs progress toward drug resistance.** *Fundamental & Clinical Pharmacology* 26: 146–161. doi:10.1111/j.1472-8206.2011.01009.x.
 22. Karn J, Stoltzfus CM (2012) **Transcriptional and Posttranscriptional Regulation of HIV-1 Gene Expression.** *Cold Spring Harb Perspect Med* 2: a006916. doi:10.1101/cshperspect.a006916.
 23. Schwartz S, Felber BK, Benko DM, Fenyö EM, Pavlakis GN (1990) **Cloning and functional analysis of multiply spliced mRNA species of human immunodeficiency virus type 1.** *Journal of Virology* 64: 2519–2529.
 24. Pollard VW, Malim MH (1998) **The HIV-1 Rev protein.** *Annu Rev Microbiol* 52: 491–532. doi:10.1146/annurev.micro.52.1.491.
 25. Jones KA, Peterlin BM (1994) **Control of RNA initiation and elongation at the HIV-1 promoter.** *Annu Rev Biochem* 63: 717–743. doi:10.1146/annurev.bi.63.070194.003441.
 26. Jones KA (1997) **Taking a new TAK on tat transactivation.** *Genes & Development* 11: 2593–2599.
 27. Feinberg MB, Jarrett RF, Aldovini A, Gallo RC, Wong-Staal F (1986) **HTLV-III expression and production involve complex regulation at the levels of splicing and translation of viral RNA.** *Cell* 46: 807–817.
 28. Sodroski J, Goh WC, Rosen C, Campbell K, Haseltine WA (1986) **Role of the HTLV-III/LAV envelope in syncytium formation and cytopathicity.** *Nature* 322: 470–474. doi:10.1038/322470a0.
 29. Zapp ML, Green MR (1989) **Sequence-specific RNA binding by the HIV-1 Rev protein.** *Nature* 342: 714–716. doi:10.1038/342714a0.
 30. Kim SY, Byrn R, Groopman J, Baltimore D (1989) **Temporal aspects of DNA and RNA synthesis during human immunodeficiency virus infection: evidence for differential gene expression.** *Journal of Virology* 63: 3708–3713.
 31. Kjems J, Calnan BJ, Frankel AD, Sharp PA (1992) **Specific binding of a basic peptide from HIV-1 Rev.** *EMBO J* 11: 1119–1129.
 32. Hope TJ, McDonald D, Huang XJ, Low J, Parslow TG (1990) **Mutational analysis of the human immunodeficiency virus type 1 Rev transactivator: essential residues near the amino terminus.** *Journal of Virology* 64: 5360–5366.
 33. Thomas SL, Oft M, Jaksche H, Casari G, Heger P, et al. (1998) **Functional analysis of the human immunodeficiency virus type 1 Rev protein oligomerization interface.** *Journal of Virology* 72: 2935–2944.
 34. Wen W, Meinkoth JL, Tsien RY, Taylor SS (1995) **Identification of a signal for rapid export of proteins from the nucleus.** *Cell* 82: 463–473.
 35. Fischer U, Huber J, Boelens WC, Mattaj IW, Lührmann R (1995) **The HIV-1 Rev activation domain is a nuclear export signal that accesses an export pathway used by specific cellular RNAs.** *Cell* 82: 475–483.
 36. Mann DA, Mikaélian I, Zimmel RW, Green SM, Lowe AD, et al. (1994) **A molecular rheostat. Co-operative rev binding to stem I of the rev-response element modulates human immunodeficiency virus type-1 late gene expression.** *Journal of Molecular Biology* 241: 193–207.

37. Dayton ET, Powell DM, Dayton AI (1989) **Functional analysis of CAR, the target sequence for the Rev protein of HIV-1.** *Science* 246: 1625–1629.
38. Olsen HS, Nelbock P, Cochrane AW, Rosen CA (1990) **Secondary structure is the major determinant for interaction of HIV rev protein with RNA.** *Science* 247: 845–848.
39. Kjems J, Brown M, Chang DD, Sharp PA (1991) **Structural analysis of the interaction between the human immunodeficiency virus Rev protein and the Rev response element.** *Proc Natl Acad Sci USA* 88: 683–687.
40. Bartel DP, Zapp ML, Green MR, Szostak JW (1991) **HIV-1 Rev regulation involves recognition of non-Watson-Crick base pairs in viral RNA.** *Cell* 67: 529–536.
41. Daly TJ, Cook KS, Gray GS, Maione TE, Rusche JR (1989) **Specific binding of HIV-1 recombinant Rev protein to the Rev-responsive element in vitro.** *Nature* 342: 816–819. doi:10.1038/342816a0.
42. Zapp ML, Hope TJ, Parslow TG, Green MR (1991) **Oligomerization and RNA binding domains of the type 1 human immunodeficiency virus Rev protein: a dual function for an arginine-rich binding motif.** *Proc Natl Acad Sci USA* 88: 7734–7738.
43. Tiley LS, Malim MH, Tewary HK, Stockley PG, Cullen BR (1992) **Identification of a high-affinity RNA-binding site for the human immunodeficiency virus type 1 Rev protein.** *Proc Natl Acad Sci USA* 89: 758–762.
44. Cook KS, Fisk GJ, Hauber J, Usman N, Daly TJ, et al. (1991) **Characterization of HIV-1 REV protein: binding stoichiometry and minimal RNA substrate.** *Nucleic Acids Research* 19: 1577–1583.
45. Iwai S, Pritchard C, Mann DA, Karn J, Gait MJ (1992) **Recognition of the high affinity binding site in rev-response element RNA by the human immunodeficiency virus type-1 rev protein.** *Nucleic Acids Research* 20: 6465–6472.
46. Powell DM, Zhang MJ, Konings DA, Wingfield PT, Stahl SJ, et al. (1995) **Sequence specificity in the higher-order interaction of the Rev protein of HIV-1 with its target sequence, the RRE.** *J Acquir Immune Defic Syndr Hum Retroviro* 10: 317–323.
47. Charpentier B, Stutz F, Rosbash M (1997) **A dynamic in vivo view of the HIV-I Rev-RRE interaction.** *Journal of Molecular Biology* 266: 950–962. doi:10.1006/jmbi.1996.0858.
48. Jain C, Belasco JG (2001) **Structural model for the cooperative assembly of HIV-1 Rev multimers on the RRE as deduced from analysis of assembly-defective mutants.** *Molecular Cell* 7: 603–614.
49. Legiewicz M, Badorrek CS, Turner KB, Fabris D, Hamm TE, et al. (2008) **Resistance to RevM10 inhibition reflects a conformational switch in the HIV-1 Rev response element.** *Proceedings of the National Academy of Sciences* 105: 14365–14370. doi:10.1073/pnas.0804461105.
50. Pond SJK, Ridgeway WK, Robertson R, Wang J, Millar DP (2009) **HIV-1 Rev protein assembles on viral RNA one molecule at a time.** *Proceedings of the National Academy of Sciences* 106: 1404–1408. doi:10.1073/pnas.0807388106.
51. Daugherty MD, D'Orso I, Frankel AD (2008) **A solution to limited genomic capacity: using adaptable binding surfaces to assemble the functional HIV Rev oligomer on RNA.** *Molecular Cell* 31: 824–834. doi:10.1016/j.molcel.2008.07.016.
52. Pallesen J, Dong M, Besenbacher F, Kjems J (2009) **Structure of the HIV-1 Rev response element alone and in complex with regulator of virion (Rev) studied by atomic force microscopy.** *FEBS Journal* 276: 4223–4232. doi:10.1111/j.1742-4658.2009.07130.x.
53. Fernandes J, Jayaraman B, Frankel A (2012) **The HIV-1 rev response element: An RNA scaffold**

References

- that directs the cooperative assembly of a homo-oligomeric ribonucleoprotein complex. *RNA Biol* 9.
54. Daugherty MD, Liu B, Frankel AD (2010) **Structural basis for cooperative RNA binding and export complex assembly by HIV Rev.** *Nat Struct Mol Biol* 17: 1337–1342. doi:10.1038/nsmb.1902.
55. Van Ryk DI, Venkatesan S (1999) **Real-time kinetics of HIV-1 Rev-Rev response element interactions. Definition of minimal binding sites on RNA and protein and stoichiometric analysis.** *J Biol Chem* 274: 17452–17463.
56. Hope TJ (1999) **The ins and outs of HIV Rev.** *Archives of Biochemistry and Biophysics* 365: 186–191. doi:10.1006/abbi.1999.1207.
57. Moebius U, Clayton LK, Abraham S, Diener A, Yunis JJ, et al. (1992) **Human immunodeficiency virus gp120 binding C'C" ridge of CD4 domain 1 is also involved in interaction with class II major histocompatibility complex molecules.** *Proc Natl Acad Sci USA* 89: 12008–12012.
58. Kwong PD, Wyatt R, Robinson J, Sweet RW, Sodroski J, et al. (1998) **Structure of an HIV gp120 envelope glycoprotein in complex with the CD4 receptor and a neutralizing human antibody.** *Nature* 393: 648–659. doi:10.1038/31405.
59. Robert-Guroff M, Reitz MS, Robey WG, Gallo RC (1986) **In vitro generation of an HTLV-III variant by neutralizing antibody.** *J Immunol* 137: 3306–3309.
60. Veazey RS, DeMaria M, Chalifoux LV, Shvetz DE, Pauley DR, et al. (1998) **Gastrointestinal tract as a major site of CD4+ T cell depletion and viral replication in SIV infection.** *Science* 280: 427–431.
61. Mattapallil JJ, Douek DC, Hill B, Nishimura Y, Martin M, et al. (2005) **Massive infection and loss of memory CD4+ T cells in multiple tissues during acute SIV infection.** *Nature* 434: 1093–1097. doi:10.1038/nature03501.
62. Li Q, Duan L, Estes JD, Ma Z-M, Rourke T, et al. (2005) **Peak SIV replication in resting memory CD4+ T cells depletes gut lamina propria CD4+ T cells.** *Nature* 434: 1148–1152. doi:10.1038/nature03513.
63. Février M, Dorgham K, Rebollo A (2011) **CD4+ T cell depletion in human immunodeficiency virus (HIV) infection: role of apoptosis.** *Viruses* 3: 586–612. doi:10.3390/v3050586.
64. Cummins NW, Badley AD (2010) **Mechanisms of HIV-associated lymphocyte apoptosis: 2010.** *Cell Death and Disease* 1: e99–e99. doi:10.1038/cddis.2010.77.
65. Kreisberg JF, Yonemoto W, Greene WC (2006) **Endogenous factors enhance HIV infection of tissue naive CD4 T cells by stimulating high molecular mass APOBEC3G complex formation.** *J Exp Med* 203: 865–870. doi:10.1084/jem.20051856.
66. Kamata M, Nagaoka Y, Chen ISY (2009) **Reassessing the role of APOBEC3G in human immunodeficiency virus type 1 infection of quiescent CD4+ T-cells.** *PLoS Pathog* 5: e1000342. doi:10.1371/journal.ppat.1000342.
67. Doitsh G, Cavrois M, Lassen KG, Zepeda O, Yang Z, et al. (2010) **Abortive HIV Infection Mediates CD4 T Cell Depletion and Inflammation in Human Lymphoid Tissue.** *Cell* 143: 789–801. doi:10.1016/j.cell.2010.11.001.
68. Blanco J (2003) **Cell-Surface-Expressed HIV-1 Envelope Induces the Death of CD4 T Cells during GP41-Mediated Hemifusion-like Events.** *Virology* 305: 318–329. doi:10.1006/viro.2002.1764.
69. Blanco J, Barretina J, Clotet B, Esté JA (2004) **R5 HIV gp120-mediated cellular contacts induce**

- the death of single CCR5-expressing CD4 T cells by a gp41-dependent mechanism.** *J Leukoc Biol* 76: 804–811. doi:10.1189/jlb.0204100.
70. Checkley MA, Lutge BG, Freed EO (2011) **HIV-1 Envelope Glycoprotein Biosynthesis, Trafficking, and Incorporation.** *Journal of Molecular Biology* 410: 582–608. doi:10.1016/j.jmb.2011.04.042.
71. Starcich BR, Hahn BH, Shaw GM, McNeely PD, Modrow S, et al. (1986) **Identification and characterization of conserved and variable regions in the envelope gene of HTLV-III/LAV, the retrovirus of AIDS.** *Cell* 45: 637–648.
72. Willey RL, Rutledge RA, Dias S, Folks T, Theodore T, et al. (1986) **Identification of conserved and divergent domains within the envelope gene of the acquired immunodeficiency syndrome retrovirus.** *Proc Natl Acad Sci USA* 83: 5038–5042.
73. Ashkenazi A, Viard M, Wexler-Cohen Y, Blumenthal R, Shai Y (2011) **Viral envelope protein folding and membrane hemifusion are enhanced by the conserved loop region of HIV-1 gp41.** *The FASEB Journal* 25: 2156–2166. doi:10.1096/fj.10-175752.
74. Leonard CK, Spellman MW, Riddle L, Harris RJ, Thomas JN, et al. (1990) **Assignment of intrachain disulfide bonds and characterization of potential glycosylation sites of the type 1 recombinant human immunodeficiency virus envelope glycoprotein (gp120) expressed in Chinese hamster ovary cells.** *J Biol Chem* 265: 10373–10382.
75. Allan JS, Coligan JE, Barin F, McLane MF, Sodroski JG, et al. (1985) **Major glycoprotein antigens that induce antibodies in AIDS patients are encoded by HTLV-III.** *Science* 228: 1091–1094.
76. Montefiori DC, Robinson WE, Mitchell WM (1988) **Role of protein N-glycosylation in pathogenesis of human immunodeficiency virus type 1.** *Proc Natl Acad Sci USA* 85: 9248–9252.
77. Ma B-J, Alam SM, Go EP, Lu X, Desaire H, et al. (2011) **Envelope Deglycosylation Enhances Antigenicity of HIV-1 gp41 Epitopes for Both Broad Neutralizing Antibodies and Their Unmutated Ancestor Antibodies.** *PLoS Pathog* 7: e1002200. doi:10.1371/journal.ppat.1002200.g010.
78. Pancera M, Majeed S, Ban Y-EA, Chen L, Huang C-C, et al. (2010) **Structure of HIV-1 gp120 with gp41-interactive region reveals layered envelope architecture and basis of conformational mobility.** *Proceedings of the National Academy of Sciences* 107: 1166–1171. doi:10.1073/pnas.0911004107.
79. Li H, Chien PC, Tuen M, Visciano ML, Cohen S, et al. (2008) **Identification of an N-linked glycosylation in the C4 region of HIV-1 envelope gp120 that is critical for recognition of neighboring CD4 T cell epitopes.** *J Immunol* 180: 4011–4021.
80. Raska M, Novak J (2010) **Involvement of envelope-glycoprotein glycans in HIV-1 biology and infection.** *Arch Immunol Ther Exp (Warsz)* 58: 191–208. doi:10.1007/s00005-010-0072-3.
81. Zhang CW-H (2001) **Expression, Purification, and Characterization of Recombinant HIV gp140. The gp41 Ectodomain of HIV or Simian Immunodeficiency Virus is Sufficient to Maintain the Retroviral Envelope Glycoprotein as a Trimer.** *Journal of Biological Chemistry* 276: 39577–39585. doi:10.1074/jbc.M107147200.
82. Johnson WE, Sauvron JM, Desrosiers RC (2001) **Conserved, N-linked carbohydrates of human immunodeficiency virus type 1 gp41 are largely dispensable for viral replication.** *Journal of Virology* 75: 11426–11436. doi:10.1128/JVI.75.23.11426-11436.2001.
83. Haynes BF, Kelsoe G, Harrison SC, Kepler TB (2012) **B-cell-lineage immunogen design in vaccine development with HIV-1 as a case study.** *Nat Biotechnol* 30: 423–433. doi:10.1038/nbt.2197.
84. Ashkenazi A, Shai Y (2011) **Insights into the mechanism of HIV-1 envelope induced membrane**

References

- fusion as revealed by its inhibitory peptides. *Eur Biophys J* 40: 349–357. doi:10.1007/s00249-010-0666-z.**
85. Olshevsky U, Helseth E, Furman C, Li J, Haseltine W, et al. (1990) **Identification of individual human immunodeficiency virus type 1 gp120 amino acids important for CD4 receptor binding.** *Journal of Virology* 64: 5701–5707.
86. Chen B, Vogan EM, Gong H, Skehel JJ, Wiley DC, et al. (2005) **Structure of an unliganded simian immunodeficiency virus gp120 core.** *Nature* 433: 834–841. doi:10.1038/nature03327.
87. Berger EA, Murphy PM, Farber JM (1999) **Chemokine receptors as HIV-1 coreceptors: roles in viral entry, tropism, and disease.** *Annu Rev Immunol* 17: 657–700. doi:10.1146/annurev.immunol.17.1.657.
88. Chernomordik LV, Leikina E, Frolov V, Bronk P, Zimmerberg J (1997) **An early stage of membrane fusion mediated by the low pH conformation of influenza hemagglutinin depends upon membrane lipids.** *J Cell Biol* 136: 81–93.
89. Chernomordik LV, Kozlov MM (2003) **Protein-lipid interplay in fusion and fission of biological membranes.** *Annu Rev Biochem* 72: 175–207. doi:10.1146/annurev.biochem.72.121801.161504.
90. Chernomordik LV, Kozlov MM (2005) **Membrane hemifusion: crossing a chasm in two leaps.** *Cell* 123: 375–382. doi:10.1016/j.cell.2005.10.015.
91. Chan DC, Kim PS (1998) **HIV entry and its inhibition.** *Cell* 93: 681–684.
92. Harada S, Yusa K, Monde K, Akaike T, Maeda Y (2005) **Influence of membrane fluidity on human immunodeficiency virus type 1 entry.** *Biochemical and Biophysical Research Communications* 329: 480–486. doi:10.1016/j.bbrc.2005.02.007.
93. Brass AL, Dykxhoorn DM, Benita Y, Yan N, Engelman A, et al. (2008) **Identification of host proteins required for HIV infection through a functional genomic screen.** *Science* 319: 921–926. doi:10.1126/science.1152725.
94. Wang XM, Nadeau PE, Lo YT, Mergia A (2010) **Caveolin-1 Modulates HIV-1 Envelope-Induced Bystander Apoptosis through gp41.** *Journal of Virology* 84: 6515–6526. doi:10.1128/JVI.02722-09.
95. Llano M, Kelly T, Vanegas M, Peretz M, Peterson TE, et al. (2002) **Blockade of human immunodeficiency virus type 1 expression by caveolin-1.** *Journal of Virology* 76: 9152–9164.
96. Ashkenazi A, Wexler-Cohen Y, Shai Y (2011) **Multifaceted action of Fuzeon as virus–cell membrane fusion inhibitor.** *BBA - Biomembranes* 1808: 2352–2358. doi:10.1016/j.bbamem.2011.06.020.
97. Lin H, Chen W, Luo L, Wu C, Wang Q, et al. (2011) **Cytotoxic effect of HIV-1 gp120 on primary cultured human retinal capillary endothelial cells.** *Mol Vis* 17: 3450–3457.
98. Cefai D, Ferrer M, Serpente N, Idziorek T, Dautry-Varsat A, et al. (1992) **Internalization of HIV glycoprotein gp120 is associated with down-modulation of membrane CD4 and p56lck together with impairment of T cell activation.** *J Immunol* 149: 285–294.
99. Orenstein JM (2000) **In vivo cytolysis and fusion of human immunodeficiency virus type 1-infected lymphocytes in lymphoid tissue.** *J Infect Dis* 182: 338–342. doi:10.1086/315640.
100. Koenig S, Gendelman H, Orenstein J, Dal Canto M, Pezeshkpour G, et al. (1986) **Detection of AIDS virus in macrophages in brain tissue from AIDS patients with encephalopathy.** *Science* 233: 1089–1093. doi:10.1126/science.3016903.
101. Eilbott DJ, Peress N, Burger H, LaNeve D, Orenstein J, et al. (1989) **Human immunodeficiency**

- virus type 1 in spinal cords of acquired immunodeficiency syndrome patients with myelopathy: expression and replication in macrophages.** *Proc Natl Acad Sci USA* 86: 3337–3341.
102. Dargent J-L, Lespagnard L, Kornreich A, Hermans P, Clumeck N, et al. (2000) **HIV-Associated Multinucleated Giant Cells in Lymphoid Tissue of the Waldeyer's Ring: A Detailed Study.** *Mod Pathol* 13: 1293–1299. doi:10.1038/modpathol.3880237.
 103. Rivera-Toledo E, López-Balderas N, Huerta L, Lamoyi E, Larralde C (2010) **Decreased CD4 and wide-ranging expression of other immune receptors after HIV-envelope-mediated formation of syncytia in vitro.** *Arch Virol* 155: 1205–1216. doi:10.1007/s00705-010-0704-2.
 104. Perfettini J-L, Castedo M, Roumier T, Andreau K, Nardacci R, et al. (2005) **Mechanisms of apoptosis induction by the HIV-1 envelope.** *Cell Death Differ* 12: 916–923. doi:10.1038/sj.cdd.4401584.
 105. Perfettini J-L, Nardacci R, Bourouba M, Subra F, Gros L, et al. (2008) **Critical Involvement of the ATM-Dependent DNA Damage Response in the Apoptotic Demise of HIV-1-Elicited Syncytia.** *PLoS ONE* 3: e2458. doi:10.1371/journal.pone.0002458.g007.
 106. Garg H, Blumenthal R (2006) **HIV gp41-induced apoptosis is mediated by caspase-3-dependent mitochondrial depolarization, which is inhibited by HIV protease inhibitor nelfinavir.** *J Leukoc Biol* 79: 351–362. doi:10.1189/jlb.0805430.
 107. Brenchley JM, Knox KS, Asher AI, Price DA, Kohli LM, et al. (2008) **High frequencies of polyfunctional HIV-specific T cells are associated with preservation of mucosal CD4 T cells in bronchoalveolar lavage.** *Mucosal Immunol* 1: 49–58. doi:10.1038/mi.2007.5.
 108. Layne SP, Merges MJ, Dembo M, Spouge JL, Conley SR, et al. (1992) **Factors underlying spontaneous inactivation and susceptibility to neutralization of human immunodeficiency virus.** *Virology* 189: 695–714.
 109. Bourinbaïar AS (1994) **The ratio of defective HIV-1 particles to replication-competent infectious virions.** *Acta Virol* 38: 59–61.
 110. Gougeon M-L, Lecoœur H, Dulioust A, Enouf MG, Crouvoiser M, et al. (1996) **Programmed cell death in peripheral lymphocytes from HIV-infected persons: increased susceptibility to apoptosis of CD4 and CD8 T cells correlates with lymphocyte activation and with disease progression.** *J Immunol* 156: 3509–3520.
 111. Ahr B, Robert-Hebmann V, Devaux C, Biard-Piechaczyk M (2004) **Apoptosis of uninfected cells induced by HIV envelope glycoproteins.** *Retrovirology* 1: 12. doi:10.1186/1742-4690-1-12.
 112. Finkel T, Tudor-Williams G, Banda N, Cotton M, Curiel T, et al. (1995) **Apoptosis occurs predominantly in bystander cells and not in productively infected cells of HIV- and SIV-infected lymph nodes.** *Nat Med* 1: 129–134.
 113. Aillet F, Masutani H, Elbim C, Raoul H, Chêne L, et al. (1998) **Human immunodeficiency virus induces a dual regulation of Bcl-2, resulting in persistent infection of CD4(+) T- or monocytic cell lines.** *Journal of Virology* 72: 9698–9705.
 114. Fernández Larrosa PN, Croci DO, Riva DA, Bibini M, Luzzi R, et al. (2008) **Apoptosis resistance in HIV-1 persistently-infected cells is independent of active viral replication and involves modulation of the apoptotic mitochondrial pathway.** *Retrovirology* 5: 19. doi:10.1186/1742-4690-5-19.
 115. Wild CT, Shugars DC, Greenwell TK, McDanal CB, Matthews TJ (1994) **Peptides corresponding to a predictive alpha-helical domain of human immunodeficiency virus type 1 gp41 are potent inhibitors of virus infection.** *Proc Natl Acad Sci USA* 91: 9770–9774.
 116. Cervia JS, Smith MA (2003) **Enfuvirtide (T-20): a novel human immunodeficiency virus type 1**

References

- fusion inhibitor. *Clin Infect Dis* 37: 1102–1106. doi:10.1086/378302.**
117. Kilby JM, Hopkins S, Venetta TM, DiMassimo B, Cloud GA, et al. (1998) **Potent suppression of HIV-1 replication in humans by T-20, a peptide inhibitor of gp41-mediated virus entry.** *Nat Med* 4: 1302–1307. doi:10.1038/3293.
118. Lazzarin A, Clotet B, Cooper D, Reynes J, Arastéh K, et al. (2003) **Efficacy of enfuvirtide in patients infected with drug-resistant HIV-1 in Europe and Australia.** *N Engl J Med* 348: 2186–2195. doi:10.1056/NEJMoa035211.
119. Lalezari JP, Henry K, O'Hearn M, Montaner JSG, Piliero PJ, et al. (2003) **Enfuvirtide, an HIV-1 fusion inhibitor, for drug-resistant HIV infection in North and South America.** *N Engl J Med* 348: 2175–2185. doi:10.1056/NEJMoa035026.
120. Bonjoch A, Negredo E, Puig J, Erkizia I, Puig T, et al. (2006) **Viral failure in HIV-infected patients with long-lasting viral suppression who discontinued enfuvirtide.** *AIDS* 20: 1896–1898. doi:10.1097/01.aids.0000244212.15951.2b.
121. Clotet B (2011) **The HIV & Hepatitis Drug Resistance and PK Guide.**
122. Coffin JM (1995) **HIV population dynamics in vivo: implications for genetic variation, pathogenesis, and therapy.** *Science* 267: 483–489.
123. Cabrera C, Marfil S, García E, Martínez-Picado J, Bonjoch A, et al. (2006) **Genetic evolution of gp41 reveals a highly exclusive relationship between codons 36, 38 and 43 in gp41 under long-term enfuvirtide-containing salvage regimen.** *AIDS* 20: 2075–2080. doi:10.1097/QAD.0b013e3280102377.
124. Wei X, Decker JM, Liu H, Zhang Z, Arani RB, et al. (2002) **Emergence of resistant human immunodeficiency virus type 1 in patients receiving fusion inhibitor (T-20) monotherapy.** *Antimicrob Agents Chemother* 46: 1896–1905.
125. Pessoa LS, Valadão ALC, Abreu CM, Calazans AR, Martins AN, et al. (2011) **Genotypic analysis of the gp41 HR1 region from HIV-1 isolates from enfuvirtide-treated and untreated patients.** *J Acquir Immune Defic Syndr* 57 Suppl 3: S197–S201. doi:10.1097/QAI.0b013e31821e9d29.
126. Ray N, Blackburn LA, Doms RW (2009) **HR-2 Mutations in Human Immunodeficiency Virus Type 1 gp41 Restore Fusion Kinetics Delayed by HR-1 Mutations That Cause Clinical Resistance to Enfuvirtide.** *Journal of Virology* 83: 2989–2995. doi:10.1128/JVI.02496-08.
127. Reeves JD, Gallo SA, Ahmad N, Miamidian JL, Harvey PE, et al. (2002) **Sensitivity of HIV-1 to entry inhibitors correlates with envelope/coreceptor affinity, receptor density, and fusion kinetics.** *Proc Natl Acad Sci USA* 99: 16249–16254. doi:10.1073/pnas.252469399.
128. Tolstrup M, Selzer-Plön J, Laursen AL, Bertelsen L, Gerstoft J, et al. (2007) **Full fusion competence rescue of the enfuvirtide resistant HIV-1 gp41 genotype (43D) by a prevalent polymorphism (137K).** *AIDS* 21: 519–521. doi:10.1097/QAD.0b013e3280187558.
129. Xu L, Pozniak A, Wildfire A, Stanfield-Oakley SA, Mosier SM, et al. (2005) **Emergence and evolution of enfuvirtide resistance following long-term therapy involves heptad repeat 2 mutations within gp41.** *Antimicrob Agents Chemother* 49: 1113–1119. doi:10.1128/AAC.49.3.1113-1119.2005.
130. Jenwitheesuk E, Samudrala R (2005) **Heptad-repeat-2 mutations enhance the stability of the enfuvirtide-resistant HIV-1 gp41 hairpin structure.** *Antivir Ther (Lond)* 10: 893–900.
131. Baatz F, Nijhuis M, Lemaire M, Riedijk M, Wensing AMJ, et al. (2011) **Impact of the HIV-1 env Genetic Context outside HR1–HR2 on Resistance to the Fusion Inhibitor Enfuvirtide and Viral Infectivity in Clinical Isolates.** *PLoS ONE* 6: e21535. doi:10.1371/journal.pone.0021535.g004.

132. Svicher V, Aquaro S, D'Arrigo R, Artese A, Dimonte S, et al. (2008) **Specific Enfuvirtide-Associated Mutational Pathways in HIV-1 Gp41 Are Significantly Correlated With an Increase in CD4 +Cell Count, Despite Virological Failure.** *J Infect Dis* 197: 1408–1418. doi:10.1086/587693.
133. Aquaro S (2006) **Specific mutations in HIV-1 gp41 are associated with immunological success in HIV-1-infected patients receiving enfuvirtide treatment.** *Journal of Antimicrobial Chemotherapy* 58: 714–722. doi:10.1093/jac/dkl306.
134. Melby TE, Despirito M, Demasi RA, Heilek G, Thommes JA, et al. (2007) **Association between specific enfuvirtide resistance mutations and CD4 cell response during enfuvirtide-based therapy.** *AIDS* 21: 2537–2539. doi:10.1097/QAD.0b013e3282f12362.
135. Garg H, Joshi A, Freed EO, Blumenthal R (2007) **Site-specific mutations in HIV-1 gp41 reveal a correlation between HIV-1-mediated bystander apoptosis and fusion/hemifusion.** *Science's STKE* 282: 16899.
136. Garg H, Joshi A, Blumenthal R (2009) **Altered bystander apoptosis induction and pathogenesis of enfuvirtide-resistant HIV type 1 Env mutants.** *AIDS Res Hum Retroviruses* 25: 811–817.
137. Garg H, Joshi A, Ye C, Shankar P, Manjunath N (2011) **Single amino acid change in gp41 region of HIV-1 alters bystander apoptosis and CD4 decline in humanized mice.** *Virol J* 8: 34. doi:10.1186/1743-422X-8-34.
138. Goubard A, Clavel F, Mammano F, Labrosse B (2009) **In vivo selection by enfuvirtide of HIV type-1 env quasispecies with optimal potential for phenotypic expression of HR1 mutations.** *Antivir Ther (Lond)* 14: 597–602.
139. Svicher V, Alteri C, D'Arrigo R, Lagana A, Trignetti M, et al. (2009) **Treatment with the Fusion Inhibitor Enfuvirtide Influences the Appearance of Mutations in the Human Immunodeficiency Virus Type 1 Regulatory Protein Rev.** *Antimicrob Agents Chemother* 53: 2816–2823. doi:10.1128/AAC.01067-08.
140. Peden K, Emerman M, Montagnier L (1991) **Changes in growth properties on passage in tissue culture of viruses derived from infectious molecular clones of HIV-1LAI, HIV-1MAL, and HIV-1ELI.** *Virology* 185: 661–672.
141. Liu S (2005) **Different from the HIV Fusion Inhibitor C34, the Anti-HIV Drug Fuzeon (T-20) Inhibits HIV-1 Entry by Targeting Multiple Sites in gp41 and gp120.** *Journal of Biological Chemistry* 280: 11259–11273. doi:10.1074/jbc.M411141200.
142. Purvis SF, Jacobberger JW, Sramkoski RM, Patki AH, Lederman MM (1995) **HIV type 1 Tat protein induces apoptosis and death in Jurkat cells.** *AIDS Res Hum Retroviruses* 11: 443–450.
143. Adachi A, Gendelman HE, Koenig S, Folks T, Willey R, et al. (1986) **Production of acquired immunodeficiency syndrome-associated retrovirus in human and nonhuman cells transfected with an infectious molecular clone.** *Journal of Virology* 59: 284–291.
144. Zuker M, Stiegler P (1981) **Optimal computer folding of large RNA sequences using thermodynamics and auxiliary information.** *Nucleic Acids Research* 9: 133–148.
145. Wilkinson KA, Merino EJ, Weeks KM (2006) **Selective 2'-hydroxyl acylation analyzed by primer extension (SHAPE): quantitative RNA structure analysis at single nucleotide resolution.** *Nat Protoc* 1: 1610–1616. doi:10.1038/nprot.2006.249.
146. Watts JM, Dang KK, Gorelick RJ, Leonard CW, Bess JW, et al. (2009) **Architecture and secondary structure of an entire HIV-1 RNA genome.** *Nature* 460: 711–716. doi:10.1038/nature08237.
147. Zuker M (2003) **Mfold web server for nucleic acid folding and hybridization prediction.** *Nucleic*

References

- Acids Research* 31: 3406–3415. doi:10.1093/nar/gkg595.
148. Sterjovski J, Churchill MJ, Ellett A, Gray LR, Roche MJ, et al. (2007) **Asn 362 in gp120 contributes to enhanced fusogenicity by CCR5-restricted HIV-1 envelope glycoprotein variants from patients with AIDS.** *Retrovirology* 4: 89. doi:10.1186/1742-4690-4-89.
 149. Dayton ET, Konings DA, Powell DM, Shapiro BA, Butini L, et al. (1992) **Extensive sequence-specific information throughout the CAR/RRE, the target sequence of the human immunodeficiency virus type 1 Rev protein.** *Journal of Virology* 66: 1139–1151.
 150. Nameki D, Kodama E, Ikeuchi M, Mabuchi N, Otaka A, et al. (2005) **Mutations conferring resistance to human immunodeficiency virus type 1 fusion inhibitors are restricted by gp41 and Rev-responsive element functions.** *Journal of Virology* 79: 764–770. doi:10.1128/JVI.79.2.764-770.2005.
 151. Ueno M, Kodama EN, Shimura K, Sakurai Y, Kajiwara K, et al. (2009) **Synonymous mutations in stem-loop III of Rev responsive elements enhance HIV-1 replication impaired by primary mutations for resistance to enfuvirtide.** *Antiviral Res* 82: 67–72. doi:10.1016/j.antiviral.2009.02.002.
 152. Gallo SA, Sackett K, Rawat SS, Shai Y, Blumenthal R (2004) **The stability of the intact envelope glycoproteins is a major determinant of sensitivity of HIV/SIV to peptidic fusion inhibitors.** *Journal of Molecular Biology* 340: 9–14. doi:10.1016/j.jmb.2004.04.027.
 153. De Clercq E, Yamamoto N, Pauwels R, Balzarini J, Witvrouw M, et al. (1994) **Highly potent and selective inhibition of human immunodeficiency virus by the bicyclam derivative JM3100.** *Antimicrob Agents Chemother* 38: 668–674.
 154. Baba M, Nishimura O, Kanzaki N, Okamoto M, Sawada H, et al. (1999) **A small-molecule, nonpeptide CCR5 antagonist with highly potent and selective anti-HIV-1 activity.** *Proc Natl Acad Sci USA* 96: 5698–5703.
 155. Dragic T, Trkola A, Thompson DA, Cormier EG, Kajumo FA, et al. (2000) **A binding pocket for a small molecule inhibitor of HIV-1 entry within the transmembrane helices of CCR5.** *Proc Natl Acad Sci USA* 97: 5639–5644. doi:10.1073/pnas.090576697.
 156. Patki AH, Lederman MM (1996) **HIV-1 Tat protein and its inhibitor Ro 24-7429 inhibit lymphocyte proliferation and induce apoptosis in peripheral blood mononuclear cells from healthy donors.** *Cell Immunol* 169: 40–46. doi:10.1006/cimm.1996.0088.
 157. Mathews DH (2006) **Revolutions in RNA Secondary Structure Prediction.** *Journal of Molecular Biology* 359: 526–532. doi:10.1016/j.jmb.2006.01.067.
 158. Gruber AR, Lorenz R, Bernhart SH, Neubock R, Hofacker IL (2008) **The Vienna RNA Website.** *Nucleic Acids Research* 36: W70–W74. doi:10.1093/nar/gkn188.
 159. Cheng D-C, Zhong G-C, Su J-X, Liu Y-H, Li Y, et al. (2010) **A sensitive HIV-1 envelope induced fusion assay identifies fusion enhancement of thrombin.** *Biochemical and Biophysical Research Communications* 391: 1780–1784. doi:10.1016/j.bbrc.2009.12.155.
 160. Sakamoto T, Ushijima H, Okitsu S, Suzuki E, Sakai K, et al. (2003) **Establishment of an HIV cell-cell fusion assay by using two genetically modified HeLa cell lines and reporter gene.** *J Virol Methods* 114: 159–166.
 161. Blanco J, Jacotot E, Cabrera C, Cardona A, Clotet B, et al. (1999) **The implication of the chemokine receptor CXCR4 in HIV-1 envelope protein-induced apoptosis is independent of the G protein-mediated signalling.** *AIDS* 13: 909–917.
 162. Scanlan CN, Pantophlet R, Wormald MR, Ollmann Saphire E, Stanfield R, et al. (2002) **The broadly neutralizing anti-human immunodeficiency virus type 1 antibody 2G12 recognizes a cluster of**

- alpha1-->2 mannose residues on the outer face of gp120.** *Journal of Virology* 76: 7306–7321.
163. Karlsson GB, Halloran M, Schenten D, Lee J, Racz P, et al. (1998) **The envelope glycoprotein ectodomains determine the efficiency of CD4+ T lymphocyte depletion in simian-human immunodeficiency virus-infected macaques.** *J Exp Med* 188: 1159–1171.
 164. Métivier D, Dallaporta B, Zamzami N, Larochette N, Susin SA, et al. (1998) **Cytofluorometric detection of mitochondrial alterations in early CD95/Fas/APO-1-triggered apoptosis of Jurkat T lymphoma cells. Comparison of seven mitochondrion-specific fluorochromes.** *Immunol Lett* 61: 157–163.
 165. Etemad-Moghadam B, Rhone D, Steenbeke T, Sun Y, Manola J, et al. (2001) **Membrane-fusing capacity of the human immunodeficiency virus envelope proteins determines the efficiency of CD+ T-cell depletion in macaques infected by a simian-human immunodeficiency virus.** *Journal of Virology* 75: 5646–5655. doi:10.1128/JVI.75.12.5646-5655.2001.
 166. LaBonte JA, Patel T, Hofmann W, Sodroski J (2000) **Importance of membrane fusion mediated by human immunodeficiency virus envelope glycoproteins for lysis of primary CD4-positive T cells.** *Journal of Virology* 74: 10690–10698.
 167. Barretina J, Blanco J, Armand-Ugón M, Gutiérrez A, Clotet B, et al. (2003) **Anti-HIV-1 activity of enfuvirtide (T-20) by inhibition of bystander cell death.** *Antivir Ther (Lond)* 8: 155–161.
 168. Tersmette M, Lange JM, de Goede RE, de Wolf F, Eeftink-Schattenkerk JK, et al. (1989) **Association between biological properties of human immunodeficiency virus variants and risk for AIDS and AIDS mortality.** *Lancet* 1: 983–985.
 169. Freed EO, Delwart EL, Buchsacher GL, Panganiban AT (1992) **A mutation in the human immunodeficiency virus type 1 transmembrane glycoprotein gp41 dominantly interferes with fusion and infectivity.** *Proc Natl Acad Sci USA* 89: 70–74.
 170. Denizot M, Varbanov M, Espert L, Robert-Hebmann V, Sagnier S, et al. (2008) **HIV-1 gp41 fusogenic function triggers autophagy in uninfected cells.** *Autophagy* 4: 998–1008.
 171. Malim MH, Hauber J, Fenrick R, Cullen BR (1988) **Immunodeficiency virus rev trans-activator modulates the expression of the viral regulatory genes.** *Nature* 335: 181–183. doi:10.1038/335181a0.
 172. Phuphuakrat A, Auewarakul P (2003) **Heterogeneity of HIV-1 Rev response element.** *AIDS Res Hum Retroviruses* 19: 569–574. doi:10.1089/088922203322230932.
 173. Chen SS-L, Yang P, Ke P-Y, Li H-F, Chan W-E, et al. (2009) **Identification of the LWYIK motif located in the human immunodeficiency virus type 1 transmembrane gp41 protein as a distinct determinant for viral infection.** *Journal of Virology* 83: 870–883. doi:10.1128/JVI.01088-08.
 174. Dimonte S, Mercurio F, Svicher V, Perno CF, Ceccherini Silberstein F (2011) **Genetic and Structural Analysis of HIV-1 Rev Responsive Element Related to V38A and T18A Enfuvirtide Resistance Mutations.** *Intervirology*. doi:10.1159/000334696.
 175. Menzo S, Castagna A, Monachetti A, Hasson H, Danise A, et al. (2004) **Genotype and phenotype patterns of human immunodeficiency virus type 1 resistance to enfuvirtide during long-term treatment.** *Antimicrob Agents Chemother* 48: 3253–3259. doi:10.1128/AAC.48.9.3253-3259.2004.
 176. Marconi V, Bonhoeffer S, Paredes R, Lu J, Hoh R, et al. (2008) **Viral Dynamics and In Vivo Fitness of HIV-1 in the Presence and Absence of Enfuvirtide.** *JAIDS Journal of Acquired Immune Deficiency Syndromes* 48: 572–576. doi:10.1097/QAI.0b013e31817bbc4e.
 177. Mink M, Mosier SM, Janumpalli S, Davison D, Jin L, et al. (2005) **Impact of human immunodeficiency virus type 1 gp41 amino acid substitutions selected during enfuvirtide treatment on gp41 binding and antiviral potency of enfuvirtide in vitro.** *Journal of Virology* 79:

References

- 12447–12454. doi:10.1128/JVI.79.19.12447-12454.2005.
178. Pérez-Alvarez L, Carmona R, Ocampo A, Asorey A, Miralles C, et al. (2005) **Long-term monitoring of genotypic and phenotypic resistance to T20 in treated patients infected with HIV-1.** *J Med Virol* 78: 141–147. doi:10.1002/jmv.20520.
179. Mink M, Greenberg M, Mosier S, Janumpalli S (2002) **Impact of HIV-1 gp41 amino acid substitutions (positions 36–45) on susceptibility to T-20 (enfuvirtide) in vitro: analysis of primary virus isolates recovered.** *Antivir. Ther.* pp.
180. Lu J, Sista P, Giguel F, Greenberg M, Kuritzkes DR (2004) **Relative replicative fitness of human immunodeficiency virus type 1 mutants resistant to enfuvirtide (T-20).** *Journal of Virology* 78: 4628–4637.
181. Shuck-Lee D, Chen FF, Willard R, Raman S, Ptak R, et al. (2008) **Heterocyclic Compounds That Inhibit Rev-RRE Function and Human Immunodeficiency Virus Type 1 Replication.** *Antimicrob Agents Chemother* 52: 3169–3179. doi:10.1128/AAC.00274-08.
182. Nicholas L Mills MDDADFRKG (2006) **An α -Helical Peptidomimetic Inhibitor of the HIV-1 Rev-RRE Interaction.** *Journal of the American Chemical Society* 128: 3496. doi:10.1021/ja0582051.
183. Gao F, Morrison SG, Robertson DL, Thornton CL, Craig S, et al. (1996) **Molecular cloning and analysis of functional envelope genes from human immunodeficiency virus type 1 sequence subtypes A through G. The WHO and NIAID Networks for HIV Isolation and Characterization.** *Journal of Virology* 70: 1651–1667.
184. Zhang PF, Chen X, Fu DW, Margolick JB, Quinnan GV (1999) **Primary virus envelope cross-reactivity of the broadening neutralizing antibody response during early chronic human immunodeficiency virus type 1 infection.** *Journal of Virology* 73: 5225–5230.
185. Nora T, Bouchonnet F, Labrosse B, Charpentier C, Mammano F, et al. (2008) **Functional diversity of HIV-1 envelope proteins expressed by contemporaneous plasma viruses.** *Retrovirology* 5: 23. doi:10.1186/1742-4690-5-23.
186. Cunyat F, Curriu M, Marfil S, García E, Clotet B, et al. (2012) **Evaluation of the Cytopathicity (Fusion/Hemifusion) of Patient-Derived HIV-1 Envelope Glycoproteins Comparing Two Effector Cell Lines.** *J Biomol Screen.* doi:10.1177/1087057112439890.
187. Ramakrishnan R, Mehta R, Sundaravaradan V, Davis T, Ahmad N (2006) **Characterization of HIV-1 envelope gp41 genetic diversity and functional domains following perinatal transmission.** *Retrovirology* 3: 42. doi:10.1186/1742-4690-3-42.
188. Joshi A, Nyakeriga AM, Ravi R, Garg H (2011) **HIV ENV Glycoprotein-mediated Bystander Apoptosis Depends on Expression of the CCR5 Co-receptor at the Cell Surface and ENV Fusogenic Activity.** *Journal of Biological Chemistry* 286: 36404–36413. doi:10.1074/jbc.M111.281659.
189. Stocker H, Scheller C, Jassoy C (2000) **Destruction of primary CD4(+) T cells by cell-cell interaction in human immunodeficiency virus type 1 infection in vitro.** *J Gen Virol* 81: 1907–1911.
190. Bär S, Alizon M (2004) **Role of the ectodomain of the gp41 transmembrane envelope protein of human immunodeficiency virus type 1 in late steps of the membrane fusion process.** *Journal of Virology* 78: 811–820.
191. LaBonte JA, Madani N, Sodroski J (2003) **Cytolysis by CCR5-using human immunodeficiency virus type 1 envelope glycoproteins is dependent on membrane fusion and can be inhibited by high levels of CD4 expression.** *Journal of Virology* 77: 6645–6659.
192. Nussbaum O, Broder CC, Berger EA (1994) **Fusogenic mechanisms of enveloped-virus**

- glycoproteins analyzed by a novel recombinant vaccinia virus-based assay quantitating cell fusion-dependent reporter gene activation. *Journal of Virology* 68: 5411–5422.**
193. Cao J, Park IW, Cooper A, Sodroski J (1996) **Molecular determinants of acute single-cell lysis by human immunodeficiency virus type 1.** *Journal of Virology* 70: 1340–1354.
194. Weiss CD, Barnett SW, Cacalano N, Killeen N, Littman DR, et al. (1996) **Studies of HIV-1 envelope glycoprotein-mediated fusion using a simple fluorescence assay.** *AIDS* 10: 241–246.
195. Huerta L, Lamoyi E, Báez-Saldaña A, Larralde C (2002) **Human immunodeficiency virus envelope-dependent cell-cell fusion: a quantitative fluorescence cytometric assay.** *Cytometry* 47: 100–106.
196. López-Balderas N, Huerta L, Villarreal C, Rivera-Toledo E, Sandoval G, et al. (2007) **In vitro cell fusion between CD4+ and HIV-1 Env+ T cells generates a diversity of syncytia varying in total number, size and cellular content.** *Virus Res* 123: 138–146. doi:10.1016/j.virusres.2006.08.009.
197. Litwin V, Nagashima KA, Ryder AM, Chang C-H, Carver JM, et al. (1996) **HIV-1 membrane fusion mediated by a laboratory-adapted strain and a primary isolate analyzed by resonance energy transfer.** *Journal of Virology* 70: 1–5.
198. Huerta L, López-Balderas N, Larralde C, Lamoyi E (2006) **Discriminating in vitro cell fusion from cell aggregation by flow cytometry combined with fluorescence resonance energy transfer.** *J Virol Methods* 138: 17–23. doi:10.1016/j.jviromet.2006.07.012.
199. Broder CC, Berger EA (1995) **Fusogenic selectivity of the envelope glycoprotein is a major determinant of human immunodeficiency virus type 1 tropism for CD4+ T-cell lines vs. primary macrophages.** *Proc Natl Acad Sci USA* 92: 9004–9008.
200. Melikyan GB, Markosyan RM, Roth MG, Cohen FS (2000) **A point mutation in the transmembrane domain of the hemagglutinin of influenza virus stabilizes a hemifusion intermediate that can transit to fusion.** *Mol Biol Cell* 11: 3765–3775.
201. Kasson PM, Pande VS (2007) **Control of Membrane Fusion Mechanism by Lipid Composition: Predictions from Ensemble Molecular Dynamics.** *PLoS Comput Biol* 3: e220. doi:10.1371/journal.pcbi.0030220.st002.
202. Lineberger JE, Danzeisen R, Hazuda DJ, Simon AJ, Miller MD (2002) **Altering expression levels of human immunodeficiency virus type 1 gp120-gp41 affects efficiency but not kinetics of cell-cell fusion.** *Journal of Virology* 76: 3522–3533.
203. Singer II, Scott S, Kawka DW, Chin J, Daugherty BL, et al. (2001) **CCR5, CXCR4, and CD4 are clustered and closely apposed on microvilli of human macrophages and T cells.** *Journal of Virology* 75: 3779–3790.
204. Steffens CM, Hope TJ (2004) **Mobility of the human immunodeficiency virus (HIV) receptor CD4 and coreceptor CCR5 in living cells: implications for HIV fusion and entry events.** *Journal of Virology* 78: 9573–9578.
205. Zhang J, Fu Y, Li G, Nowaczyk K, Zhao RY, et al. (2010) **Direct observation to chemokine receptor 5 on T-lymphocyte cell surface using fluorescent metal nanoprobe.** *Biochemical and Biophysical Research Communications* 400: 111–116. doi:10.1016/j.bbrc.2010.08.020.
206. Sáez-Ciri3n A, Nir S, Lorizate M, Agirre A, Cruz A, et al. (2002) **Sphingomyelin and cholesterol promote HIV-1 gp41 pretransmembrane sequence surface aggregation and membrane restructuring.** *J Biol Chem* 277: 21776–21785. doi:10.1074/jbc.M202255200.
207. Vincent N, Genin C, Malvoisin E (2002) **Identification of a conserved domain of the HIV-1 transmembrane protein gp41 which interacts with cholesteryl groups.** *Biochim Biophys Acta* 1567: 157–164.

References

208. Poveda E, Rod s B, Labernardi re J-L, Benito JM, Toro C, et al. (2004) **Evolution of genotypic and phenotypic resistance to Enfuvirtide in HIV-infected patients experiencing prolonged virologic failure.** *J Med Virol* 74: 21–28. doi:10.1002/jmv.20141.
209. Soria A, Cavarelli M, Sala S, Alessandrini AI, Scarlatti G, et al. (2008) **Unexpected dramatic increase in CD4⁺ cell count in a patient with AIDS after enfuvirtide treatment despite persistent viremia and resistance mutations.** *J Med Virol* 80: 937–941. doi:10.1002/jmv.21138.
210. Cunyat F, Marfil S, García E, Svicher V, Pérez-Alvárez N, et al. (2012) **The HR2 polymorphism N140I in the HIV-1 gp41 combined with the HR1 V38A mutation is associated with a less cytopathic phenotype.** *Retrovirology* 9: 15. doi:10.1186/1742-4690-9-15.
211. Reeves JD, Lee F-H, Miamidian JL, Jabara CB, Juntilla MM, et al. (2005) **Enfuvirtide resistance mutations: impact on human immunodeficiency virus envelope function, entry inhibitor sensitivity, and virus neutralization.** *Journal of Virology* 79: 4991–4999. doi:10.1128/JVI.79.8.4991-4999.2005.
212. Baldwin CE, Berkhout B (2006) **Second site escape of a T20-dependent HIV-1 variant by a single amino acid change in the CD4 binding region of the envelope glycoprotein.** *Retrovirology* 3: 84. doi:10.1186/1742-4690-3-84.
213. Bai X, Wilson KL, Seedorff JE, Ahrens D, Green J, et al. (2008) **Impact of the Enfuvirtide Resistance Mutation N43D and the Associated Baseline Polymorphism E137K on Peptide Sensitivity and Six-Helix Bundle Structure.** *Biochemistry* 47: 6662–6670. doi:10.1021/ bi702509d.
214. Sista PR, Melby T, Davison D, Jin L, Mosier S, et al. (2004) **Characterization of determinants of genotypic and phenotypic resistance to enfuvirtide in baseline and on-treatment HIV-1 isolates.** *AIDS* 18: 1787–1794.
215. Labrosse B, Morand-Joubert L, Goubard A, Rochas S, Labernardiere JL, et al. (2006) **Role of the Envelope Genetic Context in the Development of Enfuvirtide Resistance in Human Immunodeficiency Virus Type 1-Infected Patients.** *Journal of Virology* 80: 8807–8819. doi: 10.1128/JVI.02706-05.
216. Su C, Melby T, DeMasi R, Ravindran P, Heilek-Snyder G (2006) **Genotypic changes in human immunodeficiency virus type 1 envelope glycoproteins on treatment with the fusion inhibitor enfuvirtide and their influence on changes in drug susceptibility in vitro.** *J Clin Virol* 36: 249–257. doi:10.1016/j.jcv.2006.03.007.
217. Baldwin CE, Sanders RW, Deng Y, Jurriaans S, Lange JM, et al. (2004) **Emergence of a drug-dependent human immunodeficiency virus type 1 variant during therapy with the T20 fusion inhibitor.** *Journal of Virology* 78: 12428–12437. doi:10.1128/JVI.78.22.12428-12437.2004.

ACKNOWLEDGMENTS

Acknowledgments

Aquest treball no hagués estat possible si fa quatre anys la meva directora de tesi, la Dra. Cecilia Cabrera, no m'hagués donat la oportunitat a incorporar-me al seu grup, per tant, li agraeixo de tot cor.

En estos cuatro años y medio, Ceci, siempre me has sabido guiar para hacerme mejorar y formarme en el día a día como investigador. Te agradezco por haberme transmitido estas ganas de ir siempre más allá y de buscar soluciones donde a veces parece que no hay ninguna. Gracias por tu confianza y por todo lo que me has enseñado, que es mucho. También tengo que dar las gracias a Juliá porqué esa gran persona y un gran científico. Su ímpetu de hacer reuniones, comentar resultados y elaborar hipótesis las recordaré siempre. Su amabilidad y buen feeling también. También tengo que agradecer todo el resto del grupo. Algunos se han ido, otros se han incorporado, pero todos formáis parte de esta tesis, gracias: Sílvia, Eli, Jorge, las dos Martas, Lucía e Isa, que siempre me habeis ayudado en todo. Las reuniones del grupo VIC siempre han sido increíblemente amenas, y sobretodo cuando alguien traía algo para desayunar, que eso ocurría muy a menudo por suerte. Me alegro de haber podido formar parte de este grupo, y de haberos conocido.

También tengo que agradecer todo el tiempo, ayuda, amistad y conversaciones que me han brindado el resto de compañeros del laboratorio. Este tiempo ha pasado volando gracias a todos y cada uno de vosotros. Siempre tendré un fantástico recuerdo rodando escenas para tesis doctorales, abriendo regalos de amigos invisibles en las cenas de navidad o comiendo los pasteles que cada uno traía para celebrar su cumpleaños. Estoy seguro que el talento y amabilidad que se respira en Irsi será difícil de encontrar en otro sitio. Estoy seguro que os voy a echar de menos. De hecho, ya lo estoy haciendo ahora que me estoy dando cuenta que esto realmente se acaba. Parecía un túnel infinito, pero por lo que se ve, esto es la salida. Hay luz. Habrá que salir.

Gràcies en gran part a l'ajuda inmensa d'en Ventura també.

Tot i que no estiguessin dintre del laboratori, també m'agradaria donar les gràcies a la meva família per tots els seus esforços i als meus amics, que sempre s'han preocupat per mi, i que m'han donat ànims en tot moment. Aquest optimisme sempre m'ha ajudat, gràcies per ser com sou i per transmetre'm-ho cada dia que ens veiem. I

finalment m'agradaria donar especialment les gràcies a la Bea, perquè sense ella tampoc hagués pogut i perquè m'ha ajudat a desconnectar del món laboral i veure vida fora del laboratori. Tot i que ella realment no sàpiga què hi faig al laboratori.

